Title
SCATTERING OF 50.9 MeV ALPHA PARTICLES FROM Ne20 AND Ca40

Author
Springer, Arthur.

Publication Date
1965-05-06

UCRL-11681

University of California

Ernest O. Lawrence Radiation Laboratory

SCATTERING OF 50.9 MeV ALPHA PARTICELS FROM Ne^{20} AND Ca^{40}

Berkeley, California

UCRL-11681

UNIVERSITY OF CALIFORNIA

Lawrence Radiation Laboratory
Berkeley, California

AEC Contract No. W-7405-eng-48

SCATTERING OF 50.9 MeV ALPHA PARTICLES FROM Ne^{20} AND Ca^{40}

Arthur Springer

(Ph.D. Thesis)

May 6, 1965

SCATTERING OF 50.9 MeV ALPHA PARTICLES FROM Ne^{20} AND Ca^{40}

Contents

SCATTERING OF 50.9 MeV ALPHA PARTICLES FROM Ne^{20} AND Ca^{40}

Arthur Springer

Department of Chemistry and Lawrence Radiation Laboratory
University of California
Berkeley, California

May 6, 1965

ABSTRACT

More than a dozen inelastic levels of both Ne^{20} and Ca^{40} were excited by inelastic scattering of 50.9 MeV alpha particles. Differential cross sections for these excitations were measured, and by analysis with the Austern and Blair model, one-step and two-step excitation processes were distinguished from each other. Spins, parities, and reduced transition probabilities were also extracted with the aid of this model. This information was then used to discuss the collective nuclear structure of Ca^{40}, which is vibrational, and Ne^{20} which has rotational bands based on both the ground state and octupole vibrations.

I. INTRODUCTION

This thesis is completely devoted to inelastic alpha scattering, a direct surface reaction which is currently receiving considerable attention. Most of the interest is due to three observations: 1) That inelastic alpha scattering primarily excites collective states, states which are best described in terms of the vibrational or rotational model; 2) That from the phase and small-angle behavior of the regular oscillations that characterize differential cross sections for alpha excitation, the angular momentum transfer in a one-step process can be measured. It is also possible to distinguish between one-step and two-step excitation processes; 3) That the reduced transition probabilities obtained from inelastic alpha scattering are directly related to the corresponding transition probabilities of gamma decay and Coulomb excitation.

This impressive list must be tempered with one obvious limitation— the information can only be obtained if the energy resolution of the experimental system permits the observation of discrete states.

With these points in mind two nuclei were chosen for investigation; Ne^{20} and Ca^{40}. Neon-20 is the lightest nucleus known to have well-defined rotational bands[1] and the combination of the facts that it is even-even and has comparatively few nucleons causes the excited states to be well separated. Although Ca^{40} has twice the number of nucleons, it also has well-separated states since it is doubly magic. Because of its spherical symmetry no rotational bands or enhanced quadrupole vibrations are expected. An enhanced octupole vibration found throughout the nuclei[2] and higher vibrations have previously been seen.[3]

In order to extract the information obtainable from inelastic alpha scattering mentioned earlier, a model is needed. Austern and Blair,[4,5] proposed a simple adiabatic model which has up to the present time rarely been compared with experimental data.[6] This model is based on a collective picture of the nucleus. To first order in the nuclear deformation it deals with one-step processes.

Calcium-40 was analyzed first. Its one-phonon vibrational states are known to lie at about 4 MeV,[7] and since most of the states studied in this experiment are found below 8 MeV, contributions from double phonon excitation should be slight. In this case the model predicts that all differential cross sections involving the same angular momentum transfer should have the same shape. In the section on Ca^{40} results, comparisons of this type are made. Since as will be shown, the model works excellently for Ca^{40}, it was next used to analyze the more complicated Ne^{20} data.

If the rotational band assignments in Ne^{20} are correct,[1] the three lowest bands are a positive parity K=0 band based on the 0+ ground state and two negative parity bands based on octupole vibrations with K projections of 0 and 2. According to this picture the ground-state band 2+ level and the 3- levels of the two negative parity bands should be excited by enhanced single-step processes while the other members of these bands should be excited by non-enhanced two-step processes. This situation is analogous to Coulomb excitation of nuclei in the permanently deformed region and in Secs. IV-B.3 and VI the similarities of inelastic scattering of alpha particles from Ne^{20} and multiple Coulomb excitation of U^{238} are pointed out.[8]

II. EXPERIMENTAL ARRANGEMENT AND PROCEDURES

A. The Cyclotron and Beam Optics

Although the new 88-inch spiral-ridge cyclotron is capable of providing variable energy beams of all the light charged particles, in the present experiment only the 50-MeV alpha particle beam was used. The beam optical system is shown in Fig. 1. In the radial plane a quadrupole-lens doublet created an image of the effective source half-way to the analyzing magnet which then deflected the beam 57^{o}, producing a radial image on the analyzing slit. This slit was made by water-cooled tantalum jaws whose radial position and separation could be remotely controlled. Under normal conditions the slit was 0.06-inches wide. After the slit the beam passed through the main shielding wall of the cyclotron vault. The particles were then brought to a radial focus at the target position in

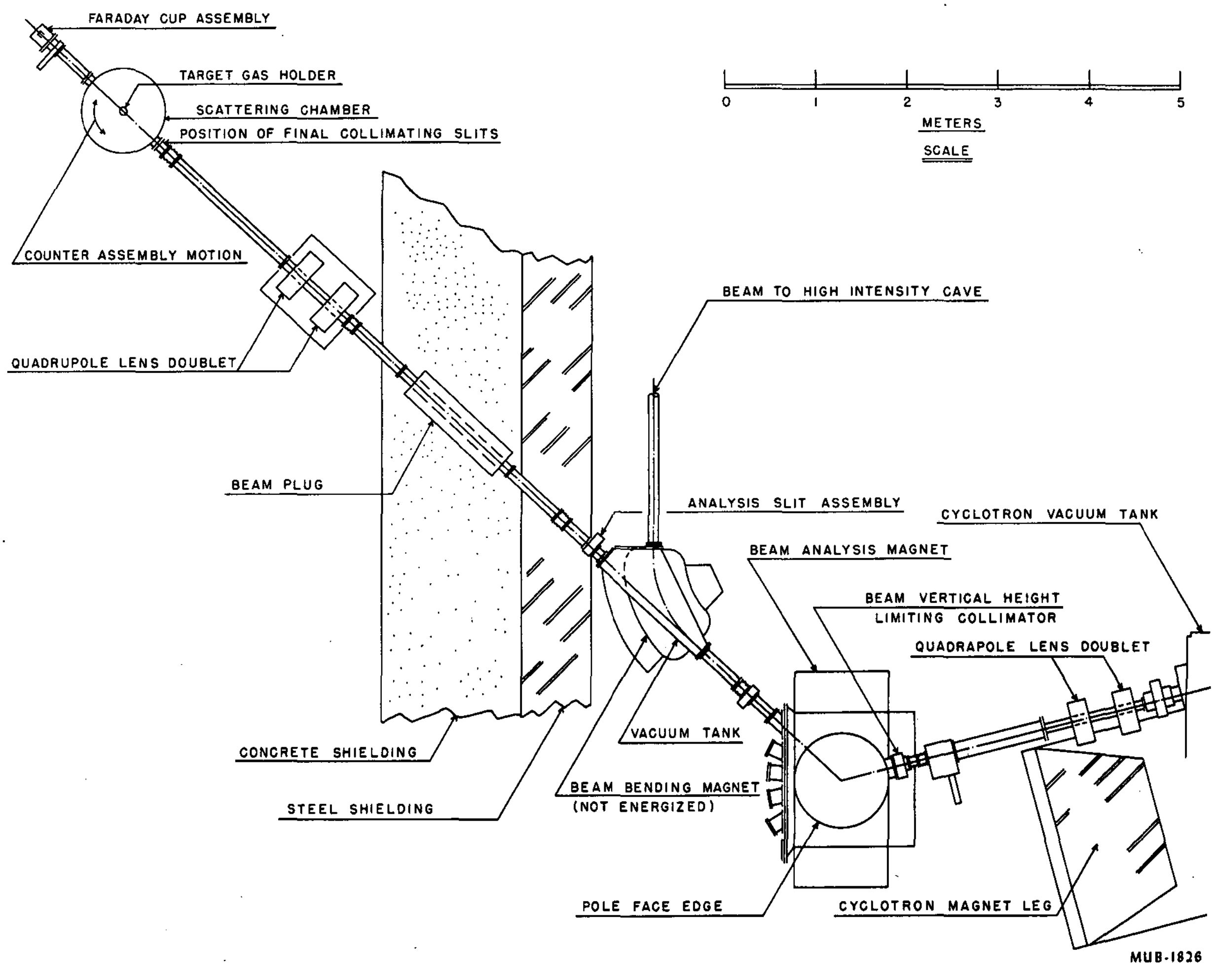

Fig. 1. Beam optics system of 88-in. cyclotron, cave 1.

the center of the scattering chamber by a second quadrupole doublet. The beam spot on the target was approximately 1/8-in. wide by 1/4-in. high. In the vertical plane the beam was roughly parallel. To minimize background due to slit scattering, no other beam collimation was used with the calcium target. Special analysis of the data was performed to correct for possible beam shifts, but no shifts corresponding to more than 0.1° were noted.

B. Scattering Equipment

The beam was measured by a magnetically protected Faraday cup and an integrating electrometer. Typically the beam intensity was 0.5μA. The energy of the beam was determined by measuring the range of the particles by a system of two remotely controlled 12-position foil wheels located directly in front of the Faraday cup. The range was converted to an equivalent energy by use of the range tables of Williamson and Boujot.[9] On the first run the energy at the center of the target was calculated to be 50.9 MeV and on subsequent runs the frequency was adjusted until the range-energy measurement was again consistent with this.

The scattering chamber consisted of a 36-in. diameter vacuum tank with a rotatable table on which the detector was placed. The table and target holder assembly could be moved by remote control. The positions of the counter and target were read on a digital volt meter. The counter assembly intercepted the beam at 6° thus limiting the useful table positions. The basic Faraday cup and scattering chamber have been described before.[10,11,12] The entire system was evacuated by a 6-in. water-cooled oil-diffusion pump backed by a Kinney mechanical pump.

C. Detectors

From a practical standpoint, one detector is sufficient to study inelastic scattering of alpha particles higher in energy than the highest energy He^3 group. This corresponds to over 12 MeV of excitation in both Ca^{40} and Ne^{20}. Particles lighter than He^3 are not stopped in the detector and cannot lose sufficient energy to overlap the energy range of interest. Particles heavier than alphas are not seen because of low cross sections or high negative Q-values. In any case, the energy scale was accurate enough to identify particle groups by energy vibration with angle.

The counters were 0.06-in. thick lithium-drifted silicon detectors made by a well described procedure.[13] The starting material was p-type silicon into which lithium was thermally diffused. Then under a reverse bias at $125^{\circ}C$ the lithium ions were drifted to form a compensated region of intrinsic resistivity. In the counter assembly (Fig. 2) contact was made by a stainless-steel pressure contact on the lithium side and by a silver ring to the gold surface-barrier side. The bias voltages applied were 250 to 300 V, the leakage currents were 1 to 4μA and the overall resolutions for alpha particles scattered from gold leaf were 70 to 80 keV.

D. Electronics

The detector was connected by a short length of low-capacity cable to a charge sensitive preamplifier[14] and by a 100-KΩ resistor to a bias supply. The preamplifier output signals traveled to the counting area through a 125Ω cable terminated at the input of the main amplifier system.[14] In the main amplifier the pulses were differentiated with a time constant of 0.5μsec, amplified, and then shaped to a 1 μsec square pulse suitable for the 4096-channel Nuclear Data pulse-height analyzer. Energy spectra were stored in the first 1024-channel group.

To avoid difficulties with pick-up of electrical noise from such sources as the cyclotron oscillator, great care was taken to maintain a one-point ground system and to avoid loops. The installation was very successful in this respect.

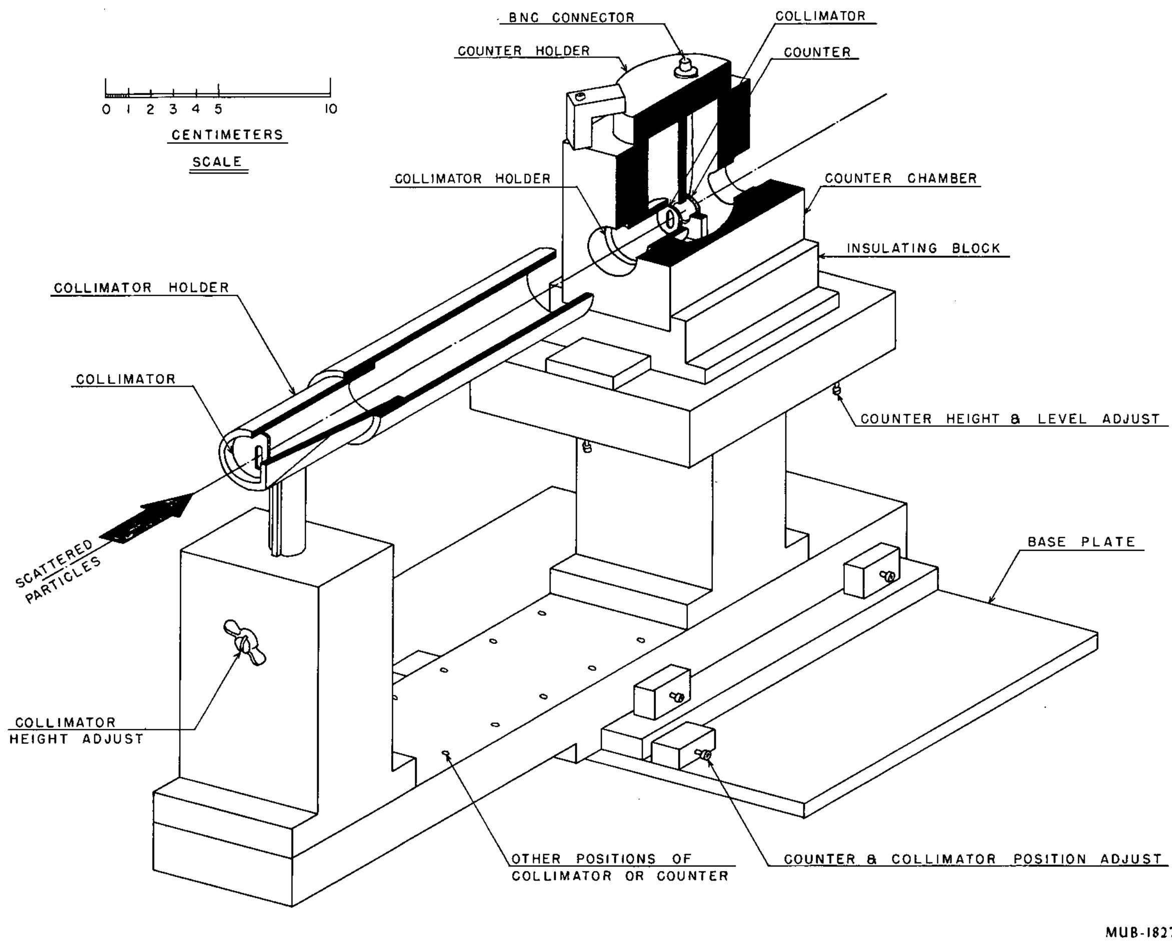

Fig. 2. Counter and gas target collimation.

E. Targets

1. Solid Targets

The calcium targets were prepared by rolling natural calcium metal turnings (97% Ca^{40}) in an inert atmosphere of dry argon. Application of a small amount of carbon tetrachloride before rolling the calcium generally reduced the tendency of the thin calcium foil to stick to the roller. All the steps of target preparation were performed in the inert atmosphere box and were as follows. The sealed commercial jar was opened and several turnings, one at a time, were hammered between two tantalum sheets until pieces thin enough to fit between the rollers were produced. All pieces which showed signs of strain or tears were discarded. One of the remaining pieces was then rolled with painstaking care, increasing the roller pressure slightly with each pass. Each time the calcium foil became longer than two inches in length it was cut in two. One piece was saved and the other was rolled further. Eventually, the foil would stick to the rollers and tear. If a piece of foil large enough for a target could be saved it was mounted at this point. If not, the piece saved from the last stage was then rolled one less time than the piece that tore, and then mounted. The mounted foil was transferred to the target mechanism of the scattering chamber and then raised into a small compartment which was closed off and quickly evacuated. Thus, exposure of the foil during the twenty minutes it took to pump down the scattering chamber was avoided. Targets prepared in this way had a thickness of 0.6 to 0.7 mg/cm^2. Carbon and oxygen were the only appreciable impurities and together were 9% by weight of the total thickness. The handicap of having the impurity peaks obscure inelastic calcium peaks at certain angles was partially compensated by the usefulness of these impurity peaks in the angle and energy scale calibration described in Sec. III-A. The target thickness was determined by a quantitative chemical analysis of the calcium in a piece of the target one square centimeter in area and centered on the spot discolored by the beam.

Figure 3 is a picture of one of the bombarded calcium foils after exposure to the air for several hours. The region hit by the beam

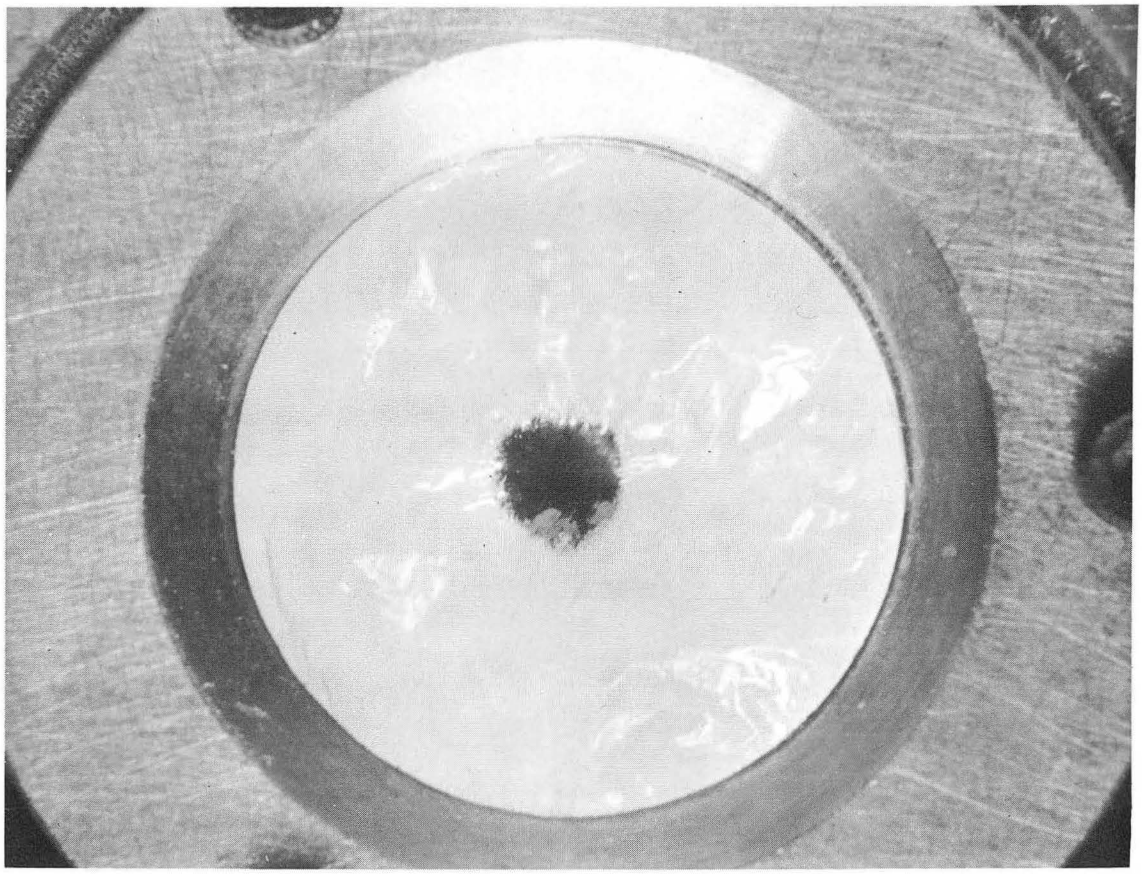

ZN-4592

Fig. 3. Beam spot on partially oxidized calcium target.

remained dark and metallic while the rest of the foil reacted to form transparent calcium carbonate. This gives some indication of how little the beam drifted and how well focused it was. The dimensions of the metallic remnant was 1/8-in. by 1/8-in. This is of concern since in Sec. II-A it was pointed out that no collimators were used between the analyzing slit and the target, a distance of twenty feet.

2. Gas Target

Ne^{20} was contained in a gas holder 3-in. in diameter at a pressure of about 10-cm Hg. The windows of the gas cell were 0.0001-in. thick Havar (from the Hamilton Watch Company) foil. The placement of the counter collimators for a gas target can be seen in Fig. 2. The resulting solid angle was 8.46×10^{-4} sr. Pressure adjustment was accomplished by a mercury Töpler pump and the pressure was measured by a mercury manometer. This system was especially designed for the recovery of rare gases. The neon (98.1% Ne^{20}) was obtained from the Mound Research Corporation.

F. Operating Procedure

The counter and electronics were tested before each cyclotron run with both a pulse generator and known energy alpha particles from decay of Th^{228}. By suitable adjustment of the bias cut and post-amplifier gain, pulses accepted by the pulse-height analyzer were made to correspond to alpha particles between 31 and 51 MeV.

The zero position of the beam was determined before and after each experiment by measuring the elastic differential cross section at a series of points separated by 0.1° in the vicinity of 26.5° on each side of the beam direction. At this angle a 0.1° shift in angle causes a 10% change in differential cross section. By averaging the two digital volt meter readings on each side of the beam direction which gave the same cross section, the digital volt meter reading corresponding to zero degrees was determined within 0.1°. A reading of 26.5 was specifically picked for Ca^{40}. A slightly different angle was used for Ne^{20}. During the experiment in which the target shown in Fig. 3 was bombarded, there was less than a 0.1° change in beam position. The beam energy was measured before and after the experiment by a range measurement described in Sec. I-B. As a final check on the beam energy and the accuracy of the counter angles, an energy scale was calculated from the pulse height of the known inelastic peaks at the first angle. At each subsequent angle the elastic-peak pulse height was converted to an equivalent alpha-particle energy by means of this scale and compared with the energy calculated for elastic alpha particles at that angle. The computer code used for all kinematic calculations is described in the Appendix in the section called LYCURGUS.

III. DATA REDUCTION

A. Energy Level Analysis

The energy spectrum at each counter angle recorded by the Nuclear Data pulse-height analyzer was punched on a paper type. The information on the paper tape was transferred to magnetic tape by an IBM-1101 computer. This magnetic tape was then used as input for a computer program named DIABLO written by Mr. Don Zurlinden. This code generated two additional magnetic tapes. One was used to operate a Calcomp plotter. Figures 4 and 5 were obtained in this way. The other was used as input for a second computer program called VARMIT. The purpose of VARMIT was to determine the peak channel number and the number of counts in each peak both for fully resolved and for overlapping peaks. As a practical consideration the counting statistics and the ability to separate overlapping peaks are related. Two peaks each containing about a thousand counts can be unfolded if separated by more than one half their full-width at half maximum, even though at the minimum separation mentioned only one smooth peak with no shoulders appears in the unresolved spectrum.

The separation was accomplished by expanding each energy spectrum as a series of Gaussian curves. A chi-squared minimization was then performed where

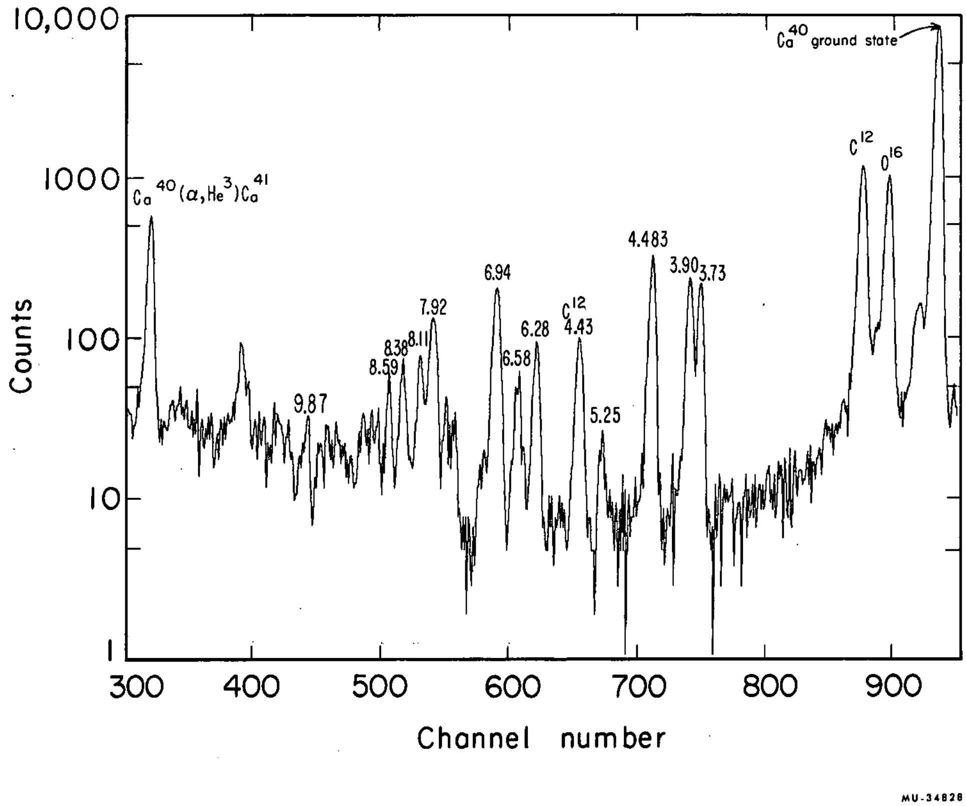

Fig. 4. A Ca^{40} energy spectrum at $\theta_{lab} = 18.5^{\circ}$.

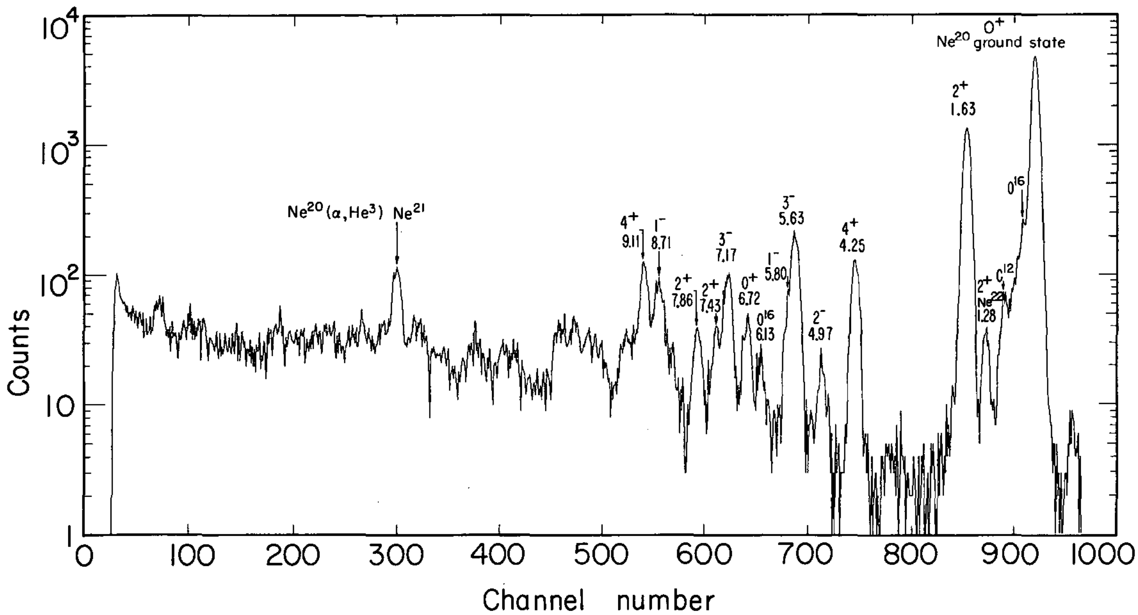

Fig. 5. Neon-20 19° lab energy spectrum.

$$\chi^2 = \sum_{i=1}^{m} \frac{(f_i - cts_i)^2}{cts_1} \qquad (1)$$

and

$$f_i = \sum_{j=1}^{n} X_j e^{-2.773 \left(\frac{i - X_{n+j}}{X_{2n+1}}\right)^2} \qquad (2)$$

where m is the number of channels, cts_i is the number of counts in the ith channel, n is the number of peaks, X_j is the height of the jth peak, X_{n+j} is the position of the jth peak and X_{2n+1} is the common full width at half maximum of all the peaks. The minimization was performed by a general minimization code written by Davidon[15] and modified by the author. The rest of the code was written by the author with the help of Mr. Joseph Good and Mr. Eric Beals. The Fortran listing and a brief description of this code appears in the Appendix. The (2n+1) parameters consisting of X_k, k=1,2..., 2n+1 were varied independently and afterwards relationships between the parameters due to calculable peak positions of known energy levels were checked as external criteria of meaningful convergence. In no case where a hand calculation for a single resolved peak was compared with the corresponding computer calculation did the two differ by as much as 5%. A typical spectrum and computer fit is shown in Fig. 6. From preliminary experimental work it was determined that Gaussian shaped peaks were a close approximation to the true peak shape only when all sources of slit scattering had been removed. This promoted the decision to not use a defining slit between the target and analyzing slit referred to in Secs. II-A and II-E.1.

With the peak positions thus determined, an energy scale was set up in the following manner. From a relativistic kinematics program called LYCURGUS described in the Appendix, the energy of scattered alpha particles and other scattered particles is given as a function of Q-value for the reaction, beam energy and angle of the scattered particle. The Q-values for the inelastic alpha scattering are obtained directly from the known energy levels.[16] The Q-values for $Ca^{40}(\alpha,He^3)Ca^{41}$ and other

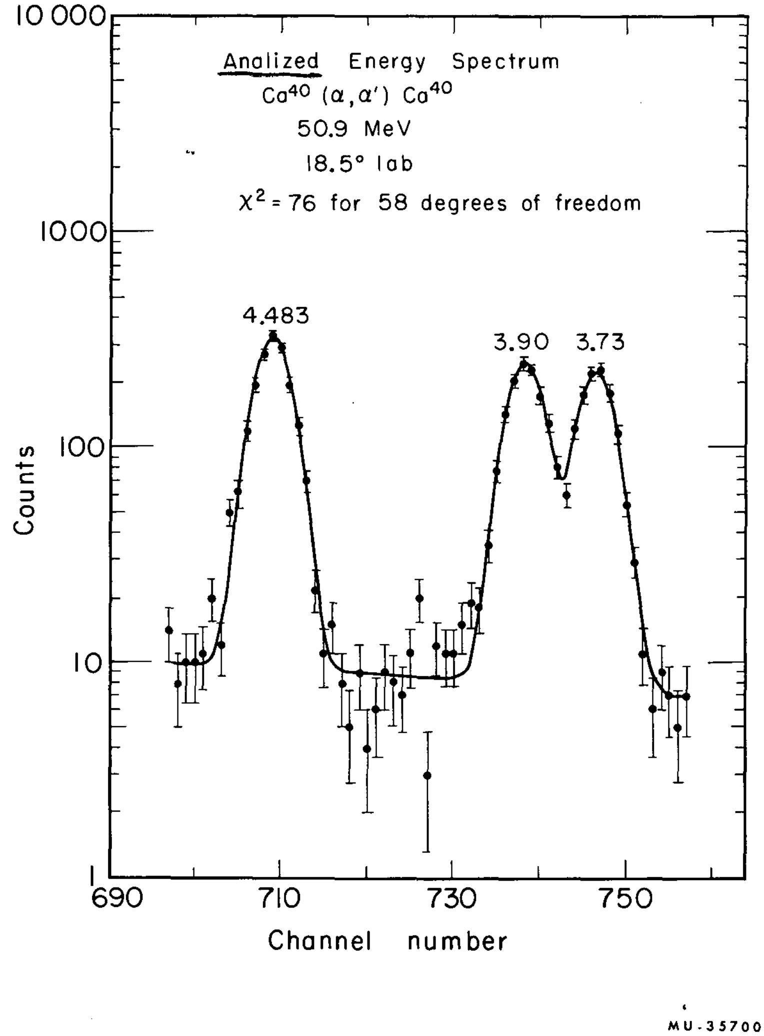

Fig. 6. The Ca^{40} energy spectrum shown in Fig. 4 was expanded in terms of a series of Gaussian peaks and a linear background. The portion of the fit shown here has a χ^2 of 76 for 58° of freedom. All the peaks have the same width, so the parameters varied correspond to the positions and heights of the peaks plus one variable width. The background was approximated by a straight line whose value was 10 counts per channel at the lowest channels shown and 7 counts per channel at the highest.

reactions were found in Ashby and Catron's tables.[17] The beam energy (see Sec. II-F) had previously been determined. A plot could therefore be made of energy versus channel for each known group from the energy spectra taken at each angle.

The functional form was found to be linear by the following, rather devious method. The energy scale was expanded in a series of polynomials with the channel number as a variable, starting first with a straight line and then successively adding higher terms up to 5th order. The coefficients were determined by a standard linear least squares method. However, χ^2 did not decrease sufficiently with increased parameters to warrant using any form beyond the linear one. With the energy scale determined to first order, second-order corrections could be made by using deviations in the points corresponding to carbon and oxygen impurities to correct the angles. This was not in fact necessary since the corrections were found to be less than 0.1° of a degree.

In the case of Ca^{40} there are two regions where the energy of the levels are well known. From inelastic proton scattering[18] the energies of levels up to 6 MeV in excitation are known to better than 10 keV. From $K^{39}(p,\gamma)Ca^{40}$ the energies of levels from 9 MeV to 11 MeV are also known to better than 10 keV.[19] Most of the levels analyzed in this thesis lie between the two known regions. If even one level in the higher region could be positively identified with one of the discrete groups excited in inelastic alpha scattering an internal interpolation could be performed which would make systematic errors highly unlikely. Finding one such level was not easy, since the resolution of this experiment (115 keV) was greater than most energy-level separations. A distinct peak does appear at 9.87 MeV which corresponds to a strong doublet at the same energy. Even if this identification had not been made, by use of the He^3 groups corresponding to the Ca^{41} ground state a slightly less trustworthy interpolation could still have been made. In Fig. 7 only peaks from the energy spectra at 30°, 35°, 40°, and 45° have been plotted to increase visual clarity. The levels whose energy have been determined

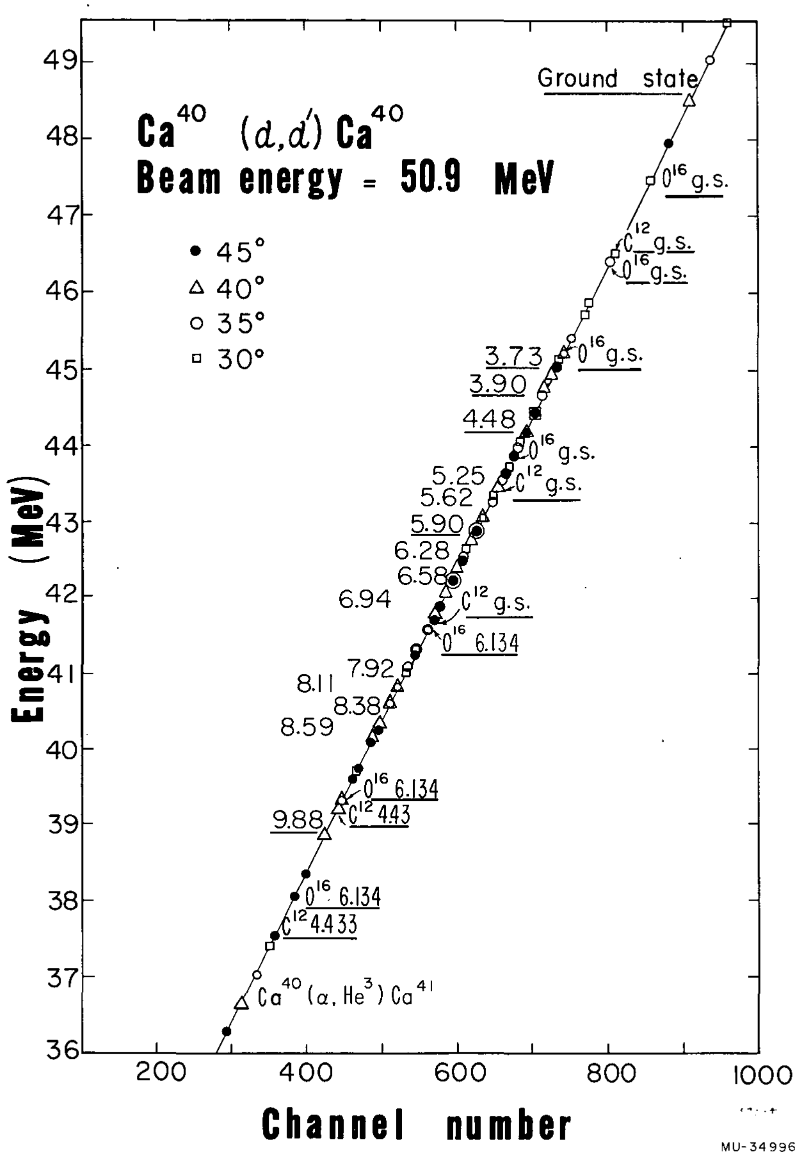

Fig. 7. Energy scale for energy spectra from θ_{lab}= 30° to θ_{lab}= 45°. Only θ_{lab}= 30°, 35°, 40°, and 45° are plotted. The ordinate is the calculated energy assuming incident beam energy of 50.9 MeV, and the Q values given in Table I. The abscissa is the channel of the peak. The states underlined were used to determine the line.

by this method are not underlined. To further strengthen the energy assignment, it can be seen from Fig. 7 that the carbon- and oxygen-impurity peaks fairly well cover the region between known levels. This can be fully appreciated if one tries to imagine what the plot would look like with just the 16 angles between 30° and 45° plotted. These arguments justify the 10 keV uncertainty in the energy assignments given in Table I.

For Ne^{20} a much simpler analysis was employed, since the energies of all the levels seen in this experiment were already known. A simple plot of excitation energy versus channel was made for two angles and it was observed that a smooth line was obtained in each case.

To conclude this section on energy scales, it must be stressed that the extreme linearity of the total counter and electronic system described in Secs. II-C and II-D greatly simplified the analysis and decreased the margin of energy uncertainty.

B. Differential Cross Sections

Differential cross sections were also calculated by the VARMIT computer code by the relationship

$$\left(\frac{d\sigma}{d\Omega}\right)_{C.M.} = G\,J\left(\frac{\text{counts}}{\mu c}\right) \tag{4}$$

where

$$J = \frac{d\cos\theta_{lab}}{d\cos\theta_{C.M.}}$$

and μc is the total charge in μ coulombs collected in the Faraday cup at the given angle.

For a solid target

$$G = \frac{1.602\times10^{-19}\,\text{coul.}}{6.023\times10^{23}\,\frac{\text{nuclei}}{\text{mole}}} \times10^{6}\,\frac{\mu\text{coul}}{\text{coul}} \times10^{27}\,\frac{\text{mb}}{\text{cm}^2}\times10^{3}\,\frac{\text{mg}}{\text{gm}}\left(\frac{R^2}{\text{area}}\right)ZA\sin\Phi \tag{5}$$

$$= 2.66\times10^{-7}\left(\frac{R^2}{\text{area}}\right)ZA\sin\Phi/T$$

Table I. Q-values, spins, and parities of Ca^{40} energy levels.

-Q value (MeV)	-Q value other experiments (MeV)	Ref.	J^{π}	J^{π} other experiments	Ref.
3.73	3.730	18	3-	3-	3,7,16,19, 26
3.90	3.900	18	2+	2+	3,7,16,19, 26
4.48	4.483	18	5-	5-	3,7,16,19, 26
5.25	5.241 5.272	18	?-	3- or 1-	26
5.62	5.606 5.621	18	?-	4+	26
5.90	5.901	18	3-	1-	26
6.28	6.29	26	3-	3-	3,26
6.58	6.56	26	3-	3-	26
6.94	6.94	26	2+ and (3- or 1-)	2+,3- 1-	3 26
7.92	7.91	26	4+	4+	3,26
8.11	8.09	26	2+	2+	26
8.38	8.37	26	4+	5-	3,26
8.59	--	--	2+	--	--
9.87	9.872 9.876	40			

where R is the distance from target to counter, "area" refers to the counter collimator, Z is the charge of the projectile, A is the atomic weight of the target, T is the thickness in mg/cm^2, and Φ is the target angle.

For a gas target

$$G = 2.66\times10^{-7}\ \frac{76\text{cm of Hg}}{\text{atm}}\ \frac{82.05\text{ atm cc}}{\text{g-mole }^{\circ}\text{K}}\times10^{-3}\ \frac{\text{gm}}{\text{mg}}\ \frac{(T+273)(\ell_1+\ell_2)^2 ZA\sin\theta}{PN\,W_1W_2h_2[1+\ \ell_1/\ell_2]}$$

$$= \frac{1.66\times10^{-6}(T+273)(\ell_1+\ell_2)^2 Z\sin\theta}{PN\,W_1W_2h_2[1+\ \ell_1/\ell_2]} \tag{6}$$

where T is the gas target temperature in degrees centigrade, ℓ_1 and ℓ_2 are the distances from the front collimator to the gas target center and from the front collimator to the rear collimator, θ is the lab scattering angle, ZA is the charge of the projectile, P is the gas pressure (cm Hg), W_1 and W_2 are the widths of the front and rear slits and h_2 is the height of the rear slit. All linear dimensions are measured in centimeters. N is the number of target-element atoms per molecule of the gas.

C. Reduced Transition Probabilities

Collective vibrations are associated with an oscillating electric multipole moment[20]

$$M(E_\lambda,\mu) = \frac{3}{4\pi} ZeR_o^{\lambda}\alpha_{\lambda\mu} \ . \tag{7}$$

The normalization has been chosen so that for a nucleus with constant density and sharp surface, the parameters $\alpha_{\lambda\mu}$ would define the surface by

$$R(\Omega) = R_o(1+\sum_{\lambda\mu}\alpha_{\lambda\mu}Y_\lambda^{\mu*}(\Omega)) \tag{8}$$

where $\Omega \equiv (\theta,\phi)$ are the polar angles of the radius vector in a space fixed coordinate system. For small oscillations the collective Hamiltonian is approximately

$$H_{coll} = \sum_{\lambda\mu} \frac{1}{2} B_\lambda |\dot{\alpha}_{\lambda\mu}|^2 + \frac{1}{2} C_\lambda |\alpha_{\lambda\mu}|^2 \qquad (9)$$

corresponding to a set of independent harmonic oscillators, with energy quanta

$$\hbar\omega_\lambda = \hbar\left(\frac{C_\lambda}{B_\lambda}\right)^{1/2} . \qquad (10)$$

Vibrational excitations are characterized by enhanced electric transition probabilities. For one phonon excitation the transition probability is given by

$$B(E_\lambda;\lambda \to 0) = \left(\frac{3}{4} ZeR_o^{\lambda}\right)^2 \frac{\hbar}{2(B_\lambda C_\lambda)^{1/2}} \qquad (11)$$

since

$$\langle\lambda|\alpha_{\lambda\mu}|0\rangle^2 = \frac{\hbar}{2(B_\lambda C_\lambda)^{1/2}} \qquad (12)$$

for a harmonic oscillator. The $B(E_\lambda;\lambda \to 0)$ are defined according to Ref. 12.

If on the other hand the nucleus has a permanent deformation and an associated set of rotational levels, then the nuclear surface is approximately described by

$$R(\omega) = R_o(1+ \sum_\ell \beta_\ell Y_\ell^{o}(\omega)) \qquad (13)$$

where $\omega \equiv (\theta',\Phi')$ and θ' is the azimuthal angle measured from the symmetry axis, see Fig. 8. The nuclear surface as veiwed from the direction $\Omega \equiv (\Theta,\Phi)$ of the fixed coordinate system, depends on the Eulerean angles $(\alpha\beta\gamma)$ corresponding to a rotation of this system into the direction

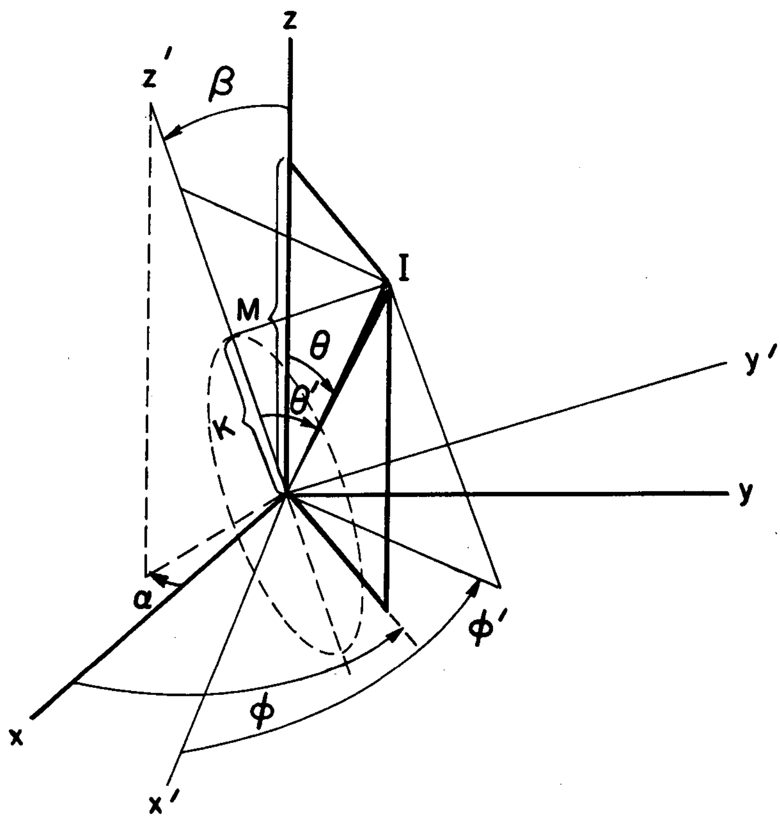

Fig. 8. Relationship between body centered and fixed coordinate systems. The last Eulerean angle γ is not shown.

of the nuclear symmetry axis.†

$$Y_\ell^{\,o}(\omega) = \sum_m Y_\ell^{m*}(\Omega)\, D^{\ell *}_{mo}(\alpha\beta\gamma). \tag{14}$$

Since in the fixed system the nuclear surface can still be represented by

$$R(\Omega) = R_o(1+\alpha_{\ell m} Y_\ell^{m*}(\Omega)) \tag{15}$$

it follows that

$$\alpha_{\ell m} = \beta_\ell D^{\ell *}_{mo}(\alpha\beta\gamma)\ . \tag{16}$$

Using the normalized wave functions of a symmetric top

$$IMK = \left(\frac{2I+1}{8\pi^2}\right)^{1/2} D^I_{MK}(\alpha\beta\gamma) \tag{17}$$

the matrix element of the operator α_{IM} can be evaluated as follows

$$\langle IMK|\alpha_{IM}|000\rangle = \int_0^{2\pi} d\alpha \int_0^{\pi} d\beta \sin\beta \int_{-\pi}^{\pi} d\gamma \left(\frac{I+1}{8\ ^2}\right)^{1/2} D^I_{MK}(\alpha\beta\gamma)\beta_I D^{I*}_{MO}(\alpha\beta\gamma)\left(\frac{1}{8\pi^2}\right)^{1/2}$$

$$= \frac{\beta_I}{(2I+1)^{1/2}}\ . \tag{18}$$

In the Austern and Blair model (Sec. V-A) the physically meaningful quantities are ξ_{IM} and δ_I which are the product of the "nuclear radius" R_o and α_{IM} and β_I respectively. Since the radius is not

†The conventions for Euler angles and rotation matrices are those of Messiah.[22]

determined in this type of analysis, to compare inelastic scattering transition probabilities with other experiments the radius must be obtained separately. In the next section a method of obtaining suitable radii is discussed.

Since the inelastic cross section is proportional to the square of the matrix element of ξ_{IM} and independent of the model assumed for the collective motion, it is convenient to report the matrix element in terms of the parameter δ_I for vibrational as well as rotational excitation.

From Eqs. (12) and (18) the relationship between the two sets of parameters is

$$\frac{\hbar R_o^2}{2(B_I C_I)^{1/2}} = \frac{\delta_I^2}{2I+1} \tag{19}$$

The connection between the electric reduced transition probability and inelastic alpha scattering is that collective inelastic scattering is induced by the variations in the radius corresponding to shape oscillations. Specifically when the optical potential is expanded in powers of $\alpha(\Omega) \equiv \sum_{\ell m} \xi_{\ell m} Y_\ell^m(\Omega)$, it is the term $\partial V/\partial R \; \alpha(\Omega)$ which leads to single excitation.

D. Evaluation of Reduced Transition Probabilities

In the last section relationships were developed between vibrational model parameters and rotational model parameters. In terms of this relationship the reduced transition probability is given by

$$B(E_\lambda; \lambda \to 0) = \left(\frac{3}{4} ZeR_o^{\lambda}\right)^2 \frac{\beta_\lambda^2}{2\lambda+1} \tag{20}$$

assuming a uniform charge distribution.

Lane and Pendelbury[2] have obtained for non-uniform charge distributions

$$\frac{B(E_\lambda;\lambda\to 0)}{e^2} = (2\lambda+1)\left[\frac{Z\langle r^{2\lambda-2}\rangle}{4\pi R_{1/2}^{\lambda-2}}\right]^2 \beta_\lambda^2 \tag{21}$$

and for a single particle transition

$$\frac{B_{sp}(E_\lambda;\lambda\to 0)}{e^2} = \frac{\langle r^\lambda\rangle^2}{4\pi} \tag{22}$$

where

$$\langle r^{2\lambda-2}\rangle = \frac{\int_0^\infty r^{2\lambda}\rho(r)dr}{\int_0^\infty r^2\rho(r)dr}$$

and

$$\rho(r) = \left(1+e^{\frac{r-R_{1/2}}{.55}}\right)^{-1}$$

where $R_{1/2}$ is the half density radius.

The quantity δ_λ is directly extracted from experimental cross sections by use of the Austern and Blair model (Sec. V-B).

Since neither the "nuclear radius" R_o or the half density radius $R_{1/2}$ is directly measurable they are both taken from electron scattering data of Hofstadter with R_o corresponding to his equivalent uniform charge radius.

IV. RESULTS AND DISCUSSION

A. Calcium-40

1. General

In the excitation of levels in Ca^{40} the states based on octupole vibrations are dominant. Most of the strength resides in the lowest 3- level at 3.73 MeV which has been seen by many experiments[16] and is known to be enhanced 11 times over single particle estimates.[2] Several other 3- states are also enhanced and are discussed in the following section. Octupole vibrational states are found widely throughout the nuclei.[2,24,25] Their excitation energy and strength are not closely related to shell structure. This is in marked contrast to quadrupole vibrations which are found at increasingly higher energies in the vicinity of closed shells and correspondingly are less enhanced. In Ca^{40} the lowest 2+ is found at 3.90 MeV and its reduced transition probability is indicative of a single particle excitation. Three other 2+ states are also seen, again without enhanced excitation. Calcium-40 is one of the few nuclei, where a one-phonon 2^5th pole vibrational state has been identified.[3] According to the prescription used in this work for calculating enhancements (Sec. III-D) the 5- level at 4.483 MeV is enhanced 24 times over single particle excitation. No higher 5- states were seen in this experiment. A one-phonon 2^4th pole excitation to a state at 7.9 MeV was first observed by inelastic electron scattering. This has been also seen in the present work along with another 2^4th pole excitation at 8.38 MeV. Both are enhanced by 2 to 4 time single-particle estimates.

Angular distributions to 13 excited states were measured. The differential cross sections are tabulated in the Appendix. The levels are the 3.73, 3.90, 4.48, 5.25, 5.62, 5.90, 6.28, 6.58, 6.94, 7.92, 8.11, and 8.59 MeV states.

Angular distributions for ℓ = 3,5,2, and 4 are grouped respectively in Figs. 9-12. The known 3.35 MeV 0+ level was possibly seen at a few angles but it was not made in sufficient strength for an angular distribution to be measured. The peaks at 5.25 and 5.62 MeV are known to be doublets.[16] They are weakly excited and because of the poor statistics

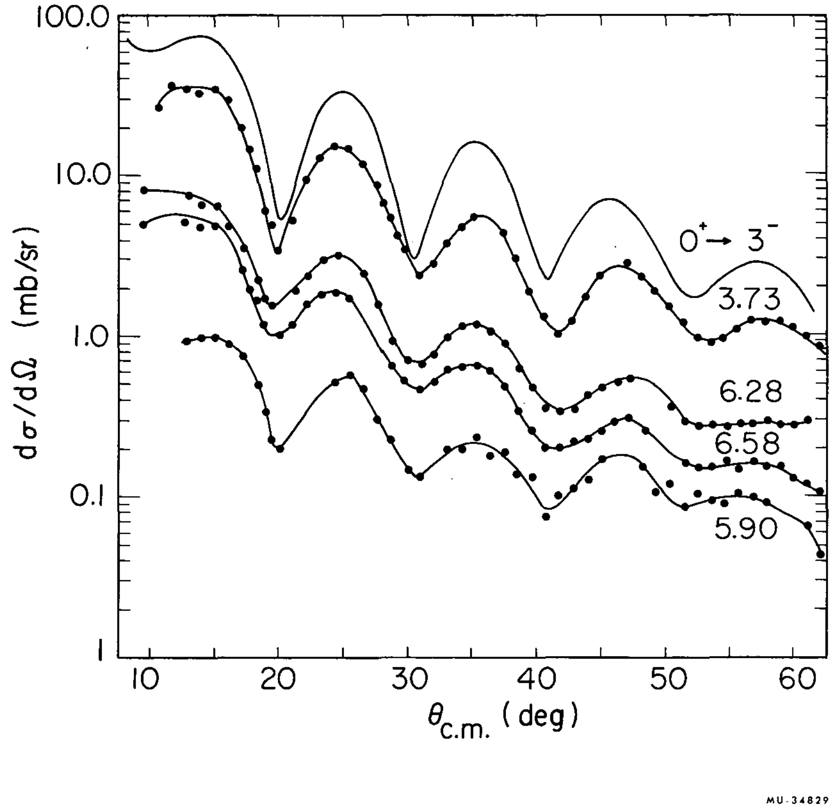

Fig. 9. Austern and Blair ℓ = 3 unnormalized angular distribution and states with similar experimental differential cross section.

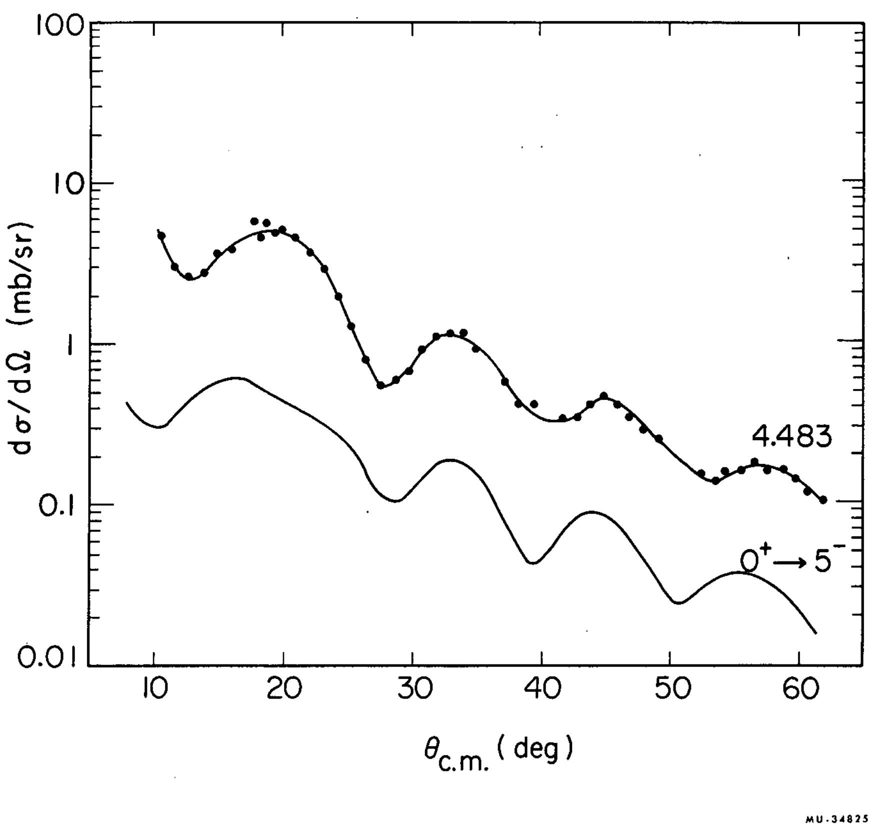

Fig. 10. Austern and Blair $\ell = 5$ unnormalized angular distribution and the 4.483-MeV level differential cross section.

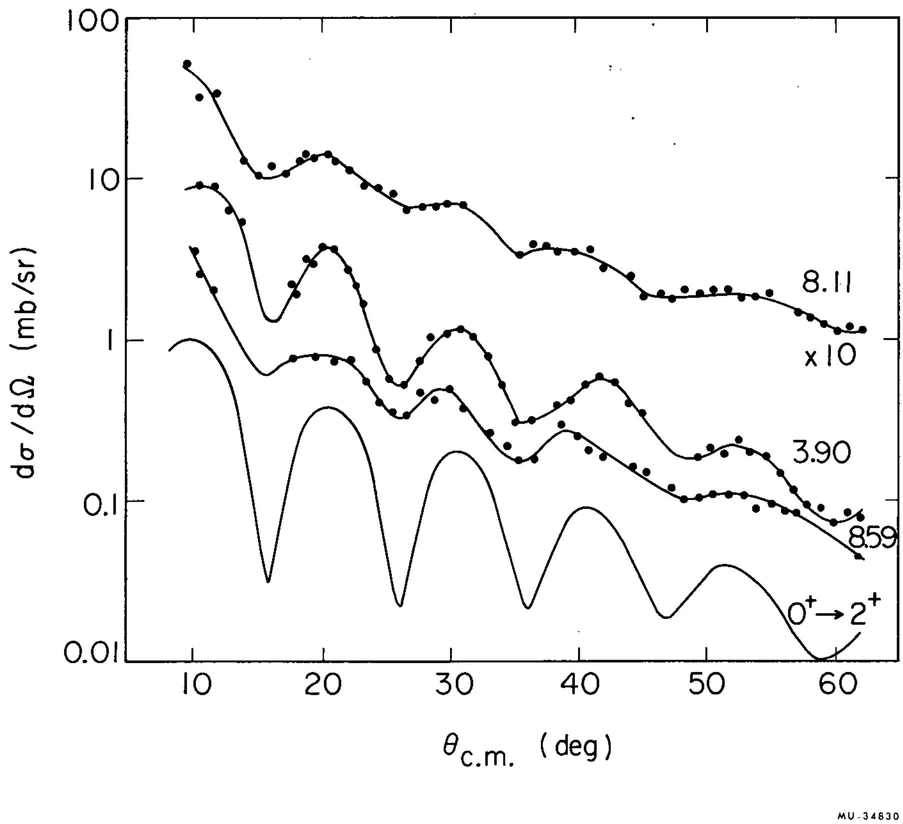

Fig. 11. Austern and Blair $\ell = 2$ unnormalized angular distribution and states with similar experimental differential cross sections.

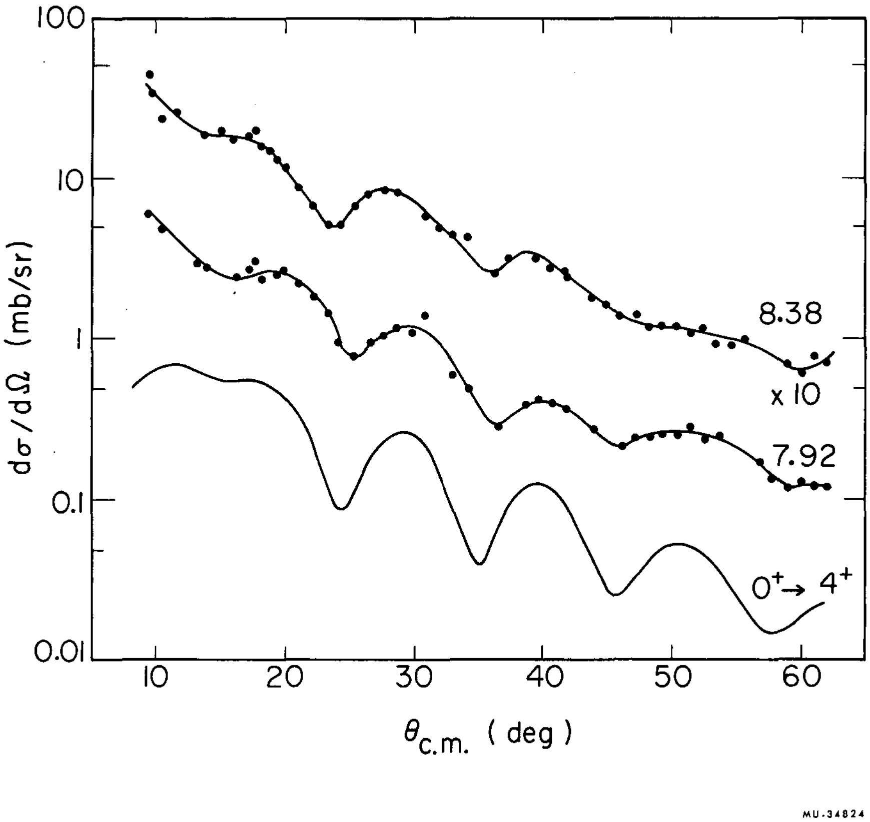

Fig. 12. Austern and Blair $\ell = 4$ unnormalized angular distribution and states with similar experimental differential cross section.

and background interference they appear to oscillate only feebly. Their phase corresponds to negative parity states. Corresponding peaks were seen in a 30 MeV inelastic scattering experiment[26] and were respectively reported as a negative parity and a 4+ level. The 4+ assignment is surprising since the gamma decay does not cascade through the 2+ level at 3.90 MeV, but occurs directly to the ground state.[14] The 6.94-MeV peak appears to be a doublet from its angular distribution. This is discussed in the last part of this section. A level or group of levels is consistently seen at 7.5 MeV but is too weak for further analysis. The 9.87-MeV doublet was identified only for purposes of energy scale calibration (see Sec. III-A).

Since the octupole states dominate the Ca^{40} energy spectra at most angles, 18^{o} lab which corresponds to a minimum in the angular distributions of octupole states and a maximum for the other types of vibrational excitation seen has been selected for Fig. 4. Two points of interest are the separation between the 3.73- and 3.90-MeV states which in other scattering experiments at equally high energies have not been resolved, and the low background up to 8 MeV excitation. This latter is due mainly to the elimination of slit scattering (see Sec. II-A).

2. Octupole Vibrations

The 3.73-MeV level of Ca^{40} is one of the examples picked by Lane and Pendlebury (see Sec. III-D) and so a direct comparison of $B(3 \rightarrow 0)/e^2$ can be made. Analyzing inelastic electron scattering data they obtain a value of 2.2×10^3 f^6 for the reduced-octupole-transition probability. This is the same as the value obtained from the present experiment. The rest of the reduced-transition probabilities obtained here are found in Table II.

The next apparent octupole vibration is the 5.90-MeV state. It is the only octupole state whose strength was found not to be enhanced. By inelastic scattering experiments at M.I.T. this level was assigned a spin and parity of 1-.[26] After careful study of their data it seems that this assignment is based on one small-angle point and may be incorrect.

Table II. Reduced-transition probabilities for de-excitation of Ca^{40} energy levels.

-Q value (MeV)	J^{π}	δ_J (fermis)	β_J[†]	$\frac{B(J\to 0)}{e^2}$[a] (fermis^{2J})	$\frac{B(J\to 0)_{sp}}{e^2}$[a] (fermis^{2J})	$\lvert\mu\rvert^2$
3.73	3-	0.85	0.19	2.2×10^3	1.9×10^2	11.4
3.90	2+	0.34	0.075	11.	12.	0.88
4.48	5-	0.35	0.077	2.1×10^6	8.7×10^4	24.
5.90	3-	0.18	0.040	10^2	1.9×10^2	0.52
6.28	3-	0.40	0.088	5.5×10^2	1.9×10^2	2.8
6.58	3-	0.31	0.069	4.2×10^2	1.9×10^2	2.2
6.94	2+	0.21	0.047	8.8	12.	0.74
	3-[b]	0.36	0.078	4.9×10^2	1.9×10^2	2.5
7.92	4+	0.29	0.064	1.4×10^4	3.7×10^3	3.8
8.11	2+	0.24	0.052	9.8	12.	0.82
8.38	4+	0.24	0.052	9.5×10^3	3.7×10^3	2.5
8.59	2+	0.19	0.041	7.7	12.	0.65

[†] Using R_o = 4.54f from electron scattering.[25]

[a] Reference 2.

[b] Though less likely a 1- assignment cannot be ruled out by our analysis.

Only a 3- assignment is consistent with the Austern and Blair model; compare Figs. 19 and 17.

The next octupole state (at 6.28 MeV), is enhanced by a factor of three. It has been seen by several other experimental groups and all agree that it is a 3- level.[3,7,16,26]

The state at 6.58 MeV is enhanced a factor of 2 and agrees well with the Austern and Blair angular distribution for $\ell = 3$. The M.I.T. group[26] agrees with this assignment.

There is one more state of probably octupole character, but it is a doublet and will be discussed separately.

3. Quadrupole Vibrations

Two higher energy 2+ states are found at 8.11 MeV and 8.59 MeV. Neither is enhanced, and the assignment of the one at 8.11 MeV agrees with Ref. 26. The other has not been previously seen. It must be stressed that the spin and parity assignments of the levels above 8 MeV are only tentative for two reasons. First, these levels are experimentally more difficult to separate both from each other and background. This causes the oscillations to be less pronounced and the distinctions between the $\ell = 2$ and $\ell = 4$ angular distributions to be less reliable. Secondly, at these high excitations there is less justification for ignoring double excitation. This is discussed in Sec. IV-A.1.

4. The 6.94-MeV State

The 6.94-MeV state is strongly excited and has been observed in numerous experiments.[3,7,26,27,28] There is wide confusion concerning its spin and parity. It has variously been reported as a 3-,[7] 3- and 2+ doublet,[3] 2+,[28] 1-,[26] and 2+ or possibly a 2+,3- doublet.[27] Part of the confusion stems from the fact that there is also a state at 7.1 MeV which is not resolved from the 6.94-MeV doublet in most of these experiments.

Figure 13 compares the present experimental differential cross section for the 6.94-MeV peak with Austern and Blair angular distributions for a 1-,2+ doublet in the upper curve, and a 3-,2+ doublet in the lower curve. The relative strength of the negative parity state to positive

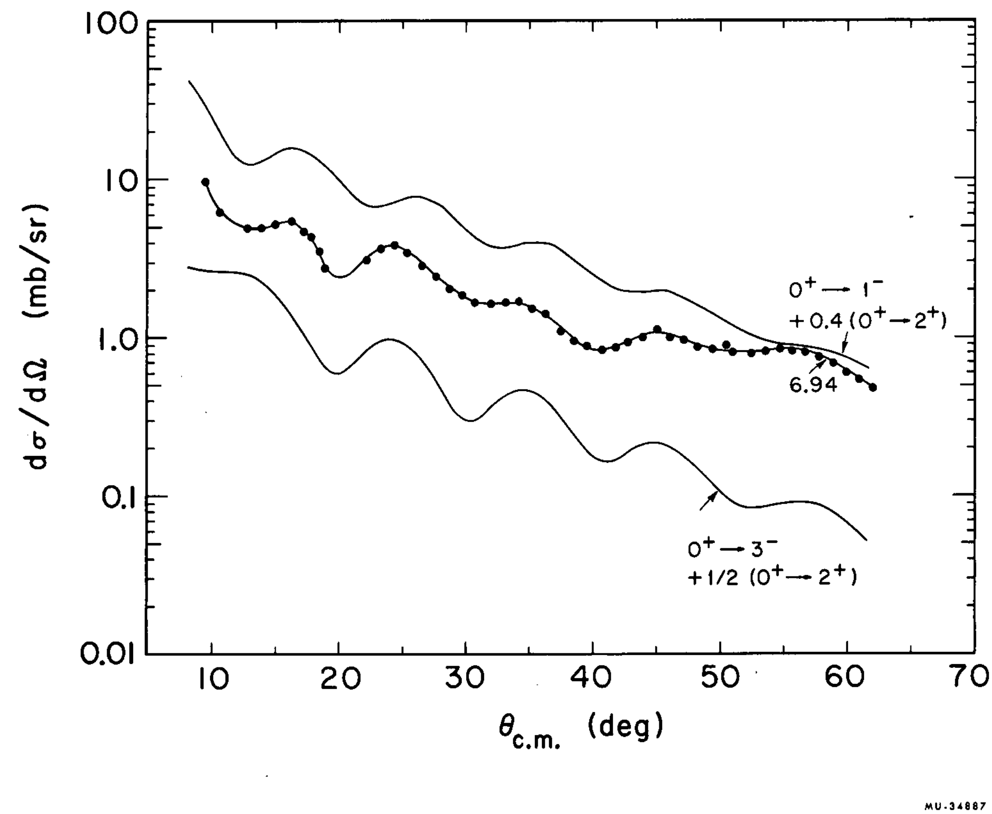

Fig. 13. The Ca^{40} 6.94-MeV state experimental differential cross section compared with two Austern and Blair angular distributions for a doublet. The upper curve is a sum of (0+ → 1−) and (0+ → 2+) in the ratio of 5 to 2. The lower curve is a sum of (0+ → 3−) and (0+ → 2+) in the ratio of 2 to 1. Except for a few small angle points the lower curve is more in phase with the experimental curve.

parity state is about 2:1 in each case. Except for a few small-angle points a 3-,2+ doublet seems more consistent with the experimental phase. This would indicate agreement with the inelastic electron scattering work.[3] The 7.1-MeV state is only weakly seen, and the differential cross section for its excitation was not obtained.

B. Neon-20

1. General

Considerable evidence for rotational band structure in Ne^{20} has been obtained through a comprehensive set of experiments by the Chalk River group.[29] The energy levels will be discussed one band at a time.

2. Ground-State Rotational Band

The 2+ member of this band is strongly excited at 1.63 MeV. Its phase is close to that expected for single excitation; however, addition of a double excitation contribution improves the fit. The sign of the deformation can be determined in this way and is positive, corresponding to a prolate shape as expected. The 4+ member of this band at 4.25 MeV is excited more weakly by an order of magnitude. Its phase is shifted noticeably from that expected for single excitation with an angular momentum transfer of 4. The best fit is obtained by a double excitation to single excitation ratio of 2. This behavior of strongly exciting the 2+ by a one-step process and the 4+ by primarily a two-step process is analogous to multiple Coulomb excitation by successive E2's. In fact the magnitude of the double excitation contribution agrees well with the value predicted from the strength of the single excitation to the 2+ (see Table III. The angular distributions are shown in Fig. 14.

3. Negative-Parity Octupole Vibrational Bands

The lowest band of this nature has K=2; its first member is the 2- level at 4.97 MeV. It is very weakly excited and no oscillations are observed in its differential cross section.

Table III. Ground state rotational band single and double excitation information.

-Q value	I^{π}	$C_1(I)$	δ_I	$C_2(I)$	$C_2'(I)$
1.63 MeV	2+	0.75	1.72	0.30	0.23
4.25 MeV	4+	0.12	0.36	0.25	0.23

$C_1(I)$ and $C_2(I)$ are extracted from the experimental cross sections by the Austern and Blair model as described in the text. $\delta_I = C_1(I)\sqrt{2I+1}$ is the deformation length. $C_2'(I)$ is the double excitation matrix element calculated from the strength of the 0+ → 2+ quadrupole excitation by the relationship

$$C_2(I) = \frac{1}{\sqrt{4\pi}} \langle 2I00|20\rangle^2 \delta_2^{\,2}.$$

The agreement between $C_2(I)$ and $C_2'(I)$ is consistent with the rotational model.

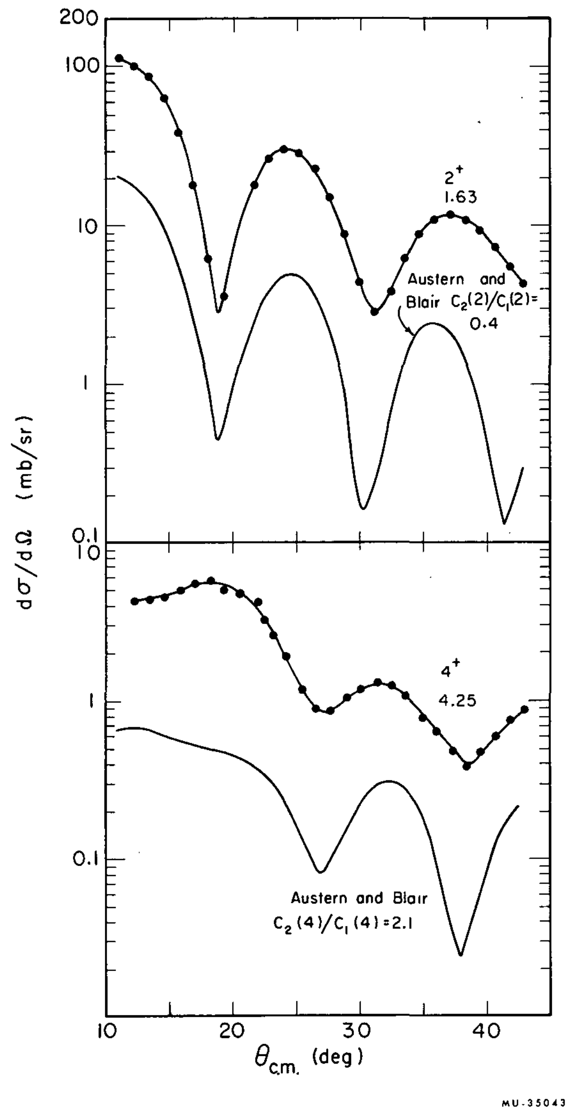

Fig. 14. Ground state band 2+ and 4+ experimental and theoretical angular distributions in Ne^{20}.

The 3- level at 5.63 MeV is the second member of the band and fit is enhanced 6 times over single particle estimates. Its differential cross section indicates a single step $\ell = 3$ excitation. The other members of the band are not seen. This is in qualitative agreement with the idea that the band is based on an octupole vibration, since the 3- is the only member of the band which can be excited by a direct octupole excitation.

The next band based on octupole vibrations has a K-projection of zero so only the odd members of the band are allowed. The 1- level at 5.80 MeV is weakly excited, an order of magnitude weaker than the 3- level at 7.17 MeV. The phase of its angular distribution is consistent with a two-step process analogous to Coulomb excitation by E3 to the 3- level followed by an E2 excitation down to the 1- level. The 3- level at 7.17 MeV is enhancee approximately as much as the 3- in the K=2 band. Again, comparing the differential cross sections for exciting this state with the Austern and Blair $\ell = 3$ angular distribtuion a single-step angular-momentum transfer of three is indicated. In this case, however, there is a slight shift in phase of 1° to 2° relative to both the 3- at 5.63 MeV and the calculated angular distribution for angular momentum transfers of three. The differential cross sections for the two 3- states and the 1- are compared with the corresponding single excitation angular distributions in Fig. 15. Reduced transition probabilities for states excited by single excitation are found in Table IV.

4. Possible Higher-Energy Rotational Bands

Two additional K=0 bands have been suggested. The lower one consists of a 0+ level at 6.71 MeV, a 2+ level at 7.43 MeV, and a 4+ level at 9.04 MeV. The differential cross section for excitation of the 0+ level is out of phase with a direct monopole excitation and is approximately the same strength as the second-order excitation of the ground-state rotational band 4+ level. The 2+ level which under ordinary circumstances would be enhanced (especially if this band were based on a quadrupole vibration), is made slightly weaker than the 0+ level and its phase also corresponds to double excitation.

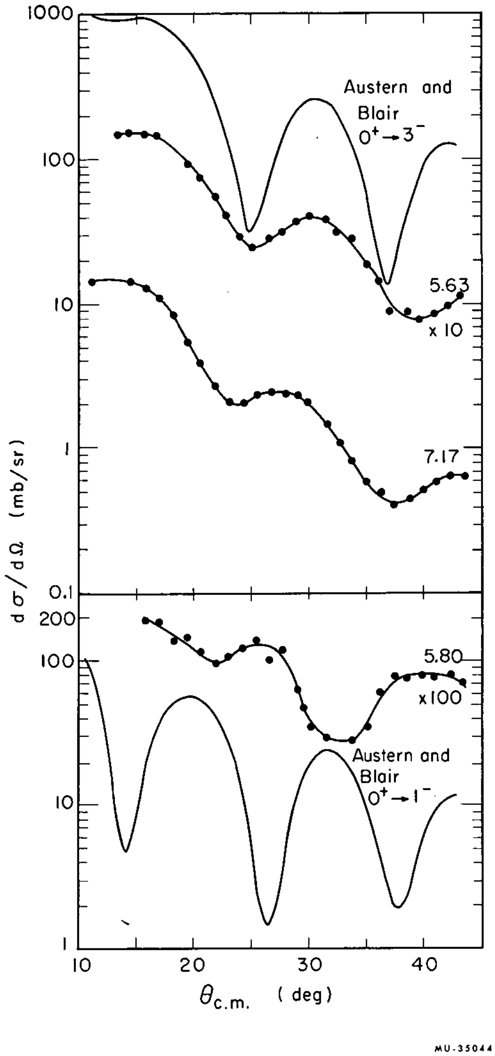

Fig. 15. Comparison of the 1- and 3- levels of the K=0 and K=2 bands in Ne^{20} with angular distribution expected for single excitation.

Table IV. Reduced transition probabilities for de-excitation of Ne^{20} energy levels.

-Q value (MeV)	J^{π}	δ_J (fermis)	β_J (fermis)	$\frac{B(J \to 0)\text{Lane}}{e^2}$ (fermis^{2J})	$\frac{B(J \to 0)_{sp}\text{Lane}}{e^2}$ (fermis^{2J})	$\|\mu\|^2$
1.63	2+	1.72	.48	53.	5.9	9.0
4.25	4+	.36	.10	6.3×10^3	1.1×10^3	5.6
5.63	3-	.84	.23	4.5×10^2	1.2×10^2	6.2
7.17	3-	.84	.23	4.5×10^2	1.2×10^2	6.2

Only the 2+ level at 7.85 MeV of the remaining band based on the 0+ level at 7.17 MeV is excited. It is made as weakly as the 2+ level at 7.43 MeV. However, this time it is in phase with the single excitation Austern and Blair $\ell = 2$ angular distribution.

V. AUSTERN AND BLAIR MODEL

The Austern and Blair model and other adiabatic models are fully described in Ref. 5, only a brief summary will be presented here. Special emphasis will be placed on the details of the calculation and the computer code developed to obtain the information inherent in elastic scattering and then used by the same code in calculating inelastic angular distributions.

A. Previous Models

A brief review of advantages and disadvantages of the earlier Fraunhofer model,[5,30,31,32] may be of use in understanding the new model. In the Fraunhofer model closed forms for the inelastic angular distributions are obtained. They have the general characteristics of the observed experimental differential cross sections except that the envelope of the experimental differential cross sections is much steeper. In spite of the simplicity of this model the differences in small-angle behavior of the angular distributions which distinguish excitations of different angular-momentum transfer are already present. The main drawbacks in using it as a spectroscopic tool are that the reduced-transition probabilities obtained from this model depend on which maximum of the angular distribution is used in normalization, and its lack of any consideration of Coulomb effects, which limits its use for low-energy or heavy nuclei.

Blair, Sharp, and Wilets[33] next developed a smooth cut-off model for monopole and quadrupole excitation that gives the same envelope as the experimental cross sections. There are also two drawbacks to this model. It cannot be used for higher multipole excitations, and Coulomb effects are still not treated.

B. The Austern and Blair Model

These last two handicaps are removed in the Austern and Blair model.[5] More sophisticated analyses can be obtained by DWBA or coupled-channel calculations, but for spectroscopic purposes the Austern and Blair model is easily used and appears to be sufficient when collective wave functions adequately describe the nuclear state.

A description of this model must start with the extended optical model. Let us consider an extended optical potential including some dynamic variables of the target nucleus, specifically internal dynamic variables closely related to the ordinary parameters of the elastic optical potential. This extended potential is an operator which connects the incident channel with reaction channels. The transition matrix elements involving this operator, by suitable approximations, may be related to derivatives of elastic scattering matrix elements with respect to these parameters. If h is one of the parameters in the elastic optical potential and we increase it by α, where α is an operator acting on the nuclear coordinates, then the extended optical potential is

$$U(h+\alpha,\vec{r}) = U(h,\vec{r}) + \Delta U(h,\alpha,\vec{r}) \tag{23}$$

and ΔU is responsible for transitions to other channels. The increment ΔU may be expanded in a Taylor series in α

$$\Delta U = \alpha \frac{\partial U}{\partial h} + \frac{1}{2!} \alpha^2 \frac{\partial U}{\partial h^2} + \ldots$$

In this thesis h is defined as a suitable nuclear radius and $\alpha(\Omega)$ is the displacement corresponding to shape oscillations of the nuclear surface in the direction of the radius vector $\Omega = (\theta,\psi)$ in the space fixed system. Expanded in multipoles

$$\alpha = \sum_{L,M} \xi_{L,M} Y_L^{M*}(\Omega) \tag{24}$$

The operators $\xi_{L,M}$ are spin-independent. The adiabatic transition amplitude

T_{ba} for inelastic scattering from initial nuclear state $|a\rangle$ to final nuclear state $\langle b|$ is to first order in α

$$T_{ba} = \langle b|\chi^{(-)}(\vec{K}_b,\vec{r}_1)|\alpha \frac{\partial U}{\partial h}|\chi^{(+)}(\vec{K}_a,\vec{r}_2)\rangle|a\rangle . \quad (25)$$

[40]

The distorted wave $\chi^{(+)}$ is the exact solution for the scattering with potential U_o and the boundary condition that at large radii the solution approaches a plane wave plus an outgoing spherical wave. $\chi^{(-)}$ is the time reversed solution related to $\chi^{(+)}$ by the equation

$$\chi^{(-)*}(\vec{k},\vec{r}) = \chi^{(+)}(-\vec{k},\vec{r}) .$$

These distorted waves may be then expanded in spherical harmonics

$$\chi^{+}(\vec{k}_a,\vec{r}) = \frac{(4\pi)^{1/2}}{k_a r} \sum_{\ell=0}^{\infty} i^{\ell}(2\ell+1)^{1/2} e^{i\sigma\ell} f_{\ell}(k_a r) Y_{\ell}^{o}(\Omega) \quad (26)$$

$$\chi^{(-)}(\vec{k}_b,\vec{r}) = \frac{4\pi}{k_b r} \sum_{\ell'=0}^{\infty} \sum_{m'=-\ell'}^{+\ell'} i^{-\ell'} e^{i\sigma\ell'} f_{\ell'}(k_b,r) Y_{\ell'}^{m'}(\theta,0) Y_{\ell'}^{m'*}(\Omega) \quad (27)$$

The Coulomb phase shifts σ_{ℓ} are given by

$$\sigma_{\ell} = \arg\Gamma(\ell + 1 + i\eta) \quad (28)$$

where η is the Coulomb parameter

$$\eta = \frac{Z'Z'e^2}{\hbar v}$$

and v is the velocity of the incident particle.

Equations (26) and (27) assume their particularly simple form due to the choice of coordinate system shown in Fig. 16

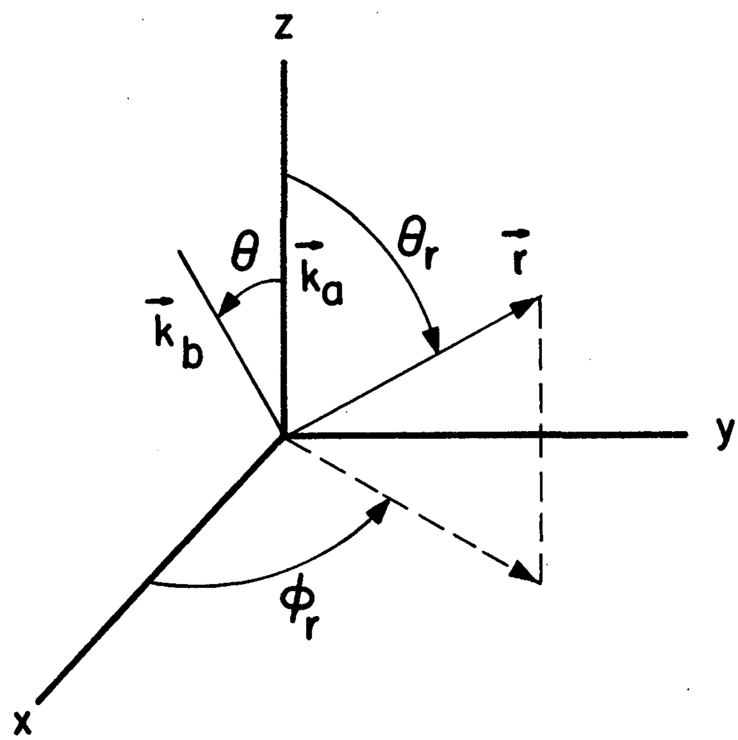

MU-35657

Fig. 16. Coordinate system chosen for the numerical calculation.

The z-axis or axis of quantization is taken in the $\vec{k}_a$ direction and the x-axis is taken in the scattering or $\vec{k}_a, \vec{k}_b$ plane. The angle between $\vec{k}_a$ and $\vec{k}_b$ is θ, the scattering angle in the center of mass system.

The regular radial functions are normalized so that

$$\lim_{r\to\infty} f_\ell = \frac{i}{2}(H_\ell^* - \eta_\ell H_\ell) \ . \tag{29}$$

This can also be considered the definition of η_ℓ. By substitution of Eqs. (1) and (4) into Eq. (2) and by performing the angular integration, Eq. (3) results. Since k_a equals k_b in the adiabatic approximation the subscripts have been dropped.

$$T_{IM_I;00} = \frac{4\pi}{k^2}(2I+1)^{1/2} \sum_{\ell\ell'} i^{\ell-\ell'}(2\ell'+1)^{1/2} e^{i(\sigma_\ell+\sigma_{\ell'})} \tag{30}$$

$$\times \ \langle \ell' I,00|\ell,0\rangle\langle \ell' I,-M_I,M_I|\ell,0\rangle \ Y_{\ell'}^{-M_I}(\theta,0)$$

$$\times \ C_1(I)\int_0^\infty f_{\ell'}(kr)\,\frac{\partial U}{\partial h}\, f_\ell(kr)dr \ .$$

This equations has been specialized for a final state having angular momentum I and z-projection M_I and an initial state of zero angular momentum. For this case the matrix element of α^n can be written as

$$\langle b(I,M_I)|\alpha^n|a(00)\rangle = C_n(I)Y_I^{M_I*}(\Omega) \tag{31}$$

When $\ell'=\ell$ the following relationship[40] is an identity

$$\int_0^\infty f_\ell\,\frac{\partial U}{\partial h}\, f_\ell dr = \frac{iE}{2k}\,\frac{\partial \eta_\ell}{\partial h} \ .$$

Austern and Blair introduce the approximation: when $\ell' \neq \ell$,

$$\int_0^\infty f_{\ell'} \frac{\partial U}{\partial h} f_\ell dr \cong \int_0^\infty f_{\bar{\ell}} \frac{\partial U}{\partial h} f_{\bar{\ell}} dr = \frac{iE}{2k} \frac{\partial \eta_{\bar{\ell}}}{\partial h} \tag{32}$$

where $\bar{\ell} = \frac{\ell+\ell'}{2}$.

Introducing this approximation in Eq. (3) the scattering amplitude $f_{IM_I;00}$ is given by

$$f_{IM_I;00} = -\frac{k^2}{4\pi E} T_{IM_I;00} .$$

Substituting from Eq. (30):

$$f_{IM_I;00} = \frac{-i}{2k} (2I+1)^{1/2} C_1(I) \sum_{\ell\ell'} i^{\ell-\ell'} (2\ell'+1)^{1/2} e^{i(\sigma_\ell+\sigma_{\ell'})}$$
$$\times \langle \ell' I,00|\ell 0\rangle \langle \ell' I,-M_I M_I|\ell 0\rangle Y_{\ell'}^{-M_I}(\theta,0) \frac{\partial \eta_{\bar{\ell}}}{\partial h} . \tag{33}$$

Explicit numerical calculation of the η_ℓ can largely be dispensed with when considering the elastic scattering of strongly-absorbed particles. The parameterization

$$\eta_\ell = \epsilon + B\Delta \frac{\partial \epsilon}{\partial \ell} + i \left(A\Delta \frac{\partial \epsilon}{\partial \ell} + D\Delta \frac{\partial^2 \epsilon}{\partial \ell^2}\right)$$
$$\epsilon = (1 + e^{(L-\ell)/\Delta})^{-1} \tag{34}$$

is adequate for good fits to the elastic scattering data. The parameters are determined by a search program described in the Appendix. Fits to the Ca^{40} and Ne^{20} elastic angular distributions are shown in Figs. 17 and 18.

Two further assumptions are needed to relate the parameterized η_ℓ to the form derived for the scattering amplitude in Eq. (33). Both are

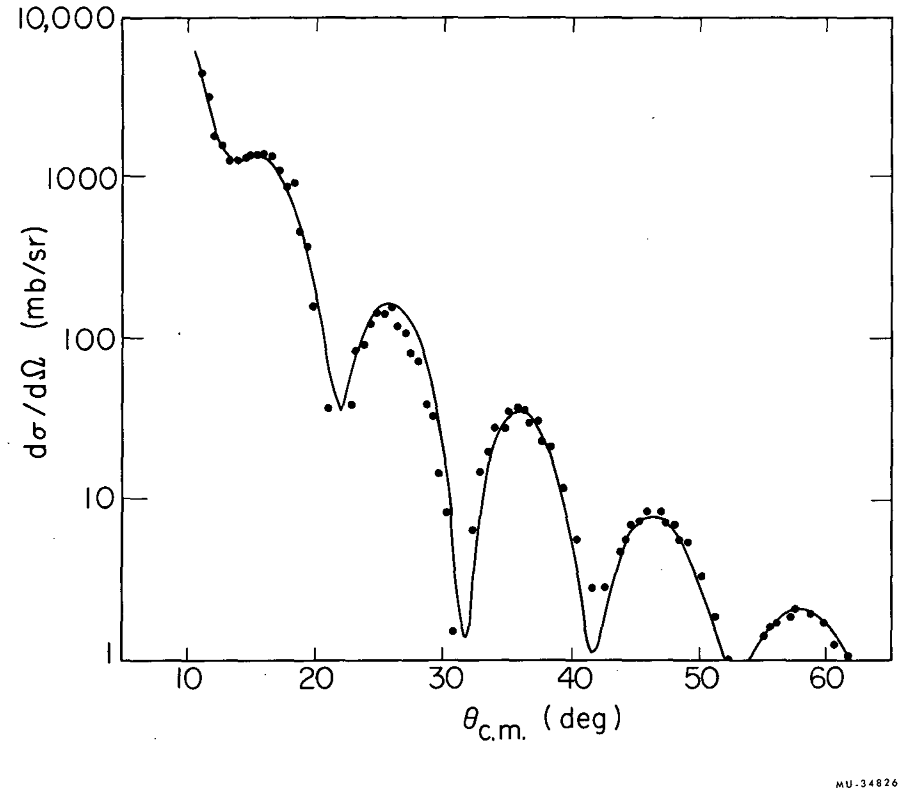

Fig. 17. Parametrized phase shift fit to Ca^{40} elastic differential cross section with the parameters; L = 16.7; Δ = 1.15; A = 0.66; B = 1.51; D = -1.92. The parameters are described in the text.

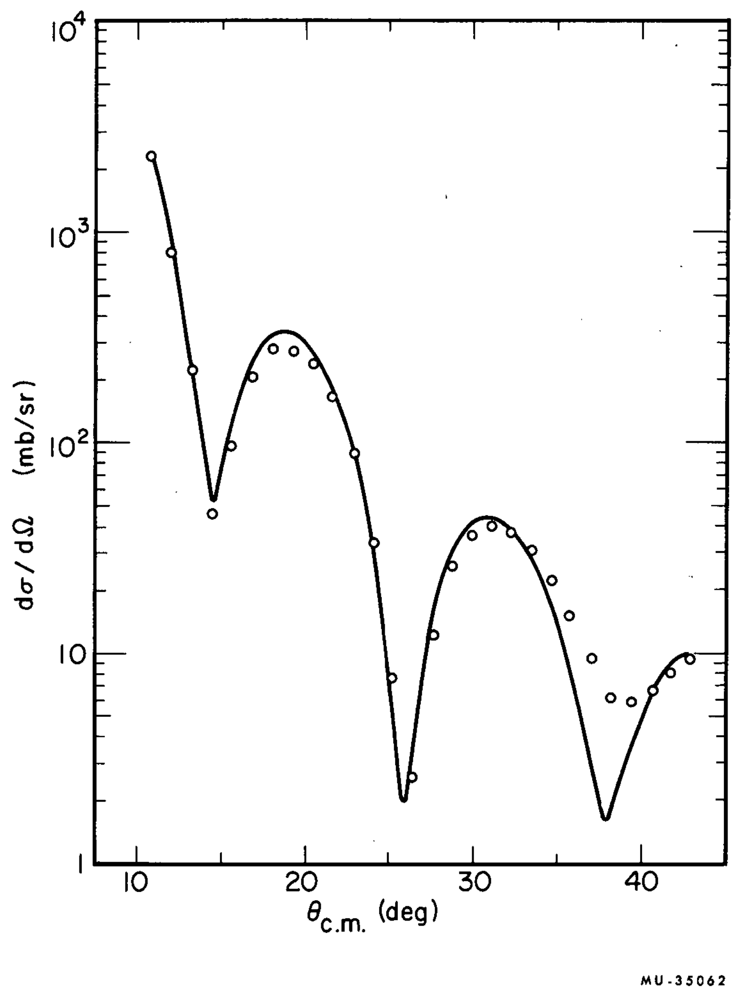

Fig. 18. Parametrized phase shift fit to Ne^{20} elastic differential cross section with the parameters; L = 15.9; Δ = 1.61; A = 1.07; B = 1.05; D = -1.22. The parameters are described in the text.

best for strong absorption. First, we assume that η_ℓ is a function only of the difference $(\ell-\ell_o)$, where ℓ_o is the critical angular momentum, and ℓ_o contains all the dependence on h. The quantity ℓ_o can be defined somewhat arbitrarily by requiring that $|\eta_{\ell_o}|$ should equal 1/2. Associated with this ℓ_o is a "cutoff radius R_o" through the relationship

$$E = \frac{ZZ'e^2}{R_o} + \frac{\hbar^2 \ell_o(\ell_o+1)}{2\mu R_o^2} \quad . \tag{35}$$

The second assumption is that R_o has the following simple relationship to the optical potential radius parameter h

$$\frac{dR_o}{dh} = 1$$

In this case

$$\frac{\partial \eta_{\overline{\ell}}}{\partial h} = \left[\frac{\partial \eta_\ell(\overline{\ell}-\ell_o)}{\partial \ell_o}\right]\left[\frac{d\ell_o}{dR_o}\right] \tag{36}$$

and since at reasonably high energies

$$\frac{d\ell_o}{dR_o} \cong k$$

$$\frac{\partial \eta_{\overline{\ell}}}{\partial h} \cong + k \frac{\partial \eta_{\overline{\ell}}}{\partial \ell_o} \tag{37}$$

In the Austern and Blair paper the derivative of η_ℓ is actually taken with respect to $\overline{\ell}$ which simply reverses the sign of the derivative. It follows that

$$f_{IM;00} = + \frac{i}{2} (2I+1)^{1/2} \hat{C}_1(I) \sum_{\ell\ell'} i^{\ell-\ell'} (2\ell'+1)^{1/2} e^{i(\sigma_\ell+\sigma_{\ell'})}$$

$$\langle \ell' I, 00 | \ell 0 \rangle \langle \ell' I - M_I M_I | \ell 0 \rangle Y_{\ell'}^{-M_I}(\theta, 0) \left[\frac{\partial \eta_{\bar{\ell}}}{\partial \bar{\ell}} \right] \quad (38)$$

In Fig. 19 angular distributions for angular momentum transfers of zero through five are shown with the first regular oscillation.

C. Double Excitation

For some levels in Ne^{20}, for example the 4+ level at 4.248 MeV which is a member of a rotational band built on the 0+ ground state, it would not be expected that a model which is first order in the nuclear deformation would even approximately describe the transition amplitude. It is experimentally observed that the differential cross section for excitation of the 4+ level is out of phase with the calculated single phonon 2^4th pole angular distribution. Austern and Blair have also extended their model to higher orders in the nuclear deformation.[5] Only second order will be considered here. A summary of the new approximations introduced by them is now given.

The exact expression for the double-excitation transition amplitude in the extended optical model is

$$T_{ba}(2) = \langle b(\xi_1) | \langle X^{(-)}(\vec{k}_b, \vec{r}_1) \left\{ \frac{1}{2} \frac{\partial^2 U(r_1)}{\vec{h}^2} \alpha^2(r_1, \xi_1) \delta(\vec{r}_1 - \vec{r}_2) \delta(\xi_1 - \xi_2) \right.$$

$$\left. + \frac{\partial U(r_1)}{\partial \vec{h}} \alpha(r_1, \xi_1) G_1(\vec{r}_1, \vec{r}_2, \xi_1, \xi_2) \frac{\partial U(r_1)}{\partial \vec{h}} \alpha(r_2, \xi_2) \right\} \left| X^{(+)}_{(\vec{k}_a, \vec{r}_1)} \right\rangle | a(\xi_2) \rangle . \quad (39)$$

Here G_1 is the exact Green's function for the problem with only the spherical potential $U(\vec{r}_1, R_0)$. G_1 satisfies the differential equation

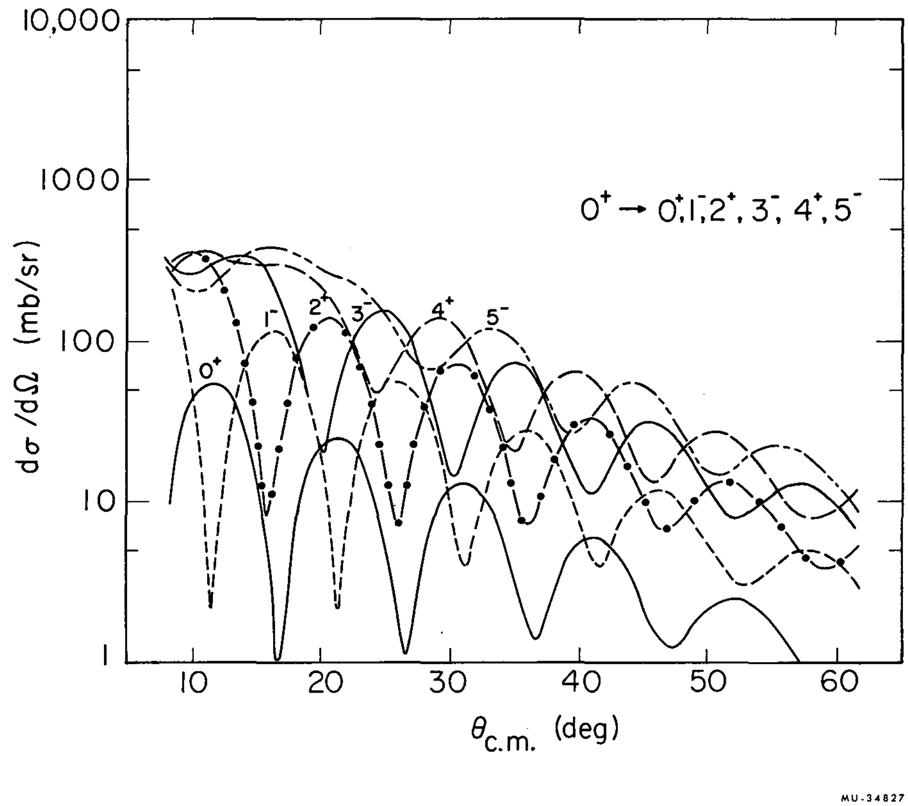

Fig. 19. Austern and Blair model angular distributions calculated with parameters determined from the Ca^{40} elastic differential cross section in Fig. 3. Transitions 0+ → 0+ through 5- are plotted with the first maximum of the regular oscillations indicated on each curve. From a spectroscopic standpoint this differentiates the different angular momentum transfers.

$$[E - K_1 - U(\vec{r}_1,R_0) - H(\xi_1) \quad G_0 = \delta(\vec{r}_1-\vec{r}_2)\delta(\xi_1-\xi_2) \qquad (40)$$

where K is the kinetic energy and $H(\xi)$ is the nuclear collective Hamiltonian.

The first approximation is to due the adiabatic Green's function in which $H(\xi)$ is absent.

The second approximation is to assume that $\alpha(\vec{r})$ commutes with this Green's function.

From this Austern and Blair arrive at the relationship

$$T^{(2)}_{I,M_I;00} = \frac{1}{2}\,\frac{C_2(I)}{C_1(I)}\,\frac{\partial}{\partial h}\,T^{(1)}_{I,M_I;00} \,. \qquad (41)$$

Following the further simplifications of Sec. V-C, the equation for double excitation corresponding to Eq. (33) has $C_1(I)\ \partial\eta_\ell/\partial\ell$ replaced by $-C_2(I)\ k/2\ \ \partial\eta_\ell/\partial\ell$.

Thus the double excitation can be affected in two ways: 1) Through the second-order term $\partial^2U/\partial h^2$ in the expansion of the nuclear deformation. This is a direct two-phonon (D2P) transition. 2) Through the first-order term $\partial U/\partial h$ acting twice. This corresponds to a multiple two-phonon (M2P) transition in which the alpha particle first excites the one-phonon 2+ level and subsequently excites a second quadrupole phonon. The ratio of D2P to M2P excitation is determined by the strength of the quadrupole phonon. If the two-phonon level is contaminated by an admixture with a single 2^4th-pole phonon, then direct one-phonon excitation (D1P) is possible. The ratio of $C_2(I)/C_1(I)$ determines the ratio of amplitudes (M2P + D2P)/D1P.

In the coupled-channel calculations of Buck[34] the D2P and M2P excitations were also considered. However, the experimental angular distribution for excitation of the 4+ two-phonon level of Ni^{58} could not be matched without arbitrarily increasing the amplitude of the D2P excitation by a factor of 1.5 to allow for the possibility of some direct excitation through a single-phonon admixture in the wave function (D1P excitation).

The angular distributions calculated for (M2P + D2P) excitation alone have nearly the correct phase but their slope actually rises with angle in comparison to experimental data (see Fig. 20). At this point Professor Blair in a private communication suggested coherently mixing one- and two-phonon excitation, varying the $R_c = C_2(I)/C_1(I)$ to obtain the closest agreement with experiment. The results are not wholly satisfactory, however, since it is not possible to obtain the best phase and the best slope with the same value of R_c. In fact the experimental slope in the range of 10 to 40°C.M. is halfway between the pure single phonon excitation and the single-double phonon mixture which gives the best phase as shown in Fig. 14. However, it should be emphasized that while quantitative agreement does not seem possible, the results of this model do qualitatively agree with experiment. In the nickel region the differential cross section for excitation of the first 4+ level has been studied as a function of energy.[35] It was found that at low energies (33 MeV) the angular distribution corresponded to single-phonon excitation and there was a gradual change of phase until at high energies (100 MeV) double excitation appeared to completely dominate. This variation with energy follows naturally from the Austern and Blair form. The radial integral is replaced by

$$\frac{iE}{2} \; C_1(I) \; \frac{\partial \eta_\ell}{\partial \ell} - \frac{k}{2} \; C_2(I) \; \frac{\partial^2 \eta_\ell}{\partial \ell^2}$$

where the double phonon term has an extra factor of k, so its importance will increase with increasing energy.

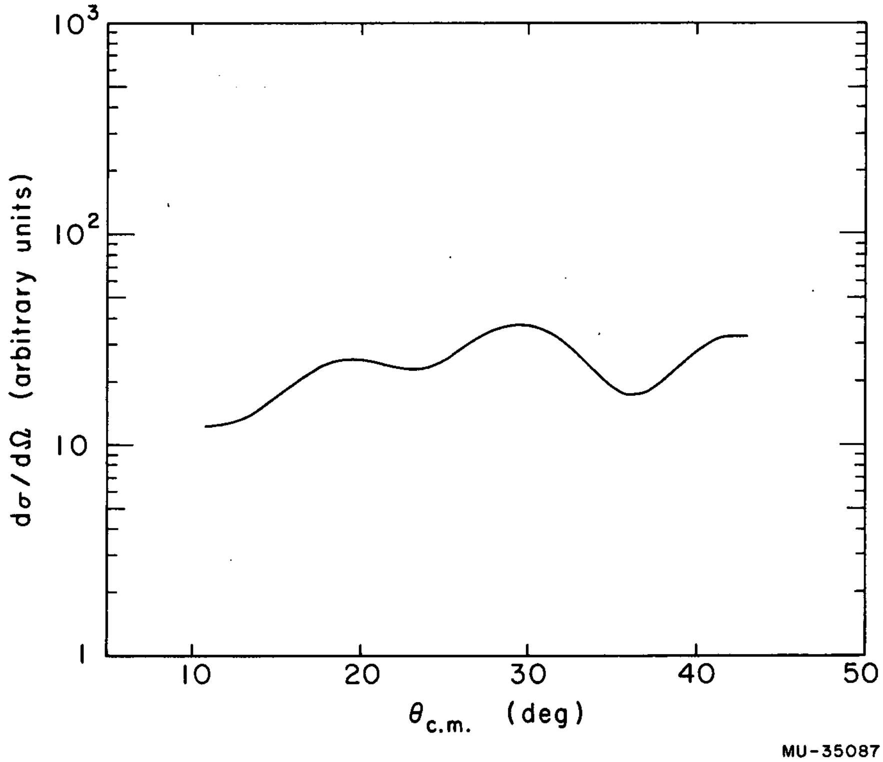

Fig. 20. Neon-20 pure double excitation.

VI. CONCLUSIONS

At the present time inelastic alpha scattering remains most useful in investigating those nuclei which have relatively well separated energy levels. An energy gap after the ground state is especially helpful since elastic scattering is so dominant that low-lying levels are often obscured by the tail of the elastic peak. It is this region where Coulomb excitation has provided the most information. On the other hand, in the lightest nuclei the pronounced regular oscillations of the scattering cross sections characteristic of surface reactions are no longer observed. For these reasons the even-even nuclei between mass number 20 and 40 would seem to offer especially rewarding targets for simple analysis of alpha-particle scattering. Neon-20 and calcium-40 bracket this region both in mass and in properties. Neon-20 appears to show a highly developed set of positive and negative rotational bands reminiscent of U^{238}. Calcium-40 is a doubly-closed magic nucleus and quite resistant to quadrupole deformations. A softness to enhanced octupole vibrations is, however, observed and to a lesser degree 2^4- and 2^5-pole vibrations. The doubly-closed shells besides providing an energy gap of over 3 MeV also seem to be responsible for the success of single-phonon mode of the Austern-Blair model for all levels investigated.

Our investigation of Ne^{20} is consistent with the rotation picture of Ne^{20}, and the similarities of Coulomb excitation on U^{238} and inelastic scattering on Ne^{20} are pointed out in Fig. 21.

Our investigation of Ca^{40} is consistent with the vibrational model. The quadrupole vibrations are weakened and raised in energy as would be expected in a doubly-magic nucleus, however, the octupole and higher multipole vibrations are at their normal strength and excitation energy.

The Austern and Blair model proved to be most useful for Ca^{40} where quantitative agreement was found and reduced transition probabilities were obtained that agree well with other measurements. All experimental differential cross sections corresponding to the same angular

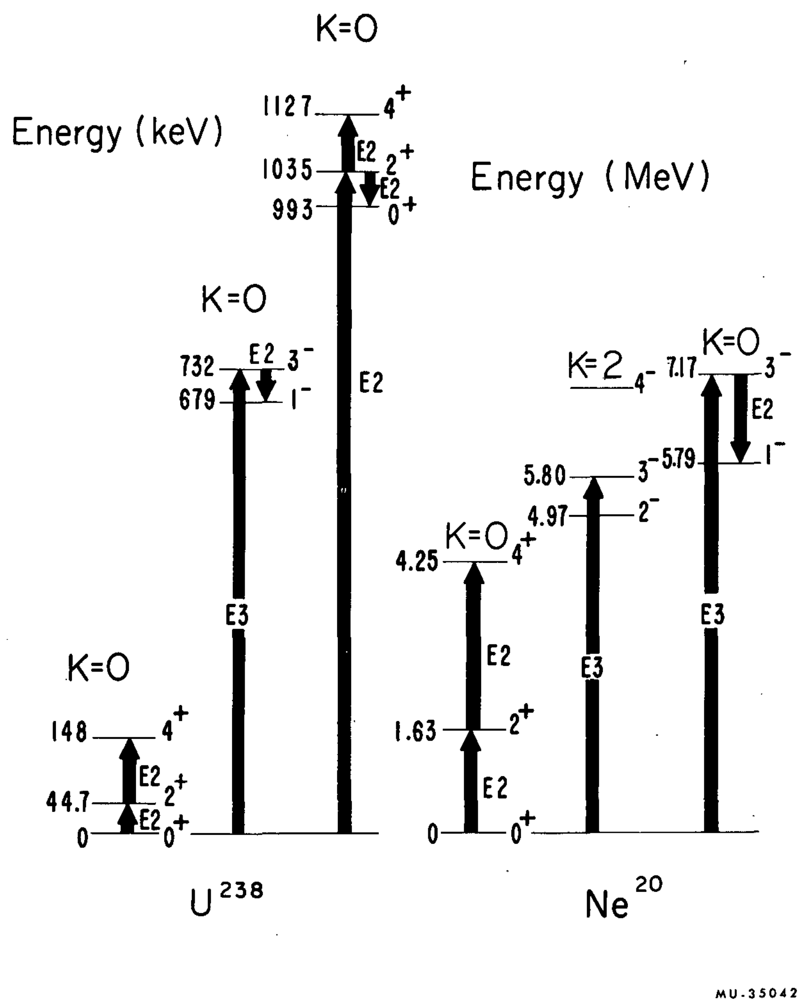

Fig. 21. Comparison of excitation of Ne^{20} by inelastic alpha scattering and U^{238} by Coulomb excitation.

momentum transfer have approximately the same shape as required by the model and can be seen in Figs. 9-12. Therefore, from a spectroscopic standpoint it does not appear that the more complicated calculations are worthwhile when the single-phonon model is applicable.

For the states in Ne^{20} which are reached by single-step processes quantitative agreement also was found and reduced-transition probabilities were obtained. For those states in Ne^{20} which are reached by two-step processes only qualitative agreement was found. However, just the information that a process is primarily single or double excitation can be quite useful in testing the applicability of nuclear models e.g., the rotational model in this case.

ACKNOWLEDGMENTS

I am indebted to all those associated with the 88-in. cyclotron whose pleasant and interesting conversations made my stay at Berkeley more enjoyable

and specifically

Dr. Bernard G. Harvey, my research advisor, for suggesting this experiment and for always being there when really needed;

Professor J. S. Blair for his frequent letters and discussions;

Mr. Pierre Darriulat for his help in my understanding the analysis of the experimental data;

Mr. Chi Chang Lu, Mr. Nolan F. Mangelson, and Professor Ernest J.-M. Rivet for their aid in the actual experiments;

Dr. John R. Meriwether for his supervision of the improvements in the scattering chamber and related equipment which greatly increased the accuracy and ease of making many measurements;

Dr. Andre Bussiere de Nercy, Dr. Homer E. Conzett, Dr. Richard H. Pehl, and Dr. H. G. Pugh for their insight into many of the problems which troubled me;

Mr. Frederick S. Goulding and Mr. Donald A. Landis for the electronic system and counters which made these experiments possible;

Professor Joseph Cerny III, Dr. Norman K. Glendenning, Dr. Daniel J. Horen, Dr. W. Barclay Jones, and Dr. Rudolpho J. Slobodrian for their enlightening discussions;

Mr. Gilbert Butler, Mr. Donald G. Fleming, Mr. Creve C. Maples, Miss Mary Reed, and Mr. Edward Shield for conversations about those topics graduate students always discuss;

Mr. Claude E. Ellsworth and Mr. Jack H. Elliott for information and aid on such varied topics as targets and detectors;

Mrs. Jolley Breckenridge, Miss. Jeannette Mahoney, Mrs. Ruth-Mary Larimer for that special feminine touch that added some cheer to a few otherwise dark days;

The 88-in. cyclotron crew in general and specifically Mr. Gary DeHaven whose company during the owl shifts was greatly appreciated and Mr. Eugene

Russell who (during the day), always seemed able to keep the beam Gary had found that morning;

And finally to those, some of whom never saw the 88-in. cyclotron or Berkeley; my dear family and friends, to mention only a few: Judy Hamermesh, Sherie and Mike Stein, and Barbara and Zev Steiger whose moral support made the long way to this degree less frightening.

This work was performed under the auspices of the A. U. Atomic Energy Commission.

APPENDIX

A. Computer Codes

1. LYCURGUS

The relativistic kinematics program mentioned in Sec. III-A is based on the formalism of a standard text.[36] It generates tables of the following two-body kinematic data; energy of scattered particle and recoil, center-of-mass angle of the scattered particle, and lab angle of the recoil, and the jacobian $d\cos\theta/d\cos\theta'$.

2. VARMIT

Many problems of analysis in experimental physics can be reduced to finding the minimum in a function of many linear or non-linear variables.

Extracting parameters from a model by comparison with data (Sec. V-B), unfolding of not fully resolved peaks in a spectrum (Sec. III-A), and generation of calibration curves (Sec. III-A) are examples which have occurred in this thesis. The problem is so important and so general that to devise the best numerical method for these cases was worth the expenditure of a considerable amount of time. For the construction of calibration curves (which is a linear least squares problem) any number of standard computer codes were acceptable.† For the other two problems no fully acceptable or easy solution was found.

In the general non-linear many-variable case there are several conditions for acceptability of a solution. The most important requirement is that the mathematical minimum should correspond to the physically meaningful values. For unfolding a spectrum, this means that the shape of the experimental peaks must closely correspond to the mathematical form chosen for a single peak. The requirements for a phase-shift analysis are more complicated and are discussed in the next section.

Secondly, one must be able to distinguish the "best" minimum from the several possible local minima; it will simply be the one with the lowest value of the function having physically reasonable parameters.

---

†A code called MLR and written by Van Hoff was used.

This is the least satisfying aspect of the general problem, for no method of determining all possible local minima was found and the practical compromise was to investigate all the minima within a small region. For unfolding Gaussian peaks this was seldom a concern. Usually it was relatively easy to start with a good enough guess so that the local minimum was the "best" minimum.

Next a method of finding a local minimum is needed. A computer code named VARMIT based closely on Davidson's method[15] was developed for this purpose with the assistance of Mr. Eric Beals. With proper scaling this method rarely fails to converge rapidly. Similar codes have previously been found superior to several other methods by other investigators.[37,38]

The last aspect of the problem to be discussed is the criteria for convergence and the related problem of error limits on determination of the parameters.

Since VARMIT does not necessarily take monotonically decreasing steps in finding a minimum, convergence criteria based on step size may possibly cause false indications of convergence. This is especially significant since intermediate values of the parameters along the minimization path can be further from the final values of the parameters than the initial guess.

The criterion which was found to be most satisfactory was to look for inconsistencies caused by machine rounding errors. For a well scaled problem these inconsistencies tend to occur only in the neighborhood of the minimum. The final check on the minimum is to choose a few new starting points obtained by moving from the minimum a distance in each parameter corresponding to the standard deviation in that parameter, and after a new search to compare the new and old values of the minimum. In all fairness it must be added that no criterion works in all cases and experience with the properties of a particular type of problem is invaluable.

For the problem of analyzing spectra with Gaussian-shaped peaks a function subroutine with many options has been coded. One has the choice of letting the height, position, and width of each Gaussian vary or restricting these parameters by any set of linear constants. Often the same width has been used for each peak either as a fixed or variable parameter. Background can easily be subtracted. Often satisfactory results can only be obtained after this is done. Figure 6 shows a fit to part of the spectrum in Fig. 4. From ten to seven counts of background were subtracted and one variable width for all peaks was used. The accuracy with which relative cross sections can be extracted by this method is limited by the presence of small peaks arising from maxima in the angular distributions of elastic scattering from trace impurities and even from collectively-excited states in carbon and oxygen which are usually present in substantial amounts.

A listing of VARMIT and subroutines for the spectrum resolving case follow.

3. PIERRE

PIERRE is the name of a program which determines parameterized reflection coefficients η_ℓ from a least squares fit of elastic scattering data and then calculates inelastic angular distributions by means of the Austern and Blair model (Sec. V-A,B). The least squares fit is done by Davidson's[15] method and is described in the section on VARMIT.

Finding the "best" local minimum in this case is far harder than the preceding case of resolving a spectrum into Gaussian peaks. A parameterization suggested by Blair[39] is physically easy to understand and is suggested by η_ℓ generated from optical-model parameters:

$$\eta_\ell = \epsilon + iA\Delta \frac{d\epsilon}{d\ell}$$

where

$$\epsilon = (1 + e^{(L-\ell)/\Delta})^{-1}$$

The parameter L corresponds to the critical angular momentum semiclassically related to the nuclear radius. As L increases, the period of oscillation of the angular distribution decreases. The parameter Δ corresponds to a diffuseness in the nuclear surface and as Δ increases, the rate of decrease of the cross section with angle increases. The final parameter A gives the strength of the imaginary part of η_ℓ which interferes with the Coulomb phase shift, so by varying A the depth of the minima changes. The parameters are reasonably uncorrelated and a least squares fit is straight forward. Unfortunately, three parameters does not give enough freedom and the fits are poor. To improve the fits a new 5- parameter form for η_ℓ was chosen

$$\eta_\ell = \epsilon + B \frac{d\epsilon}{d\ell} + i\left(A \frac{d\epsilon}{d\ell} + D \frac{d^2\epsilon}{d\ell^2}\right) .$$

As expected, this form gives much better fits; however, the properties of the parameters are now correlated and the original meaning of L, Δ, and A is lost. Now depending on the quality of the data and other factors, several local minima can be found within the physical constraint $|\eta_\ell|^2 \leq 1$.

One finds small comfort in the fact that with the optical model the situation is much worse since each local minimum in η_ℓ can correspond to a set of local minima in the optical-model parameters. No satisfactory solution beyond the suggestions of the last section have been found.

Assuming a best set of η_ℓ's has finally been determined, PIERRE now calculates the inelastic angular distributions. Some care has been taken in making the computer code fast. All quantities used often have been stored in tables and symmetry considerations have been used to reduce the calculations.

For the case of double excitation, single and double excitation are coherently mixed and the ratio is varied to reproduce the observed phase of the oscillations of the experimental differential cross section.

$Ca^{40}(\alpha,\alpha')Ca^{40}$
Beam energy = 50.9 MeV
Elastic

$\theta_{C.M.}$	$\frac{\partial\sigma}{\partial\Omega}$	Fractional statistical error	$\theta_{C.M.}$	$\frac{\partial\sigma}{\partial\Omega}$	Fractional statistical error	$\theta_{C.M.}$	$\frac{\partial\sigma}{\partial\Omega}$	Fractional statistical error
8.3	33,100.	.002	26.4	122.	.003	44.8	7.04	.008
9.4	17,300.	.002	26.9	109.	.003	45.4	7.39	.008
10.5	8,050.	.002	27.5	81.0	.003	45.9	8.31	.008
11.0	4,330.	.003	28.0	73.4	.004	46.4	7.96	.008
11.6	3,120.	.003	28.6	39.4	.005	47.0	8.40	.007
12.1	1,820.	.005	29.1	32.8	.007	47.5	7.47	.008
12.7	1,590.	.006	29.6	14.9	.008	48.0	7.15	.008
13.2	1,280.	.006	30.2	8.4	.013	48.6	5.65	.009
13.8	1,260.	.006	30.7	1.5	.019	49.1	5.41	.009
14.3	1,330.	.006	31.3	0.6	.015	50.2	3.47	.010
14.9	1,340.	.006	31.8	4.0	.015	51.2	1.89	.015
15.4	1,380.	.006	32.4	6.5	.009	52.3	1.01	.018
16.0	1,390.	.006	32.9	15.1	.008	53.4	.85	.019
16.5	1,340.	.006	33.5	20.1	.006	54.5	1.16	.016
17.1	1,080.	.004	34.0	28.0	.006	55.0	1.40	.015
17.6	875.	.003	34.5	28.0	.005	55.5	1.59	.014
18.2	939.	.003	35.1	35.9	.005	56.1	1.69	.014
18.7	457.	.003	35.6	37.4	.005	56.6	1.96	.013
19.3	368.	.004	36.2	36.4	.005	57.1	1.89	.013
19.8	158.	.004	36.7	30.4	.005	57.6	2.14	.012
20.9	38.0	.007	37.3	30.6	.006	58.7	1.97	.013
22.0	34.4	.008	37.8	23.2	.007	59.8	1.73	.013
22.5	39.9	.006	38.3	21.2	.007	60.8	1.26	.016
23.1	80.0	.003	39.4	12.3	.009	61.9	1.09	.017
23.6	91.0	.004	40.5	5.8	.011			
24.2	125.	.003	41.6	2.8	.015			
24.7	142.	.003	42.7	2.8	.013			
25.3	142.	.003	43.7	4.73	.010			
25.8	154.	.003	44.3	5.64	.009			

$Ca^{40}(\alpha,\alpha')Ca^{40}$
Beam energy = 50.9 MeV
Q = -3.73

$\theta_{C.M.}$	$\frac{\partial\sigma}{\partial\Omega}$	Fractional statistical error	$\theta_{C.M.}$	$\frac{\partial\sigma}{\partial\Omega}$	Fractional statistical error
10.5	27.0	.019			
11.6	36.2	.017	42.8	1.22	.019
12.7	35.4	.012	43.9	1.71	.017
13.8	32.9	.012	45.0	2.38	.015
14.9	34.9	.012	47.1	2.84	.012
16.0	29.4	.013	48.2	2.38	.014
17.1	20.2	.016	49.3	1.94	.015
17.7	14.6	.024	50.4	1.54	.017
18.2	11.0	.022	51.4	1.20	.019
18.8	6.02	.020	52.5	.98	.022
19.3	4.87	.024	53.6	.90	.018
19.9	3.36	.020	54.6	.99	.017
21.0	5.19	.018	55.7	1.11	.017
22.1	9.15	.015	56.8	1.24	.016
23.2	12.6	.012	57.8	1.24	.016
24.3	15.0	.010	58.9	1.25	.016
25.4	14.7	.010	60.0	1.16	.016
26.5	12.0	.009	61.0	1.02	.017
27.6	8.80	.010	62.1	.87	.019
28.7	5.27	.012			
29.8	3.41	.016			
30.8	2.31	.020			
31.9	2.76	.018			
33.0	3.67	.015			
34.1	4.72	.013			
35.2	5.42	.013			
37.4	4.40	.014			
38.5	3.07	.017			
39.6	1.93	.021			
40.6	1.32	.022			
41.7	1.04	.024			

$Ca^{40}(\alpha,\alpha')Ca^{40}$
Beam energy = 50.9 MeV
Q = -3.90

$\theta_{C.M.}$	$\frac{\partial\sigma}{\partial\Omega}$	Fractional statistical error	$\theta_{C.M.}$	$\frac{\partial\sigma}{\partial\Omega}$	Fractional statistical error
10.5	9.20	.033	45.0	0.35	.037
11.7	9.11	.034	49.3	0.19	.050
12.7	6.43	.029	50.4	0.21	.047
13.8	5.46	.040	51.4	0.20	.048
17.7	2.24	.062	52.5	0.24	.044
18.2	1.84	.054	53.6	0.20	.038
18.8	3.20	.030	54.7	0.19	.041
19.3	3.00	.030	55.7	0.15	.045
19.9	3.80	.026	56.8	0.18	.051
21.0	3.66	.022	57.8	0.09	.058
22.1	2.72	.028	58.9	0.09	.058
23.2	1.70	.032	60.0	0.07	.068
24.3	0.90	.040	61.0	0.08	.061
25.4	0.57	.050	62.1	0.08	.063
26.5	0.53	.045			
27.6	0.73	.034			
28.7	1.04	.030			
30.8	1.19	.027			
31.9	1.06	.028			
33.0	0.79	.032			
34.1	0.52	.042			
35.2	0.31	.053			
36.3	0.32	.053			
38.5	0.40	.047			
39.6	0.42	.045			
40.7	0.53	.033			
41.7	0.61	.031			
42.8	0.55	.028			
43.9	.40	.035			

$Ca^{40}(\alpha,\alpha')Ca^{40}$
Beam energy = 50.9 MeV
Q = -4.483

$\theta_{C.M.}$	$\frac{\partial\sigma}{\partial\Omega}$	Fractional statistical error	$\theta_{C.M.}$	$\frac{\partial\sigma}{\partial\Omega}$	Fractional statistical error
10.5	4.68	.047	41.8	0.33	.043
11.6	2.93	.060	42.8	0.34	.037
12.7	2.57	.045	43.9	0.40	.036
13.8	2.67	.028	45.0	0.46	.033
14.9	3.53	.039	46.1	0.41	.036
16.0	3.82	.037	47.2	0.35	.036
17.1	4.48	.034	48.2	0.28	.041
17.7	5.61	.039	49.3	0.25	.044
18.2	4.43	.035	52.5	0.15	.058
18.8	5.42	.023	53.6	0.13	.048
19.3	4.73	.024	54.7	0.16	.045
19.9	4.98	.020	55.8	0.16	.044
21.0	4.49	.019	56.8	0.17	.042
22.1	3.66	.024	57.9	0.16	.044
23.2	2.83	.025	58.9	0.16	.045
24.3	1.96	0.27	60.0	.14	.048
25.4	1.27	.034	61.0	.12	.051
26.5	0.77	.038	62.1	.10	.056
27.6	0.54	.040			
28.7	0.59	.040			
29.8	0.66	.037			
30.9	0.90	.033			
32.0	1.06	.029			
33.1	1.11	.029			
34.1	1.13	.027			
35.2	0.94	.031			
36.3	0.75	.034			
37.4	0.56	.040			
38.5	0.40	.047			
39.6	0.40	.047			

$Ca^{40}(\alpha,\alpha')Ca^{40}$
Beam energy = 50.9 MeV
Q =-5.25

$\theta_{C.M.}$	$\frac{\partial\sigma}{\partial\Omega}$	Fractional statistical error	$\theta_{C.M.}$	$\frac{\partial\sigma}{\partial\Omega}$	Fractional statistical error
11.6	1.25	.091	47.2	.11	.064
12.7	0.99	.072	48.3	.08	.073
13.8	0.96	.080	49.4	.12	.064
16.0	0.71	.085	50.4	.09	.070
17.1	0.74	.087	51.5	.07	.081
18.2	0.52	.100	52.6	.06	.083
19.4	0.34	.088	53.7	.07	.067
19.9	0.44	.070	54.7	.08	.041
21.0	0.49	.060	57.9	.07	.070
22.1	0.43	.070	59.0	.05	.073
23.2	0.46	.060	60.0	.05	.078
24.3	0.42	.058	61.1	.05	.076
25.4	0.34	.066	62.2	.04	.090
26.5	0.31	.058			
27.6	0.24	.060			
28.6	0.24	.068			
29.8	0.18	.070			
30.9	0.20	.066			
32.0	0.20	.067			
33.1	0.21	.068			
34.2	0.21	.067			
35.3	0.18	.070			
36.4	0.15	.075			
37.4	0.14	.080			
38.5	0.09	.098			
39.6	0.09	.100			
40.7	0.10	0.77			
41.8	.10	.075			
46.1	.11	.070			

$Ca^{40}(\alpha,\alpha')Ca^{40}$
Beam energy = 50.9 MeV
Q = -5.62

$\theta_{C.M.}$	$\frac{\partial\sigma}{\partial\Omega}$	Fractional statistical error	$\theta_{C.M.}$	$\frac{\partial\sigma}{\partial\Omega}$	Fractional statistical error
11.6	1.18	.094	49.4	0.06	.088
12.7	0.74	.083	50.5	0.06	.088
16.1	0.51	.100	51.5	0.07	.083
15.0	0.58	.095	52.6	0.04	.100
17.2	0.40	.112	53.7	0.05	.087
18.3	0.48	.104	54.7	0.04	.091
19.4	0.50	.072	55.8	0.04	.091
22.1	0.43	.070	60.1	0.03	.105
23.2	0.38	.065	61.1	0.03	.106
24.3	0.28	.070	62.2	0.02	.130
25.4	0.25	.076			
26.5	0.19	.072			
27.6	0.20	.067			
28.7	0.18	.066			
29.8	0.21	.065			
30.9	0.18	.071			
32.0	0.19	.070			
33.1	0.19	.068			
34.2	0.19	.070			
35.3	0.16	.074			
36.4	0.14	.080			
37.5	0.13	.080			
38.6	0.11	.088			
39.6	0.11	.091			
40.7	0.09	.079			
41.8	0.09	.083			
42.9	0.09	.070			
44.0	0.11	.069			
47.2	0.08	.072			
48.3	0.06	.085			

$Ca^{40}(\alpha,\alpha')Ca^{40}$
Beam energy = 50.9 MeV
Q = -5.90

$\theta_{C.M.}$	$\frac{\partial\sigma}{\partial\Omega}$	Fractional statistical error	$\theta_{C.M.}$	$\frac{\partial\sigma}{\partial\Omega}$	Fractional statistical error
12.7	0.94	.074	49.4	.11	.066
15.0	0.99	.072	50.5	.12	.061
16.1	0.89	.076	51.5	0.08	.072
17.2	0.75	.089	52.6	0.11	.064
18.3	0.51	.100	53.7	0.09	.057
18.8	0.35	.091	54.8	0.09	.057
19.4	0.23	.108	55.8	0.10	.054
19.9	0.20	.055	56.9	0.10	.056
24.3	0.52	.053	58.0	0.09	.058
25.4	0.58	.050	61.2	0.07	.070
26.5	0.47	.048	62.2	0.04	.085
27.6	0.30	.054			
28.7	0.23	.060			
29.8	0.15	.078			
30.9	0.13	.083			
32.0	0.16	.075			
33.1	0.20	.068			
34.2	0.20	.071			
35.3	0.24	.061			
36.4	0.18	.070			
37.5	0.19	.070			
38.6	0.14	.080			
39.7	0.13	.088			
40.7	0.07	.091			
41.8	0.10	.078			
42.9	0.11	.064			
44.0	0.13	.064			
45.1	0.17	.054			
48.3	0.15	.056			

$Ca^{40}(\alpha,\alpha')Ca^{40}$
Beam energy = 50.9 MeV
Q =-6.28

$\theta_{C.M.}$	$\frac{\partial\sigma}{\partial\Omega}$	Fractional statistical error	$\theta_{C.M.}$	$\frac{\partial\sigma}{\partial\Omega}$	Fractional statistical error
9.4	8.26	.040	44.0	0.42	.034
12.7	7.76	.026	45.1	0.47	.032
13.9	6.57	.028	46.2	0.51	.031
15.0	6.48	.029	47.3	0.53	.030
16.1	5.14	.032	50.5	0.36	.045
17.2	3.54	.039	51.6	0.29	.039
17.7	3.02	.054	52.6	0.27	.040
18.3	2.19	.049	53.7	0.28	.032
18.8	1.70	.041	54.8	0.27	.033
19.4	1.52	.042	55.9	0.28	.033
19.9	1.62	.035	56.9	0.28	.033
21.0	1.91	.030	58.0	0.29	.032
22.1	2.40	.030	59.1	0.28	.033
23.2	2.93	.024	60.1	0.28	.033
24.3	3.30	.021	61.2	0.29	.033
26.5	2.50	.022			
27.6	1.57	.024			
28.7	0.94	.030			
29.8	0.71	.035			
30.9	0.67	.036			
32.0	0.77	.034			
33.1	0.97	.030			
34.2	1.15	.028			
35.3	1.17	.028			
36.4	1.07	.029			
37.5	0.90	.031			
38.6	0.63	.040			
39.7	0.50	.043			
40.8	0.37	.040			
41.8	0.33	.044			

$Ca^{40}(\alpha,\alpha')Ca^{40}$
Beam energy = 50.9 MeV
Q =-6.58

$\theta_{C.M.}$	$\frac{\partial\sigma}{\partial\Omega}$	Fractional statistical error	$\theta_{C.M.}$	$\frac{\partial\sigma}{\partial\Omega}$	Fractional statistical error
9.4	4.87	.051	41.9	0.20	.056
10.5	5.94	.042	42.9	0.22	.048
12.7	5.21	.031	44.0	0.23	.047
13.9	4.81	.032	45.1	0.26	.044
15.0	4.93	.032	46.2	0.28	.044
16.1	4.73	.033	47.3	0.30	.039
17.2	2.67	.045	48.4	0.26	.043
17.7	1.97	.066	51.6	0.16	.053
18.3	1.65	.056	52.7	0.15	.055
18.8	1.20	.049	53.7	0.15	.046
19.4	1.00	.052	54.8	0.16	.043
19.9	0.99	.052	55.9	0.15	.044
21.0	1.17	.039	56.9	0.16	.045
22.1	1.61	.036	58.0	0.15	.045
23.2	1.83	.031	59.1	0.16	.045
24.3	1.92	.027	60.1	.13	.048
25.4	1.72	.029	61.2	.12	.051
28.7	0.65	.031	62.3	.11	.053
29.8	0.52	.041			
30.9	0.46	.044			
32.0	0.51	.041			
33.1	0.63	.037			
34.2	0.64	.038			
35.3	0.65	.037			
36.4	0.61	.038			
37.5	0.61	.043			
38.6	0.35	.050			
39.7	0.26	.058			
40.8	0.20	.054			

$Ca^{40}(\alpha,\alpha')Ca^{40}$
Beam energy = 50.9 MeV
Q = -6.94

$\theta_{C.M.}$	$\frac{\partial\sigma}{\partial\Omega}$	Fractional statistical error	$\theta_{C.M.}$	$\frac{\partial\sigma}{\partial\Omega}$	Fractional statistical error
9.4	9.75	.036	43.0	0.95	.022
10.5	6.19	.041	44.0	1.00	.023
12.8	4.95	.033	45.1	1.09	.022
13.9	4.98	.032	46.2	1.00	.022
15.0	5.22	.032	47.3	0.96	.022
16.1	5.43	.031	48.4	0.88	.022
17.2	4.68	.044	49.5	0.85	.023
17.7	4.38	.033	50.5	0.87	.023
18.3	3.57	.038	52.7	0.80	.023
18.8	2.80	.032	53.8	0.82	.019
22.1	3.11	.026	54.8	0.84	.019
23.3	3.59	.022	55.9	0.82	.019
24.4	3.80	.020	57.0	0.80	.020
25.5	3.43	.021	58.0	0.74	.021
26.6	2.84	.019	59.1	0.67	.021
27.7	2.43	.019	60.2	0.60	.022
28.8	2.01	.020	61.2	0.54	.024
29.9	1.86	.022	62.3	0.48	.025
31.0	1.61	.024			
32.1	1.64	.023			
33.1	1.65	.023			
34.2	1.67	.022			
35.3	1.52	.023			
36.4	1.39	.025			
37.5	1.11	.027			
38.6	0.94	.031			
39.7	0.86	.032			
40.8	0.83	.027			
41.9	0.86	.027			

$Ca^{40}(\alpha,\alpha')Ca^{40}$
Beam energy = 50.9 MeV
Q = -7.92

$\theta_{C.M.}$	$\frac{\partial\sigma}{\partial\Omega}$	Fractional statistical error	$\theta_{C.M.}$	$\frac{\partial\sigma}{\partial\Omega}$	Fractional statistical error
9.4	6.30	.046	44.1	0.28	.041
10.6	5.06	.045	45.2	0.24	.045
13.9	2.81	.045	46.3	0.22	.049
15.0	2.72	.045	47.3	0.24	.044
16.1	2.55	.045	48.4	0.25	.045
17.2	2.88	.045	49.5	0.26	.045
17.8	3.30	.051	50.6	0.26	.041
18.3	2.44	.046	51.7	0.28	.040
18.9	2.71	.033	52.7	0.24	.043
19.4	2.66	.031	53.8	0.24	.035
20.0	2.68	.030	57.0	0.17	.042
21.1	2.32	.027	58.1	0.14	.046
22.2	1.94	.033	59.2	0.12	.050
23.3	1.49	.033	60.2	0.13	.048
24.4	1.00	.038	61.3	0.12	.050
25.5	0.82	.041	62.3	0.12	.050
26.6	0.95	.029			
27.7	1.07	.030			
28.8	1.20	.029			
29.9	1.13	.028			
31.0	1.46	.024			
33.2	0.61	.037			
34.3	0.51	.041			
36.5	0.29	.055			
38.7	0.38	.048			
39.7	0.43	.045			
40.8	0.40	.038			
41.9	0.37	.040			
43.0	0.35	.036			

$Ca^{40}(\alpha,\alpha')Ca^{40}$
Beam energy = 50.9 MeV
Q =-8.11

$\theta_{C.M.}$	$\frac{\partial\sigma}{\partial\Omega}$	Fractional statistical error	$\theta_{C.M.}$	$\frac{\partial\sigma}{\partial\Omega}$	Fractional statistical error
9.4	5.27	.049	44.1	0.25	.045
10.6	3.24	.058	45.2	0.19	.051
11.7	3.34	.055	46.3	0.20	.050
13.9	1.28	.060	47.4	0.18	.050
16.1	1.20	.067	48.4	0.20	.048
17.2	1.07	.070	49.5	0.19	.050
17.8	1.54	.075	50.6	0.21	.048
18.3	1.25	.065	51.7	0.21	.047
18.8	1.42	.045	52.8	0.19	.049
19.4	1.34	.045	53.8	0.18	.041
20.0	1.40	.040	54.9	0.19	.040
21.1	1.27	.037	58.1	0.14	.048
22.2	1.12	.044	59.2	0.13	.049
23.3	0.90	.044	60.2	0.11	.051
24.4	0.87	.041	61.3	0.12	.050
25.5	0.79	.040	62.4	0.11	.052
26.6	0.63	.033			
27.7	0.66	.038			
28.8	0.67	.037			
29.9	0.68	.036			
31.0	0.67	.037			
35.4	0.34	.050			
36.5	0.38	.044			
37.6	0.38	.049			
38.7	0.36	.050			
39.8	0.35	.050			
40.8	0.37	.040			
41.9	0.32	.043			
43.0	0.28	.041			

$Ca^{40}(\alpha,\alpha')Ca^{40}$
Beam energy = 50.9 MeV
Q = -8.38

$\theta_{C.M.}$	$\frac{\partial\sigma}{\partial\Omega}$	Fractional statistical error	$\theta_{C.M.}$	$\frac{\partial\sigma}{\partial\Omega}$	Fractional statistical error
9.4	4.41	.054	41.9	0.26	.048
10.6	2.40	.066	43.0	0.24	.043
11.7	2.58	.063	44.1	0.18	.052
13.9	1.92	.060	45.2	0.16	.058
15.0	1.97	.061	46.3	0.14	.059
16.1	1.79	.053	47.4	0.14	.058
17.2	1.85	.052	48.5	0.12	.062
17.8	2.01	.065	49.5	0.12	.059
18.3	1.60	.057	50.6	0.12	.061
18.9	1.51	.043	51.7	0.11	.065
19.4	1.36	.045	52.8	0.12	.062
20.0	1.20	.045	53.8	0.09	.057
21.1	0.89	.044	54.9	0.09	.057
22.2	0.69	.053	56.0	0.10	.054
23.3	0.53	.058	59.2	0.07	.068
24.4	0.51	.053	60.3	0.06	.071
25.5	0.69	.045	61.3	0.08	.063
26.6	0.79	.038	62.4	0.07	.068
27.7	0.80	.033			
28.8	0.81	.034			
29.9	0.71	.035			
31.0	0.58	.043			
32.1	0.49	.043			
33.2	0.45	.044			
34.3	0.43	.045			
36.5	0.25	.058			
37.6	0.31	.052			
39.8	0.32	.044			
40.9	0.28	.045			

$Ca^{40}(\alpha,\alpha')Ca^{40}$
Beam energy = 50.9 MeV
Q = -8.59

$\theta_{C.M.}$	$\frac{\partial\sigma}{\partial\Omega}$	Fractional statistical error	$\theta_{C.M.}$	$\frac{\partial\sigma}{\partial\Omega}$	Fractional statistical error
9.5	4.45	.054	47.4	0.12	.063
10.6	2.62	.066	48.5	0.10	.069
11.7	2.01	.072	49.5	0.11	.067
17.8	0.78	.105	50.6	0.11	.064
18.3	0.79	.082	51.7	0.11	.065
18.9	0.82	.058	52.8	0.11	.066
19.4	0.80	.057	53.9	0.11	.058
20.0	0.88	.050	54.9	0.10	.058
21.1	0.72	.049	56.0	0.09	.058
22.2	0.76	.053	57.1	0.08	.059
23.3	0.55	.058	62.4	0.04	.085
24.4	0.41	.058			
25.5	0.35	.066			
26.6	0.33	.058			
27.7	0.47	.043			
28.8	0.42	.042			
29.9	0.50	.041			
31.0	0.38	.052			
32.1	0.31	.055			
33.2	0.26	.057			
34.3	0.22	.064			
35.4	0.18	.070			
36.5	0.18	.070			
38.7	0.30	.054			
40.9	0.21	.052			
43.0	0.19	.058			
44.1	0.17	.058			
45.2	0.15	.058			
46.3	0.12	.066			

$Ne^{20}(\alpha,\alpha')Ne^{20}$

Beam energy = 50.9 MeV

Elastic			Q = -1.63			Q = -4.25		
$\theta_{C.M.}$	$\frac{\partial\sigma}{\partial\Omega}$	Fractional statistical error	$\theta_{C.M.}$	$\frac{\partial\sigma}{\partial\Omega}$	Fractional statistical error	$\theta_{C.M.}$	$\frac{\partial\sigma}{\partial\Omega}$	Fractional statistical error
10.9	2290.	.001	12.1	97.5	.01	12.1	4.18	.02
12.0	792.0	.002	13.3	85.9	.01	13.3	4.28	.02
13.2	220.0	.002	14.5	63.6	.009	14.5	4.35	.02
14.4	46.6	.004	15.7	39.2	.008	15.7	4.78	.02
15.6	96.8	.005	16.9	17.8	.01	17.0	5.27	.02
16.8	203.	.004	18.1	6.04	.01	18.2	5.42	.02
18.0	272.	.003	19.3	3.52	.02	19.4	4.83	.02
19.2	269.	.003	20.5	9.89	.02	20.6	4.62	.02
20.4	235.	.003	21.7	17.9	.01	21.8	3.97	.03
21.6	163.	.003	22.9	25.6	.009	23.0	2.61	.03
22.8	89.9	.005	24.0	29.3	.009	24.2	1.80	.04
24.0	33.4	.01	25.2	28.0	.01	25.4	1.15	.05
25.2	7.72	.02	26.4	22.5	.01	26.6	0.87	.05
26.3	2.60	.03	27.6	15.2	.01	27.8	0.85	.06
27.5	12.3	.02	28.8	8.74	.02	29.0	1.05	.06
28.7	25.7	.01	30.0	4.42	.02	30.2	1.17	.05
29.9	36.1	.008	31.2	2.86	.02	31.4	1.26	.05
31.1	40.3	.007	32.4	3.83	.03	32.6	1.20	.05
32.3	37.7	.008	33.6	6.13	.02	33.7	1.06	.05
33.5	31.0	.01	34.7	8.73	.02	34.9	0.78	.06
34.6	22.1	.01	35.9	10.9	.02	36.1	0.64	.07
35.8	15.0	.01	37.1	11.5	.01	37.3	0.48	.07
37.0	9.34	.01	38.3	10.7	.02	38.5	0.39	.06
38.2	6.15	.02	39.5	9.43	.02	39.7	0.47	.06
39.3	5.73	.02	40.6	7.43	.02	40.8	0.59	.06
40.5	6.61	.02	41.8	5.62	.02	42.0	0.75	.06
41.7	8.01	.02	43.0	4.30	.02			
42.8	9.57	.01						

$Ne^{20}(\alpha,\alpha')Ne^{20}$
Beam energy = 50.9 MeV

Q = -4.97			Q = -5.63			Q = -5.80		
$\theta_{C.M.}$	$\frac{\partial\sigma}{\partial\Omega}$	Fractional statistical error	$\theta_{C.M.}$	$\frac{\partial\sigma}{\partial\Omega}$	Fractional statistical error	$\theta_{C.M.}$	$\frac{\partial\sigma}{\partial\Omega}$	Fractional statistical error
17.0	0.55	.10	13.4	14.7	.02	15.8	1.91	.03
18.2	0.46	.10	14.6	15.4	.02	17.0	1.85	.03
19.4	0.39	.10	15.8	14.8	.01	18.2	1.39	.04
20.6	0.40	.09	17.0	14.3	.01	19.4	1.45	.04
21.8	0.44	.09	18.2	12.5	.02	20.6	1.17	.05
23.0	0.43	.09	19.4	9.09	.02	21.9	0.98	.05
24.2	0.31	.09	20.6	7.62	.02	23.1	1.06	.05
25.4	0.35	.09	21.8	5.56	.02	24.3	1.20	.05
26.6	0.32	.09	23.1	3.98	.03	25.5	1.36	.05
27.8	0.32	.09	24.3	2.81	.03	26.7	1.01	.05
29.0	0.28	.10	25.5	2.44	.03	27.9	1.17	.07
30.2	0.28	.10	26.7	2.92	.03	29.1	0.64	.08
31.4	0.26	.10	27.9	3.17	.03	30.3	0.35	.09
32.6	0.25	.10	29.1	3.72	.03	31.5	0.29	.12
33.8	0.23	.13	30.3	4.03	.03	33.8	0.27	.10
35.0	0.17	.14	31.5	3.84	.03	35.1	0.35	.09
36.2	0.18	.14	32.7	3.05	.03	36.2	0.61	.09
37.4	0.18	.14	33.9	2.84	.03	37.4	0.78	.08
38.5	0.15	.15	35.0	1.86	.03	38.6	0.76	.08
39.7	0.13	.15	36.2	1.46	.04	39.8	0.81	.08
40.9	0.09	.15	37.4	0.88	.04	41.0	0.79	.07
42.1	0.08	.15	38.6	0.86	.04	42.2	0.79	.08
43.3	0.06	.15	39.7	0.79	.04	43.3	0.70	.05
			41.0	0.86	.04			
			42.2	0.96	.04			
			43.3	1.14	.04			

$Ne^{20}(\alpha,\alpha')Ne^{20}$
Beam energy = 50.9 MeV

Q = -6.72			Q = -7.17			Q = -7.43		
$\theta_{C.M.}$	$\frac{\partial\sigma}{\partial\Omega}$	Fractional statistical error	$\theta_{C.M.}$	$\frac{\partial\sigma}{\partial\Omega}$	Fractional statistical error	$\theta_{C.M.}$	$\frac{\partial\sigma}{\partial\Omega}$	Fractional statistical error
17.1	0.92	.06	11.0	14.3	.02	17.1	1.02	.04
18.3	0.77	.06	14.6	14.1	.02	18.3	1.14	.04
19.5	0.46	.06	15.9	12.4	.02	19.5	1.08	.04
20.7	0.73	.06	17.1	10.5	.02	20.7	1.10	.04
21.9	0.80	.06	18.3	8.31	.02	21.9	0.94	.04
23.1	0.93	.07	19.5	5.28	.02	23.2	0.78	.04
24.3	1.08	.07	20.7	3.79	.02	24.4	0.54	.04
25.5	0.84	.07	21.9	2.67	.03	25.6	0.55	.04
26.7	0.61	.07	23.1	2.08	.03	26.8	0.47	.03
27.9	0.51	.07	24.4	2.04	.03	28.0	0.52	.03
29.1	0.53	.07	25.6	2.34	.03	29.2	0.61	.04
30.3	0.47	.07	26.8	2.46	.03	30.4	0.65	.04
31.5	0.62	.07	28.0	2.38	.03	31.6	0.73	.05
32.7	0.68	.07	29.2	2.34	.03	32.8	0.60	.07
33.9	0.72	.07	30.4	1.98	.03	34.0	0.52	.07
35.1	0.69	.07	31.6	1.47	.04	35.2	0.43	.08
36.3	0.64	.07	32.8	1.10	.04	36.4	0.44	.08
37.5	0.51	.07	34.0	0.77	.05	37.6	0.31	.08
38.7	0.31	.07	35.2	0.57	.05	38.8	0.27	.08
39.9	0.21	.07	36.4	0.49	.05	40.0	0.29	.08
41.1	0.21	.07	37.6	0.41	.05	41.2	0.25	.08
42.3	0.17	.07	38.7	0.45	.05	42.3	0.30	.08
43.4	0.25	.06	40.0	0.52	.05	43.5	0.28	.08
			41.1	0.56	.05			
			42.3	0.66	.05			
			43.5	0.64	.05			

$Ne^{20}(\alpha,\alpha')Ne^{20}$
Beam energy = 50.9 MeV

Q = -7.86			Q = -8.71			Q = -9.11		
$\theta_{C.M.}$	$\frac{\partial\sigma}{\partial\Omega}$	Fractional statistical error	$\theta_{C.M.}$	$\frac{\partial\sigma}{\partial\Omega}$	Fractional statistical error	$\theta_{C.M.}$	$\frac{\partial\sigma}{\partial\Omega}$	Fractional statistical error
14.7	2.85	.04	17.1	2.18	.03	15.9	3.3	.03
15.9	1.82	.04	18.4	2.35	.03	17.2	3.01	.03
17.1	1.18	.05	19.6	2.24	.03	18.4	2.75	.03
18.3	0.93	.05	20.8	2.36	.04	19.6	2.60	.03
19.5	0.66	.05	22.0	2.24	.04	20.8	2.72	.03
20.8	0.73	.06	23.2	1.89	.04	22.0	2.66	.03
22.0	0.77	.06	24.5	1.51	.04	23.3	2.47	.04
23.2	0.81	.06	25.7	1.26	.04	24.5	2.04	.04
24.4	0.76	.06	26.9	1.19	.04	25.7	1.93	.05
25.6	0.81	.06	28.1	1.14	.04	26.9	1.58	.05
26.8	0.73	.06	29.3	1.30	.04	28.1	1.37	.05
28.0	0.67	.08	30.5	1.36	.04	29.3	1.18	.05
29.2	0.51	.09	31.7	1.42	.04	30.5	1.03	.06
30.4	0.41	.10	32.9	1.40	.04	31.7	0.92	.06
31.6	0.23	.11	34.1	1.49	.05	32.9	0.79	.06
34.0	0.24	.11	35.3	1.29	.05	34.1	0.84	.06
35.2	0.20	.12	36.5	1.31	.05	35.3	0.77	.06
36.4	0.25	.10	37.7	1.15	.05	36.5	0.92	.06
37.6	0.28	.09	38.9	0.97	.05	37.7	0.84	.06
38.8	0.25	.09	40.1	0.89	.05	38.9	0.89	.06
40.0	0.30	.08	41.3	0.84	.05	40.1	0.81	.06
41.2	0.36	.08	42.5	0.88	.05	41.3	0.71	.06
42.4	0.31	.07	43.7	0.78	.05	42.5	0.61	.07
43.6	0.31	.07				43.7	0.54	.07

```
$ID   465001,V        ,10, SPRINGER
$IBJOB
$IBFTC FCN     LIST,REF
      SUBROUTINE FCN(N,G,F,X,M1)
C
C     SEE SPRINGER 5631 OR 5088
C 9-21-64  CAL-COMP OF DATA,ELASTIC, O+, AND I=1,IMAX
C MAXIMUM VALUES OF INDICES  ITMAX=85, LMAX=50, IMAX=8
C
      COMMON/CCPOOL/XMIN,XMAX,YMIN,YMAX,CCXMIN,CCXMAX,CCYMIN,CCYMAX
      DIMENSION G(5),X(5),ZD(5)
      DIMENSION SLL( 85),SXL( 85),SNL( 85),IML(5),CHARS(11),
     1FINA( 85) ,FOA( 85),FA( 85),FO( 85),ETAA(100),FCC( 85),FON( 85),
     2GSIG( 85),DSIGEX( 85),PD(5),WEIGHT( 85),YLM(51, 85),PS(100),
     3YLO(52, 85),Y(6),XX(6),SIG(51),GE(100) ,SIGIN( 85, 8),  T(99),
     4SIGEX( 85),C(5),SIGEL( 85),E(100),SIGR( 85),TH( 85),S(5),MW (5),
     5AW(5),FNS(50),WW( 85),WW1( 85),SQ(100),CE(50),FNN( 85),ETTA(100)
      LOGICAL  LOGIC,FLAGE
         REAL K,MA,MX,MB,MEV
      INTEGER  PRINT
      COMPLEX FINA,FOA,FOO,FCC,FON,FNN,IML,IMO,PS,CLOG,CABS
      COMPLEX FIN,ZERO   ,E,GE,IM,CEXP,FC,FN ,EO,FNS,CE,FNSY,ZD,SQK,CSQ
      IF(M1.NE.1) GO TO 36
      CCXMIN=0.
      CCXMAX=2000./1024.
      CCYMAX=1000./1024.
      CCYMIN=0.
      XMIN=0.
      XMAX=100.
      YMIN=0.
      YMAX=4.
      DATA RADIAN,MEV,HC,IBGN/.01745329,931.478,197.323,0/
      DATA (CHARS(I),I=1,11)/3H0.0,3H10.,3H20.,3H30.,3H40.,3H50.,3H60.,
     13H70.,3H80.,3H90.,4H100./
      DATA(IML(I),I=1,5)/(1.,0.),(0.,1.),(-1.,0.),(0.,-1.),(1.,0.)/
      DATA IM,PI,ZERO  / (0.,1.),3.14159265 ,   (0.,0.)  /
      DATA(T(I),I=1,99),(S(I),I=1,5),(
     X                                MW(I),I=1,5),(AW(I),I=1,5)/1HH,2HHE
     1,2HLI,2HBE,1HB,1HC,1HN,1HO,1HF,2HNE,2HNA,2HMG,2HAL,2HSI,1HP,1HS,2H
     2CL,2HAR,1HK,2HCA,2HSC,2HTI,1HV,2HCR,2HMN,2HFE,2HCO,2HNI,2HCU,2HZN,
     32HGA,2HGE,2HAS,2HSE,2HBR,2HKR,2HRB,2HSR,1HY,2HZR,2HNB,2HMO,2HTC,2H
     4RU,2HRH,2HPD,2HAG,2HCD,2HIN,2HSN,2HSB,2HTE,1HI,2HXE,2HCS,2HBA,2HLA
     5,2HCE,2HPR,2HND,2HPM,2HSM,2HEU,2HGD,2HTB,2HDY,2HHO,2HER,2HTM,2HYB,
     62HLU,2HHF,2HTA,1HW,2HRE,2HOS,2HIR,2HPT,2HAU,2HHG,2HTL,2HPB,2HBI,2H
     7PO,2HAT,2HRN,2HFR,2HRA,2HAC,2HTH,2HPA,1HU,2HNP,2HPU,2HAM,2HCM,2HBK
     8,2HCF,2HES,1HP,1HD,3HHE3,3HHE4,1HT,1,1,2,2,1,1.007825,2.014102,3.0
     91603,4.002604,3.016049/
      N=5
      READ(2,21) NZX,NA,NB,PRINT,ITMAX,LMIN,LMAX,IMAX,MM,    MX,EA,ELL,DE
     1LTA,A,B,D
   21 FORMAT(I3,3I1,I3,4I2,3X,5F10.5/7F10.5)
      IF(-1.NE.MM) GO TO 606
      DO 51 IT=1,ITMAX
      READ(2,131) SIGEX(IT),TH(IT)
  131 FORMAT(30X,2F10.5)
      DSIGEX(IT)=.1*SIGEX(IT)
```

```
 51 CONTINUE
606 CONTINUE
    IF(MM.EQ.7) READ(2,31) AIT,BIT
    IF((MM.EQ.7).OR.(-1.EQ.MM)) GO TO 302
    READ (2,31) (SIGEX(IT),DSIGEX(IT),TH(IT),IT=1,ITMAX)
    READ (2,31)DTHETA
302 CONTINUE
 31 FORMAT(6F10.5)
    X(1)=ELL
    X(2)=DELTA
    X(3)=A
    X(4)=B
    X(5)=D
    GSIG(1)=(SIGEX(1)-SIGEX(2))/(TH(1 )-TH(2))
    ITMAX1=ITMAX-1
    DO 32 IT=2,ITMAX1
 32 GSIG(IT)= (SIGEX(IT+1)-SIGEX(IT-1))/(TH(IT+1)-TH(IT-1))
    GSIG(ITMAX)=(SIGEX(ITMAX)-SIGEX(ITMAX1))/(TH(ITMAX)-TH(ITMAX1))
    L2MAX=2*LMAX
    ZA=MW(NA)
    Z=NZX
     MA=AW(NA)
     MB=AW(NB)
    NUMX= MX+0.5
    NUMY=MA+MX-MB+.5
    NZY=NZX+MW(NA)-MW(NB)
    UMX=MX
    MX=MX*MEV
    MA=MA*MEV
    MB=MB*MEV
    SQPI=SQRT(PI)
    C(1)=.5/SQPI
    C(2)=SQRT(3.)*C(1)
    C(3)=SQRT(1.5)*C(1)
    C(4)=SQRT(7.5)*C(1)
    C(5)=SQRT(1.25)*C(1)
    DO 29 ISQ=1,100
    UISQ=ISQ
    SQ(ISQ)=SQRT(UISQ)
 29 CONTINUE
    DO 11 IT=1,ITMAX
    IF(MM.NE.7) GO TO 303
    UIT=IT
    TH(IT)=AIT*UIT+BIT
303 CONTINUE
    W=COS(TH(IT)*RADIAN)
    WW(IT)=W
    WW1(IT)=SQRT(1.-W*W)
 11 CONTINUE
    ETO=SQRT(MA         /2./EA)/137.037*ZA*Z
    K=SQRT(2.*MA*EA)*MX/(MA+MX)/HC
    WRITE(3,22) T(NZX),NUMX,S(NA),S(NB),T(NZY),NUMY,UMX,EA,ETO,K
 22 FORMAT(1H1///51X,A2,I3,1H(,A3,1H,,A3,1H),A2,I3//22X,11HTARGET MASS
   1F10.5, 3X,11HBEAM ENERGY,F10.5,3X,3HETA,F10.5,5X,1HK,F10.5//)
    WRITE(3,23) ITMAX,LMIN,LMAX,IMAX,X
 23 FORMAT(1 X,5HITMAX,I4,7X,4HLMIN,I4, 9X,4HLMAX,I4,8X,4HIMAX,I4,6X,
```

```
     11HL,F 7.3,3X,5HDELTA,   F 7.3,5X,1HA,F 7.3,5X,1HB,F7.3,5X,1HD,F7.3
     2//)
      SIG(1)=ATAN(ETO)
      DO12 L=1,LMAX
      UL=L
      L2L=2*L+1
      SIG(L+1)=SIG(L)+ATAN(ETO/(UL+1.))
      CE(L)=                  CEXP(   IM*SIG(L))
      FNS(L )=SQ  (L2L    )*CE(L)*CE(L)
   12 CONTINUE
      DO 13 IT=1,ITMAX
      W=WW(IT)
      W1=WW1(IT)
      YLO(1,IT)=W*C(2)
      YLO(2,IT)=(3.*W*W-1.)*C(5)
      FCC(IT)=-ETO*CEXP(-IM*ALOG((1.-W)/2.)*ETO)/(K*(1.-W))
      DO 13 L=1,LMAX
      UL=L
      L2L=2*L+3
      YLO(L+2,IT)=(W*SQ(L2L)*SQ(L2L+2)*YLO(L+1,IT)- (UL+1.)*SQ (L2L+2)/
     1SQ(L2L-2)*YLO(L,IT))/(UL+2.)
   13 CONTINUE
      IF(MM.EQ.2) READ(2,31)(E(L2),L2=2,L2MAX,2)
   36 CONTINUE
      ELL=X(1)
      DELTA=X(2)
      A=X(3)
      B=X(4)
      D=X(5)
      F=0.
      DO 33 J=1,5
      G(J)=0.
   33 CONTINUE
      EX=EXP(ELL/DELTA)
      EXE=EXP(-.5/DELTA)
      EXD=EXE*EXE
      EXS=EX
      FLAGE=.FALSE.
      DO 2 L=1,LMAX
      L2=2*L
      EX=EX*EXD
      UL=L
      CURE=(ELL-UL)/DELTA
      IF((CURE.GT.88.).OR.FLAGE)GO TO 54
      EX=EXP(CURE)
      FLAGE=.TRUE.
   54 CONTINUE
      ETA=1./(1.+EX)
      ET=ETA*(1.-ETA)
      ETT=ET *(1.-2.*ETA)
      ETTT=ET*(1.-6.*ET)
      E(L2)=CMPLX((ETA+B*ET),(A*ET+D*ETT))
      GE(L2)=CMPLX((ET+B*ETT),(A*ETT+D*ETTT))/DELTA
      ETAA(L2)=ET
      ETTA(L2)=ETT
    2 CONTINUE
```

```
      DO 1 IT=1,ITMAX
      W=WW(IT)
      DO 15 J=1,5
      ZD(J)=ZERO
   15 CONTINUE
      FN=CMPLX(C(1),0.)
      DO 7 L=1,LMAX
      UL=L
      L2=2*L
      FNSY=FNS(L)*YLO(L,IT)
      FN=FN+FNSY*(1.-E(L2))
      ZD(1)=ZD(1)+FNSY*GE(L2)
      ZD(2)=ZD(2)+FNSY*GE(L2)*(UL-ELL)/DELTA
      ZD(4)=ZD(4)-FNSY*ETAA(L2)
      ZD(5)=ZD(5)-FNSY*ETTA(L2)*IM
    7 CONTINUE
      ZD(3)=ZD(4)*IM
      SQK=IM*SQPI/K
      FN=FN*SQK
      FC=FCC(IT)
      CSQ=SQK*CONJG(FN+FC)
      FIT       =REAL((FN+FC)*CONJG(FN+FC))*10.
      WEIGHT(IT)=1./(DSIGEX(IT)**2+(GSIG(IT)*DTHETA)**2)
      F=F+WEIGHT(IT)*(FIT-SIGEX(IT))**2
      DO 34 J=1,5
      PD(J)=   REAL(CSQ*ZD(J))*20.
      G(J)=G(J)+(FIT-SIGEX(IT))*PD(J)*2.*WEIGHT(IT)
   34 CONTINUE
      SIGEL(IT)=FIT
      SIGR(IT)=REAL(FC*CONJG(FC))*10.
    1 CONTINUE
      IF(M1.NE.1) GO TO 445
      SCALEF=F
      WRITE(3,446) F
  446 FORMAT(8H SCALEF=F10.2)
  445 CONTINUE
      IF(M1.EQ.3) GO TO 444
      F=F/SCALEF
      DO 434 J=1,5
  434 G(J)=G(J)/SCALEF
  444 CONTINUE
      IF(MM.GT.0) M1=3
      IF(M1.NE.3)GO TO 35
      WRITE(3,447) F
  447 FORMAT(3H F=F10.3)
      EX=EXS/EXE
      WRITE(3,25)
   25 FORMAT(1X,1HL,14X,
     X              6HETA(L),11X,10HDERIVITIVE,13X,7HNUCLEAR,13X,8HRELAT
     1IVE,14X,9HSPHERICAL
     X   /34X,9HOF ETA(L),12X,10H  PHASE   ,11X,7HCOULOMB/55X,9H  SHIFT
     2 ,11X,11HPHASE SHIFT,12X,8HHARMONIC//)
      DO 8 L=1,LMAX
      L2=2*L
      PS(L2)=CLOG(E(L2))/.0174533/2./IM
   24 FORMAT                     (1X,I2,3X,2F10.5,1HI,2F10.5,1HI,2F10.5,1HI,3
```

```
     1X,F10.5,13X,F10.5)
              WRITE(3,24) L,E(L2),GE(L2),PS(L2),SIG(L)
      EX=EX*EXD
      ETA=1./(1.+EX)
      ET=ETA*(1.-ETA)
      ETT=ET *(1.-2.*ETA)
      ETTT=ET*(1.-6.*ET)
      E(L2-1)=CMPLX((ETA+B*ET),(A*ET+D*ETT))
      GE(L2-1)=CMPLX((ET+B*ETT),(A*ETT+D*ETTT))/DELTA
    8 CONTINUE
C     ETA,K,YLO,SIGMA L,FN, HAVE BEEN EVALUATED.  GOOD PLACE TO DEBUG BY
C     WRITING
C
      DO 17 IT=1,ITMAX
      SXL(IT)=ALOG10(SIGEX(IT))
      SLL(IT)=ALOG10(SIGEL(IT))
      FOO    =ZERO
      DO 18 L=LMIN,LMAX
      L2=2*L
      FOO    =FOO    +FNS(L)*GE(L2)*YLO(L,IT)
   18 CONTINUE
      FO(IT)=        REAL(FOO    *CONJG(FOO    ))*2.5
      SNL(IT)=ALOG10(FO(IT))
   17 CONTINUE
      IF(IBGN.EQ.0) CALL CCBGN
      IF(IBGN.EQ.0) GO TO 300
      CALL CCPLOT(0.,0.,1)
      CALL CCNEXT
  300 CONTINUE
      IBGN=1
      WRITE (99,52)
   52 FORMAT( 61H$ PUT ORIGIN ON INTERSECTION OF VERTICAL LINE AND BOTTO
     1M LINE)
      WRITE(99,53)
   53 FORMAT(1H=)
      WRITE(98,44)T(NZX),NUMX,S(NA),S(NB),T(NZY),NUMY,    EA,ETO,K
   44 FORMAT(       51X,A2,I3,1H(,A3,1H,,A3,1H),A2,I3/ 22X,7HELASTIC
     1       13X,11HBEAM ENERGY,F10.5,3X,3HETA,F10.5,5X,1HK,F10.5)
      WRITE(98,23)ITMAX,LMIN,LMAX,IMAX,X
      CALL CCLTR(0.,1020./1024.,0,2)
      DO 46 IX=1,11
      UIX=IX
      UUI=200./1024.*(UIX-1.)
      CALL CCLTR(UUI,-20./1024.,0,2,CHARS(IX),6)
   46 CONTINUE
      CALL CCPLOT(TH,SLL,ITMAX,4HJOIN)
      CALL CCPLOT(TH,SXL,ITMAX,6HNOJOIN,1,1)
      I=0
      CALL CCPLOT(0.,0.,1)
      CALL CCNEXT
      WRITE(99,53)
      WRITE(98,43)T(NZX),NUMX,S(NA),S(NB),T(NZY),NUMY, I,EA,ETO,K
      WRITE(98,23)ITMAX,LMIN,LMAX,IMAX,X
      CALL CCLTR(0.,1020./1024.,0,2)
      DO 48 IX=1,11
      UIX=IX
```

```
      UUI=200./1024.*(UIX-1.)
      CALL CCLTR(UUI,-20./1024.,0,2,CHARS(IX),6)
   48 CONTINUE
      WRITE (99,52)
      CALL CCPLOT(TH,SNL,ITMAX,1,1)
      LMIN2=2*LMIN
      LMAX2=2*LMAX
      DO 601 L=LMIN2,LMAX2
      AEL=REAL(CABS(E(L)))
      IF(AEL.GT..5) GO TO 603
  601 CONTINUE
  603 IL=L
      AIL=REAL(CABS(E(IL-1)))
      RR=(.5-AIL)/(AEL-AIL)
      UIL1=IL-1
      ER=(UIL1+RR)/2.
      WRITE (3,602) ER
  602 FORMAT(4H ER=F20.5)
      R=(ETO+SQRT(ETO*ETO+ER *(ER +1.)))/K
      WRITE(3,47) R
   47 FORMAT(/51X,2HR=,F10.5/)
      DO 9 I=1,IMAX
      UI=I
      U2I=2.*UI+1.
      DO 37 IT=1,ITMAX
      W=WW(IT)
      W1=WW1(IT)
      YLM(1,IT)=-C(3)*W1
      YLM(2,IT)=-C(4)*W*W1
      FA(IT)=0.
   37 CONTINUE
      DO 10 M=1,I
      UM=M
      M2=M+1
      M2M=2*M+2
      DO  3 IT=1,ITMAX
      W=WW(IT)
      W1=WW1(IT)
      FOA(IT)=ZERO
      FINA(IT)=ZERO
      DO 3 L=M2,LMAX
      UL=L
      L2L=2*L+1
      LMP=L+M+1
      LMM=L-M+1
      YLM(L+1,IT)=W*SQ(L2L)*SQ(L2L+2)/(SQ(LMP)*SQ(LMM))*YLM(L,IT)
     1-SQ(LMP-1)*SQ(LMM-1)*SQ(L2L+2)/(SQ(LMP)*SQ(LMM)* SQ(L2L-2  ))*YLM(
     2L-1,IT)
    3 CONTINUE
C
C  YLM,FN,FC   HAVE BEEN EVALUATE  GOOD PLACE TO DEBUG BY WRITING
C
      DO 6 L=LMIN,LMAX
      LLMIN=L-I
      LLMIN=MAX0(LLMIN,LMIN)
      LLMIN=LLMIN-MOD(LLMIN+L+I,2)
```

```
      LLMAX=L+I
      LLMAX=MINO(LLMAX,LMAX)
      UL=L
      L2L=2*L+1
      DO 40 IT=1,ITMAX
      FON(IT)=ZERO
      FNN(IT)=ZERO
   40 CONTINUE
      DO 5 LL=LLMIN,LLMAX,2
      LLL= LL+L
      ULL=LL
      XX(1)=UL
      XX(2)=UI
      XX(3)=ULL
      XX(4)=0.
      XX(5)=0.
      XX(6)=0.
      CSH2=CLEB  (XX)
      Y(1)=UL
      Y (2)=UI
      Y (3)=ULL
      Y(4)=-UM
      Y(5)=UM
      Y(6)=0.
      CSH1=CLEB  (Y)
      MO=MOD(LL,4)+1
      IMO=IML(MO)
      DO  5 IT=1,ITMAX
      FNN(IT)=FNN(IT)+CE(LL)*CSH1*CSH2*GE(LLL)*IMO
      IF(M.NE.I) GO TO 19
      FON(IT)=FON(IT)+CE(LL)*CSH2*CSH2*GE(LLL)*IMO
   19 CONTINUE
    5 CONTINUE
      MO=5-MOD(L,4)
      IMO=IML(MO)
      DO 41 IT=1,ITMAX
      FINA(IT)=FINA(IT)+FNN(IT)*CE(L)*YLM(L,IT)*SQ(L2L)*IMO
      IF(M.NE.I) GO TO 49
      FOA(IT)=FOA(IT)+FON(IT)*CE(L)*YLO(L,IT)*SQ(L2L)*IMO
   49 CONTINUE
   41 CONTINUE
    6 CONTINUE
      DO 10 IT=1,ITMAX
      W1=WW1(IT)
      FA(IT)=FA(IT)+2.*REAL(FINA(IT)*CONJG(FINA(IT)))
      YLM(M+2,IT    )=-W1*SQ(M2M+3)/SQ(M2M )*YLM(M+1,IT   )
      YLM(M+1,IT    )=-W1*SQ(M2M+1)/SQ(M2M )*YLM(M,IT   )
   10 CONTINUE
      DO  4 IT=1,ITMAX
      FA(IT)=FA(IT)+REAL(FOA(IT)*CONJG(FOA(IT)))
      SIGIN(IT,I)=FA(IT)*2.5*U2I
      SNL(IT)=ALOG10(SIGIN(IT,I))
    4 CONTINUE
C
C     THE DIFFERENTIAL CROSS SECTION SIGCAL
C     HAS BEEN EVALUATED.  GOOD PLACE TO DEBUG BY WRITING
```

```
C
      CALL CCPLOT(0.,0.,1)
      CALL CCNEXT
      WRITE(99,53)
      WRITE(98,43)T(NZX),NUMX,S(NA),S(NB),T(NZY),NUMY, I,EA,ETO,K
   43 FORMAT(        51X,A2,I3,1H(,A3,1H,,A3,1H),A2,I3/ 22X,10HFINAL SPIN
     1I5,     8X,11HBEAM ENERGY,F10.5,3X,3HETA,F10.5,5X,1HK,F10.5)
      WRITE(98,23)ITMAX,LMIN,LMAX,IMAX,X
      CALL CCLTR(0.,1020./1024.,0,2)
      DO 45 IX=1,11
      UIX=IX
      UUI=200./1024.*(UIX-1.)
      CALL CCLTR(UUI,-20./1024.,0,2,CHARS(IX),6)
   45 CONTINUE
      WRITE (99,52)
      CALL CCPLOT(TH,SNL,ITMAX,1,1)
    9 CONTINUE
      WRITE(3,30)
   30 FORMAT(124H1THETA RUTHERFORD  ELASTIC  DATA       I= 0         1
     1        2          3          4          5          6          7
     28      )
      DO 16 IT=1,ITMAX
      WRITE(3,26) TH(IT),SIGR(IT),SIGEL(IT), SIGEX(IT),
     1                                         FO(IT),(SIGIN(IT,I),I=1,IMAX
     2)
   26 FORMAT(1X,F6.2,2F10.2,F8.2,9F10.2)
   16 CONTINUE
   35 CONTINUE
      RETURN
      END
                   *** 'END-OF-FILE' CARD ***
```

```
$IBFTC MAIN     LIST,REF
      DIMENSION H( 5, 5),X( 5),G( 5),S( 5),XP( 5),GP( 5), T( 5),GB( 5)
      DIMENSION V(3),C( 5, 5)
      COMMON  F     ,    FP     ,    FB     ,    FO     ,    X     ,    XP
      COMMON  T     ,    S      ,    G      ,    GS     ,    GP    ,    GSP
      COMMON  GB    ,    GSB    ,    GSS    ,    GTP    ,    GTT   ,    H
      COMMON  DELTA,     N      ,    M      ,    L      ,    M1    ,    MS
      COMMON  IT    ,    E      ,    K      ,    P      ,    TO    ,    SL
      COMMON  Z     ,    Q      ,    A      ,    EL     ,    V     ,     C
      COMMON /WRITE/ISHOT,IPERP,IMOVE,ILOOP,IDRESS,IWRITE,IFIN
      ID=40
 1000 DO 99 I=1,3
 99   V(I)=0.0
      MS=0
      CALL READIN
  120 L=1
  121 CALL READY
  122 L=L
  123 GO TO (139,159,133,126),L
  124 L=2
  125 GO TO 121
  126 CALL AIM
  128 GO TO (129,132,133,139),L
  127 L=L
  129 CALL FIRE
  130 L=L
  131 GO TO (135,132,126,139),L
  132 L=1
  133 CALL DRESS
      GO TO (124,139),L
  135 L=3
      GO TO 133
  159 L=4
      GO TO 133
  139 CALL RITEOT(2)
      CALL STUFF
      L=L
      GO TO (120,142),L
  142 CONTINUE
      M1=3
      CALL FCN(N,G,F,X,M1)
      GO TO 1000
      END
```

```
$IBFTC READY   LIST,REF
      SUBROUTINE READY
      DIMENSION H( 5, 5),X( 5),G( 5),S( 5),XP( 5),GP( 5), T( 5),GB( 5)
      DIMENSION V(3),C( 5, 5)
      COMMON  F     ,  FP    ,  FB    ,  FO    ,  X     ,  XP
      COMMON  T     ,  S     ,  G     ,  GS    ,  GP    ,  GSP
      COMMON  GB    ,  GSB   ,  GSS   ,  GTP   ,  GTT   ,  H
      COMMON  DELTA,   N     ,  M     ,  L     ,  M1    ,  MS
      COMMON  IT    ,  E     ,  K     ,  P     ,  TO    ,  SL
      COMMON  Z     ,  Q     ,  A     ,  EL    ,  V     ,   C
      COMMON /ERR/IERR,IPOS
      COMMON /WRITE/ISHOT,IPERP,IMOVE,ILOOP,IDRESS,IWRITE,IFIN
      L=L
      GO TO (200,201),L
  200 IT=1
      HIGH=2.0
      IERR=0
      DOUBLE=1.0
  201 CALL MATMPY(N,N,H,G,S)
      DO 203 I=1,N
  203 S(I)=-S(I)
      M=1
  207 CALL MATMPY(M,N,S,G,GS)
      IF (GS .LE. 0.0) GO TO 208
      CALL ERROR(1)
      GO TO 201
  208 EL=AMIN1(1.0,-HIGH*F/GS)
      SL=-GS
  210 DO 211 I=1,N
  211 XP(I)=X(I)+EL*S(I)
      M1=2
      CALL FCN(N,GP,FP,XP,M1)
      CALL OVERFL(KOOOFX)
      IF (KOOOFX .NE. 1) GO TO 215
      L=2
      CALL ERROR(5)
      IERR=IERR+1
      IF (L .EQ. 1) RETURN
      HIGH=HIGH/2.0
      EL=EL/2.0
      GO TO 210
  215 CALL MATMPY (M,N,S,GP,GSP)
      IERR=0
      IF ((GSP .LT. 0.0) .AND. (FP .LT. F)) GO TO 218
C   GOES TO AIM
      L=4
      ISHOT=0
      RETURN
  218 FB=FP
      DO 234 I=1,N
      GB(I)=GP(I)
  234 T(I)=XP(I)
      IF (EL .GE. 1.0) GO TO 223
C   GOES TO DRESS 3 WHICH DOESN' MODIFY H
      HIGH=2.0*HIGH
      L=3
```

```
      ISHOT=1
      RETURN
  223 DELTA=(DOUBLE+1.0)*DELTA
      TO=DOUBLE/SL
      DOUBLE=DOUBLE+2.0
      L=2
      ISHOT=2
      RETURN
      END
```

```
$IBFTC AIM      LIST,REF
      SUBROUTINE AIM
      DIMENSION H( 5, 5),X( 5),G( 5),S( 5),XP( 5),GP( 5), T( 5),GB( 5)
      DIMENSION V(3),C( 5, 5)
      COMMON  F     ,    FP    ,    FB    ,    FC    ,    X     ,    XP
      COMMON  T     ,    S     ,    G     ,    GS    ,    GP    ,    GSP
      COMMON  GB    ,    GSB   ,    GSS   ,    GTP   ,    GTT   ,    H
      COMMON  DELTA,     N     ,    M     ,    L     ,    M1    ,    MS
      COMMON  IT    ,    E     ,    K     ,    P     ,    TO    ,    SL
      COMMON  Z     ,    Q     ,    A     ,    EL    ,    V     ,     C
      COMMON /WRITE/ISHOT,IPERP,IMOVE,ILOOP,IDRESS,IWRITE,IFIN
      M=M
      L=0
      IPERP=0
      GO TO (301,313),M
 301  Z=GS+GSP+3.0*(F-FP)/EL
      TO=GS/Z
      TI=GSP/Z
      Q=ABS(Z*SQRT(1.0-TO*TI))
      A=(GSP+Q-Z)/(GSP-GS+Q+Q)
      IF ((A .GT. 0.0) .AND. (A .LT. 1.0)) GO TO 305
      L=4
      RETURN
  305 TO=(EL*(GSP+Z+Q+Q)*A*A)/3.0
      FO=FP-TO
      CALL MATMPY(N,N,H,GP,T)
      CALL MATMPY(M,N,T,S,SP)
      CALL MATMPY(M,N,S,S,SS)
      TP1=SP/SS
      DO 308 I=1,N
  308 T(I)=-T(I)+TP1*S(I)
      M=1
      CALL MATMPY(M,N,T,GP,GTP)
      TP1=F+GTP/2.0
      IF((TO-GTP/2.0 .LE. 0.0) .AND. (TP1 .GE. 0.0)) GO TO 318
 312  CALL OVERFL(KOOOFX)
      IF (KOOOFX .EQ. 1) CALL ERROR(15)
 313  TP1=1.0-A
      DO 314 I=1,N
  314 T(I)=A*X(I)+TP1*XP(I)
      L=1
C   GOES TO FIRE
      RETURN
  318 DO 319 I=1,N
  319 T(I)=T(I)+XP(I)
      M1=2
 321  CALL FCN (N,GB,FB,T,M1)
      CALL OVERFL(KOOOFX)
      IF (KOOOFX .NE. 1) GO TO 322
      CALL ERROR(20)
      GO TO 313
  322 IF (FB .GE. FO) GO TO 312
      IPERP=1
      DO 325 I=1,N
      S(I)=T(I)-X(I)
      G(I)=GB(I)-G(I)
  325 CONTINUE
```

```
      CALL MATMPY(M,N,S,GB,GTT)
      GSS=GTT-EL*GS
      IF (GSS .LE. 0.0) GO TO 335
      SL=-GTP+EL*EL*SL
      EL=1.0
C   GOES TO DRESS 1
      L=2
      RETURN
  335 L=3
C   GOES TO DRESS 3 H IS NOT MODIFIED
      RETURN
      END
```

```
$IBFTC FIRE    LIST,REF
      SUBROUTINE FIRE
      DIMENSION H( 5, 5),X( 5),G( 5),S( 5),XP( 5),GP( 5), T( 5),GB( 5)
      DIMENSION V(3),C( 5, 5)
      COMMON  F     ,  FP    ,  FB    ,  FO    ,  X     ,  XP
      COMMON  T     ,  S     ,  G     ,  GS    ,  GP    ,  GSP
      COMMON  GB    ,  GSB   ,  GSS   ,  GTP   ,  GTT   ,  H
      COMMON  DELTA,   N     ,  M     ,  L     ,  M1    ,  MS
      COMMON  IT    ,  E     ,  K     ,  P     ,  TO    ,  SL
      COMMON  Z     ,  Q     ,  A     ,  EL    ,  V     ,  C
      COMMON /WRITE/ISHOT,IPERP,IMOVE,ILOOP,IDRESS,IWRITE,IFIN
      COMMON /AAAAAA/LOOPF
    1 M1=2
      CALL FCN(N,GB,FB,T,M1)
      CALL OVERFL(KOOOFX)
      IF (KOOOFX .NE. 1) GO TO 403
      CALL ERROR(25)
      M=2
C   GOES TO AIM 2
      L=3
      RETURN
  403 M=1
      CALL MATMPY(M,N,S,GB,GSB)
      TP1=AMIN1(F,FP)
      ABAR=1.0-A
      IF (TP1 .LT. FB) GO TO 418
       LOOPF=0
      IMOVE=0
  406 TP1=A/ABAR
      TP2=ABAR/A
      TO=GSB*(TP1-TP2)
  413 GSS=TO+Q+Q
      IF (GSS .LE. 0.0) GO TO 410
      DO 415 I=1,N
  415 G(I)=(GB(I)-G(I))*TP1+(GP(I)-GB(I))*TP2
      L=2
C   GOES TO DRESS 1
      RETURN
  410 L=1
C   GOES TO DRESS 3 H IS NOT MODIFIED
      RETURN
418    CONTINUE
      L=4
      RETURN
      END
```

```
$IBFTC DRESS   LIST,REF
      SUBROUTINE DRESS
      DIMENSION H( 5, 5),X( 5),G( 5),S( 5),XP( 5),GP( 5), T( 5),GB( 5)
      DIMENSION V(3),C( 5, 5)
      COMMON  F     ,  FP    ,  FB    ,  FO    ,  X     ,  XP
      COMMON  T     ,  S     ,  G     ,  GS    ,  GP    ,  GSP
      COMMON  GB    ,  GSB   ,  GSS   ,  GTP   ,  GTT   ,  H
      COMMON  DELTA,   N     ,  M     ,  L     ,  M1    ,  MS
      COMMON  IT    ,  E     ,  K     ,  P     ,  TO    ,  SL
      COMMON  Z     ,  Q     ,  A     ,  EL    ,  V     ,   C
      COMMON /WRITE/ISHOT,IPERP,IMOVE,ILOOP,IDRESS,IWRITE,IFIN
      L=L
      IDRESS=L
      GO TO (500,525,529,510),L
C   CALCULATE LENGTH OF THE 2ND DERIVATIVE IN THE DIRECTION OF THE STEP
  500 CALL MATMPY(N,N,H,G,X)
      M=1
      CALL MATMPY(M,N,X,G,TO)
  505 DO 507 I=1,N
      DO 507 J=1,N
  507 H(I,J)=H(I,J)-X(I)*X(J)/TO
      DELTA=DELTA*(EL*GSS/TO)
      TO=EL/GSS
  510 DO 512 I=1,N
      DO 512 J=1,N
  512 H(I,J)=H(I,J)+TO*S(I)*S(J)
  529 CALL OVERFL(KOOOFX)
      IF (KOOOFX .EQ. 1) CALL ERROR(35)
  519 F=FB
      DO 522 I=1,N
      G(I)=GB(I)
  522 X(I)=T(I)
      L=1
C   SAME VALUE FOR F CHECK
      IF (V(3) .NE. F) GO TO 523
      L=2
      RETURN
C    GOES TO STUFF
  564 CALL RITEOT(1)
      IT=IT+1
C   GOES TO READY FOR A NEW ITERATION
      RETURN
 523  V(3)=V(2)
      V(2)=V(1)
      V(1)=F
      ILOOP=0
  525 GO TO 564
      END
```

```
$IBFTC STUFF
      SUBROUTINE STUFF
      DIMENSION H( 5, 5),X( 5),G( 5),S( 5),XP( 5),GP( 5), T( 5),GB( 5)
      DIMENSION V(3),C( 5, 5)
      COMMON  F    ,  FP   ,  FB   ,  FO   ,  X    ,  XP
      COMMON  T    ,  S    ,  G    ,  GS   ,  GP   ,  GSP
      COMMON  GB   ,  GSB  ,  GSS  ,  GTP  ,  GTT  ,  H
      COMMON  DELTA,  N    ,  M    ,  L    ,  M1   ,  MS
      COMMON  IT   ,  E    ,  K    ,  P    ,  TO   ,  SL
      COMMON  Z    ,  Q    ,  A    ,  EL   ,  V    ,  C
      L=2
      IF (MS .GE. K) RETURN
      MS=MS+1
      WRITE (3,5) MS
    5 FORMAT (19H-RANDOM STEP NUMBER,I4)
      M=(MS+1)/2
      DO 7120 I=1,N
      M=MOD(I,M)+MOD(MS,2)
      T(I)=2*MOD(M,2)-1
      T(I)=2*MOD (T(I),2)-1
 7120 CONTINUE
      CALL MATMPY (N,N,H,T,S)
      M=1
      CALL MATMPY (M,N,S,T,TO)
      EL=0.1*P/SQRT(TO)
 7130 DO 7140 I=1,N
      X(I)=X(I)+EL*S(I)
 7140 CONTINUE
      M1=2
      CALL FCN (N,G,F,X,M1)
      L=1
      IT=0
      CALL RITEOT(1)
      RETURN
      END
```

```
BFTC READIN  LIST,REF
      SUBROUTINE READIN
      DIMENSION H( 5, 5),X( 5),G( 5),S( 5),XP( 5),GP( 5), T( 5),GB( 5)
      DIMENSION V(3),C( 5, 5)
      COMMON  F     ,   FP    ,   FB    ,   FO    ,   X     ,   XP
      COMMON  T     ,   S     ,   G     ,   GS    ,   GP    ,   GSP
      COMMON  GB    ,   GSB   ,   GSS   ,   GTP   ,   GTT   ,   H
      COMMON  DELTA,    N     ,   M     ,   L     ,   M1    ,   MS
      COMMON  IT    ,   E     ,   K     ,   P     ,   TO    ,   SL
      COMMON  Z     ,   Q     ,   A     ,   EL    ,   V     ,    C
      COMMON /WRITE/ISHOT,IPERP,IMOVE,ILOOP,IDRESS,IWRITE,IFIN
      COMMON /PUNCH/IPUNCH,ICLOCK
      COMMON /IDENTY/IDENT
      COMMON /READ/IREAD
      READ (2,1) IREAD,IWRITE,K,ISIZE,ISTEP,IPUNCH,ICK,IDENT,ICLOCK
    1 FORMAT (16I5)
      E=10.0**(ISIZE-3)+1.E-8
      P=10.0**ISTEP
      M1=1
      CALL FCN (N,G,F,X,M1)
      WRITE (3,20) (X(I),I=1,N)
   20 FORMAT (17H1INITIAL GUESS IS/(1X,10E13.5))
      IF (IREAD .GE. 0) GO TO 50
      DO 30 I=1,N
      DO 29 J=1,N
      C(I,J)=0.0
      H(I,J)=0.0
   29 CONTINUE
      H(I,I)=1.0
   30 CONTINUE
      DELTA=1.0
   32 FORMAT (34H WHICH IS  LINEARLY CONSTRAINED BY)
      WRITE (3,32)
      NUMCON=-IREAD
      DO 40 I=1,NUMCON
      READ(2,10) (C(I,J),J=1,N)
   10 FORMAT (5E14.5)
      WRITE (3,37) (C(I,J),J=1,N)
   37 FORMAT (10E13.5)
   40 CONTINUE
      CALL CSTRAN(0)
      GO TO 150
   50 IREAD=IREAD+1
      GO TO (100,200,300                              ),IREAD
    H STARTED AS IDENTITY
  100 DO 110 I=1,N
      DO 108 J=1,N
      H(I,J)=0.0
  108 CONTINUE
      H(I,I)=1.0
  110 CONTINUE
      DELTA=1.0
      WRITE (3,120)
  120 FORMAT (39HOH SET INITIALLY TO THE IDENTITY MATRIX)
  150 M1=2
      CALL FCN (N,G,F,X,M1)
```

```
      CALL OVERFL(KOOOFX)
      WRITE (3,160) F,(G(I),I=1,N)
  160 FORMAT (24HOAT THE INITIAL GUESS F=,E13.5/9H AND G IS/(10E13.5))
      IF (M1 .NE. 10) GO TO 168
      DO 165 I=1,N
      G(I)=100.0*G(I)/F
  165 CONTINUE
      F=100.0
  168 IF (ICK .EQ. 1) CALL DIFCK
      WRITE (3,170)
  170 FORMAT (1H0)
      RETURN
C   READ IN DIAGONAL ELEMENTS OF H
  200 DO 210 I=1,N
      DO 209 J=1,N
      H(I,J)=0.0
  209 CONTINUE
  210 CONTINUE
      READ (2,10) (H(I,I),I=1,N)
      DELTA=1.0
      DO 230 I=1,N
      IF (H(I,I) .NE. 0.0) DELTA=DELTA*H(I,I)
  230 CONTINUE
      WRITE (3,240) (H(I,I),I=1,N)
  240 FORMAT (31HOTHE DIAGONAL ELEMENTS OF H ARE/(10E13.5))
      WRITE (3,250) DELTA
  250 FORMAT (24HOTHE DETERMINANT OF H IS,E13.5)
      GO TO 150
C   READ IN H AND DELTA
  300 READ (2,10) ((H(I,J),J=1,N),I=1,N)
      READ (2,10) DELTA
      WRITE (3,310) ((H(I,J),J=1,N),I=1,N)
  310 FORMAT (1H0,20X,1HH/(10E13.5))
      WRITE (3,250) DELTA
      GO TO 150
      END
```

```
$IBFTC RITEOT  LIST,REF
      SUBROUTINE RITEOT(NN)
      DIMENSION H( 5, 5),X( 5),G( 5),S( 5),XP( 5),GP( 5), T( 5),GB( 5)
      DIMENSION V(3),C( 5, 5)
      COMMON  F     ,  FP    ,  FB    ,  FO    ,  X     ,  XP
      COMMON  T     ,  S     ,  G     ,  GS    ,  GP    ,  GSP
      COMMON  GB    ,  GSB   ,  GSS   ,  GTP   ,  GTT   ,  H
      COMMON  DELTA,   N     ,  M     ,  L     ,  M1    ,  MS
      COMMON  IT    ,  E     ,  K     ,  P     ,  TO    ,  SL
      COMMON  Z     ,  Q     ,  A     ,  EL    ,  V     ,   C
      COMMON /WRITE/ISHOT,IPERP,IMOVE,ILOOP,IDRESS,IWRITE,IFIN
      COMMON /PUNCH/IPUNCH,ICLOCK
      IF (((IT .NE. 11) .AND. (IT .NE. 1) .AND. (NN .NE. 2) .AND. (ISETU
     *P .NE. 1)) .OR. (ICLOCK .NE. 0)) GO TO 3
      IF (ISETUP .EQ. 1) GO TO 2
      IF (IT .NE. 1) GO TO 1
      CALL CLOCKI(TIME1)
      GO TO 3
    1 CALL CLOCKI(TIME2)
      TIME=(TIME1-TIME2)/FLOAT(IT-1)+0.2
      ISETUP=1
    2 CALL CLOCKI(TIME3)
      IF (TIME .LT. TIME3) GO TO 3
      WRITE (3,1002)
 1002 FORMAT (25H1/-/-/-/-/-/-/-/-/-/-/-/-/13H-RAN OVERTIME)
      JEND=-1
      GO TO 1003
    3 IF (NN .EQ. 2) GO TO 1000
      IF (IT .EQ. ICLOCK) GO TO 900
      IF (IWRITE .EQ. 0) GO TO 35
      WRITE (3,4)
    4 FORMAT (130H - - - - - - - - - - - - - - - - - - - - - - - - - - - - - -
     * - - - - - - - - - - - - - - - - - - - - - - - - - - - - - - - - -
     * - - - - -               )
      JWRITE=IWRITE+1
      GO TO (35,25,15,6,5,49                                      ),JWRITE
   49 WRITE (3,51) (XP(I),I=1,N),(GP(I),I=1,N),GSP,FP,(S(I),I=1,N),EL
   51 FORMAT (18HOXP,GP,GSP,FP,S,EL/(10E13.5))
    5 WRITE (3,50) ((H(I,J),J=1,N),I=1,N)
   50 FORMAT (1H0,20X,1HH/(10E13.5))
    6 IF (ISHOT .EQ. 1) WRITE (3,100)
      IF (ISHOT .EQ. 2) WRITE (3,110)
      ISHOT=0
      IF (IPERP .EQ. 1) WRITE (3,200)
      IPERP=0
      IF (IMOVE .GT. 0) WRITE (3,300)
      IF (IMOVE .LT. 0) WRITE (3,310)
      IMOVE=0
      WRITE (3,500) IDRESS
      IF (ILOOP .EQ. 1) WRITE (3,400)
      WRITE (3,40) GS,DELTA
   40 FORMAT (59HOTHE COMPONENT OF THE GRADIENT IN THE DIRECTION OF THE
     *STEP,E14.5/7HODELTA=,E14.5)
   15 WRITE (3,30) (G(I),I=1,N)
   30 FORMAT (1H0,19X,1HG/(10E13.5))
   25 WRITE (3,20) F,(X(I),I=1,N)
   20 FORMAT (3HOF=,E14.5/1H0,19X,1HX/(10E13.5))
```

```
      WRITE (3,10) IT,MS
   10 FORMAT (17H0ITERATION NUMBER,I4,16H OF STEP NUMBER,I4/130H0- - - -
     *- - - - - - - - - - - - - - - - - - - - - - - - - - - - - - - - -
     *- - - - - - - - - - - - - - - - - - - - - - - - - - -      )
   35 IF (-1 .NE. JEND) RETURN
      CALL EXIT
  900 WRITE (3,1006)
 1006 FORMAT (41H0   TERMINATED DUE TO TOO MANY ITERATIONS,//)
 1000 WRITE (3,1001) MS
 1001 FORMAT (25H1/-/-/-/-/-/-/-/-/-/-/-/-/21H-FINAL VALUES OF STEP,I4)
 1003 M1=4
      CALL FCN(N,G,F,X,M1)
      IF (IPUNCH .GT. 0) WRITE(14,1005) (X(I),I=1,N)
      IF (IPUNCH .EQ. 2) WRITE(14,1005) (H(I,I),I=1,N)
      IF (IPUNCH .NE. 3) GO TO 5
      WRITE(14,1005) ((H(I,J),J=1,N),I=1,N)
      WRITE(14,1005) DELTA
      GO TO 5
  100 FORMAT (27H0UNDERSHOT   H NOT MODIFIED)
  110 FORMAT (54H0UNDERSHOT   H MODIFIED SO AS TO DOUBLE LENGTH OF STEP)
  200 FORMAT (9H0RICICHET)
  300 FORMAT (11H0MOVE RIGHT)
  310 FORMAT (10H0MOVE LEFT)
  400 FORMAT (43H0FOUR CONSECUTIVE VALUES OF F WERE THE SAME)
  500 FORMAT (6H0DRESS,I3)
 1005 FORMAT (5E14.5)
      END
```

```
$IBFTC ERROR   LIST,REF
      SUBROUTINE ERROR(KK)
      DIMENSION H( 5, 5),X( 5),G( 5),S( 5),XP( 5),GP( 5), T( 5),GB( 5)
      DIMENSION V(3),C( 5, 5),DIAG( 5)
      COMMON  F     ,  FP    ,  FB    ,  FO    ,  X     ,  XP
      COMMON  T     ,  S     ,  G     ,  GS    ,  GP    ,  GSP
      COMMON  GB    ,  GSB   ,  GSS   ,  GTP   ,  GTT   ,  H
      COMMON  DELTA,   N     ,  M     ,  L     ,  M1    ,  MS
      COMMON  IT    ,  E     ,  K     ,  P     ,  TO    ,  SL
      COMMON  Z     ,  Q     ,  A     ,  EL    ,  V     ,   C
      COMMON /WRITE/ISHOT,IPERP,IMOVE,ILOOP,IDRESS,IWRITE,IFIN
      COMMON /ERR/IERR,IPOS
      COMMON /AAAAAA/LOOPF
      COMMON /IDENTY/IDENT
      COMMON /READ/IREAD
      KKK=1+KK/5
      GO TO (100,200,400,400,400,600,400,800),KKK
  100 WRITE (3,110) GS
  110 FORMAT(41HOH IS NO LONGER POSITIVE DEFINITE FOR GS=,E13.5)
      IF (IDENT .GE. 2) WRITE (3,112) ((H(I,J),J=1,N),I=1,N)
  112 FORMAT (27HOH SET TO IDENTITY. H WAS =/ (10E13.5))
      DELTA=1.0
      DO 120 I=1,N
      DIAG(I)=ABS(H(I,I))
      DO 118 J=1,N
      H(J,I)=0.0
  118 CONTINUE
      H(I,I)=DIAG(I)
      IF ((IDENT .GE. 2) .AND. (DIAG(I) .NE. 0.0)) H(I,I)=1.0
      IF (H(I,I) .NE. 0.0) DELTA=DELTA*H(I,I)
  120 CONTINUE
      IF (IDENT .GE. 2) GO TO 117
      WRITE (3,116)
  116 FORMAT (67HODIAGONAL ELTS. OF H ARE SET POSITIVE AND OFF DIAGONAL
     *ELTS. ZEROED)
  117 IF ( IREAD .GE. 0) RETURN
      CALL CSTRAN(1)
      RETURN
  200 WRITE (3,201)
  201 FORMAT (58HOREADY OVERFLOW   LENGTH OF STEP IS HALVED FOR ANOTHER
     *TRY)
      IF (IERR .LT. 5) RETURN
      L=1
      IF ((MS .NE. 0) .AND. (IT .EQ. 1)) STOP
      RETURN
  400 WRITE (3,401)
  401 FORMAT (13HOAIM OVERFLOW)
      RETURN
  600 WRITE (3,601)
  601 FORMAT (83HOFIRE OVERFLOW   TRY POINT HALFWAY BETWEEN INTERPOLATED
     * MINIMUM AND LOWER END POINT)
      IF (FP .GT. F) A=A-1.0
      IMOVE=ISIGN(1,IFIX(A))
      A=(1.0+A)/2.0
      RETURN
  800 WRITE (3,801)

  801 FORMAT (15HODRESS OVERFLOW)
      STOP
      END
```

```
$IBFTC DIFCK   LIST,REF
      SUBROUTINE DIFCK
      DIMENSION H( 5, 5),X( 5),G( 5),S( 5),XP( 5),GP( 5), T( 5),GB( 5)
      DIMENSION V(3),C( 5, 5)
      DIMENSION GPL(5),GM(5)
      COMMON  F     ,  FP    ,  FB    ,  FO    ,  X     ,  XP
      COMMON  T     ,  S     ,  G     ,  GS    ,  GP    ,  GSP
      COMMON  GB    ,  GSB   ,  GSS   ,  GTP   ,  GTT   ,  H
      COMMON  DELTA,   N     ,  M     ,  L     ,  M1    ,  MS
      COMMON  IT    ,  E     ,  K     ,  P     ,  TO    ,  SL
      COMMON  Z     ,  Q     ,  A     ,  EL    ,  V     ,   C
      IFAIL=0
      M1=2
      DO 100 I=1,N
      DO 50 ITRY=1,5
      TRY=AMAX1(AMIN1(1.0/ABS(G(I)),1.0),ABS(X(I))*1.0E-4)/(10.0**(ITRY-
     *1))
      X(I)=X(I)-TRY
      CALL FCN (N,GM,FM,X,M1)
      X(I)=X(I)+2.0*TRY
      CALL FCN (N,GPL,FPL,X,M1)
      X(I)=X(I)-TRY
      FN=(GM(I)+4.0*G(I)+GPL(I))/3.0*TRY
        IF (ABS((FPL-FM-FN)/FN) .LE. 1.0E-4) GO TO 98
      GN=(FPL-FM)/(2.0*TRY)
      IF (ABS((GN-G(I))/GN) .LE. 1.0E-3) GO TO 98
   50 CONTINUE
      WRITE (3,55) I,FPL,F,FM,FN,GPL(I),G(I),GM(I),GN,TRY
   55 FORMAT (4H-THE,I4,82H-TH COMPONENT OF THE ANALYTICAL DERIVATIVE DO
     $ESN'T AGREE TO WITHIN .1 OF 1 PERCENT/29HOFPL,F,FM,FN,GPL,G,G7,GN
     *ARE /10E13.5)
      IFAIL=1
   98 WRITE (3,99) I,ITRY
   99 FORMAT (16H-SUCCESS FOR THE,I4,20H-TH COMPONENT ON THE,I4,4H TRY)
  100 CONTINUE
      IF (IFAIL .EQ. 1) CALL EXIT
      RETURN
      END
```

```
$IBFTC CSTRAN  LIST,REF
      SUBROUTINE CSTRAN (ITEST)
      DIMENSION H( 5, 5),X( 5),G( 5),PERM( 5),XP( 5),GP( 5),IPERM( 5),
     1GB( 5),V(3),C( 5, 5)
      INTEGER P,PERM
      COMMON  F     ,  FP     ,  FB     ,  FO     ,  X      ,  XP
      COMMON  PERM  ,  IPERM  ,  G      ,  GS     ,  GP     ,  GSP
      COMMON  GB    ,  GSB    ,  GSS    ,  GTP    ,  GTT    ,  H
      COMMON  DELTA,   N      ,  M      ,  L      ,  M1     ,  MS
      COMMON  IT    ,  E      ,  K      ,  P      ,  TO     ,  SL
      COMMON  Z     ,  Q      ,  A      ,  EL     ,  V      ,   C
      COMMON /READ/IREAD
      DELTA=1.0
      IF (ITEST .NE. 0) GO TO 100
      NUMCON=-IREAD+1
      DO 5 I=1,N
      PERM(I)=I
      IPERM(I)=I
    5 CONTINUE
      P=1
      DO 50 J=1,N
      PIVOT=0.0
      DO 10 I=P,N
      II=PERM(I)
      SAVE=ABS(C(II,J))
      IF (SAVE .LE. PIVOT) GO TO 10
      PIVOT=SAVE
      IBIG=II
   10 CONTINUE
      IF (PIVOT .LE. 0.0) GO TO 50
      ISAVE=PERM(P)
      PERM(P)=J
      IP=IPERM(J)
      PERM(IP)=ISAVE
      IPERM(J)=P
      IPERM(ISAVE)=IP
      P=P+1
      PIVOT=C(IBIG,J)
      DO 20 JJ=J,N
      SAVE=C(IBIG,JJ)/PIVOT
      C(IBIG,JJ)=C(J,JJ)
      C(J,JJ)=SAVE
   20 CONTINUE
      C(J,J)=1.0
      IF (P .GE. N) GO TO 100
      J1=J+1
      DO 30 I=P,N
      II=PERM(I)
      DO 28 JJ=J1,N
      C(II,JJ)=C(II,JJ)-C(II,J)*C(J,JJ)
   28 CONTINUE
      C(II,J)=0.0
   30 CONTINUE
   50 CONTINUE
  100 IF (C(N,N) .EQ. 0.0) GO TO 105
      H(N,N)=0.0
```

```
      GO TO 110
  105 DELTA=DELTA*H(N,N)
  110 DO 150 I=2,N
      II=N-I+1
      IF (C(II,II) .NE. 0.0) GO TO 120
      DELTA=DELTA*H(II,II)
      GO TO 150
  120 H(II,II)=0.0
      I1=II+1
      DO 140 J=I1,N
      DO 130 JJ=I1,N
      H(II,J)=H(II,J)-C(II,JJ)*H(JJ,J)
  130 CONTINUE
  140 CONTINUE
  150 CONTINUE
      DO 200 I=1,N
      DO 180 J=I,N
      SAVE=0.0
      DO 170 JJ=J,N
      SAVE=SAVE+H(I,JJ)*H(J,JJ)
  170 CONTINUE
      H(I,J)=SAVE
  180 CONTINUE
      DO 190 J=1,I
      H(I,J)=H(J,I)
  190 CONTINUE
  200 CONTINUE
      RETURN
      END

$IBFTC MATMPY  LIST,REF
      SUBROUTINE MATMPY(M,N,H,G,S)
      DIMENSION H( 5, 5),X( 5),G( 5),S( 5)
      IF (M-1) 705,705,702
 702  DO 703 I=1,M
      S(I)=0.0
      DO 703 J=1,N
  703 S(I)=H(I,J)*G(J)+S(I)
      RETURN
 705  S(1)=0.0
      DO 706 I=1,N
 706  S(1)=H(I,1)*G(I)+S(1)
      RETURN
      END
```

```
$IBMAP CLB
 CLEB  SAVE     1,2
       AXT      6,1
       AXT      0,2
       CLA      3,4
       ADD      =6
       STA      LOOP
 LOOP  CLA      **,1
       STO      ARRAY,2
       TXI      *+1,2,1
       TIX      LOOP,1,1
 CL    TSX      E0,4
       TSX      ARRAY
       RETURN   CLEB
E0     CLA      1,4
       STA    E11
       TRA    E620
E3     STA    E14
       SXD    COMMON+7,2
       SXD    COMMON+8,1
       LXA    E327,2
       LXA    E423,1
E10    CLA    E424
E11    UFA    0,2
       RQL    9
       LGL    8
E14    STO    0,1
       TXI    E16,2,1                      TCH    801A+
E16    TIX    E10,1,1                      IORP   +019+8
E17    LAC      E451,2
       CLA    0,2
       ADD    1,2
       ADD    2,2
       ADD    E425
       STO    COMMON+9
       ANA    E426
       TNZ    E324
       CLA    COMMON+9
       SUB    E427
       TPL    E324
       CLA    COMMON+9
       ARS    18
       ADD    E433
       STA    E176
       CLA    0,2
       ADD    1,2
       SUB    2,2
       TZE    E43
       TMI    E324
E43    ARS    18
       STA    E172
       STO    E435
       CLA    2,2
       SUB    1,2
       ADD    0,2
       TZE    E53
```

```
        TMI   E324
E53     ARS   18
        STA   E173
        CLA   2,2
        ADD   1,2
        SUB   0,2
        TZE   E62
        TMI   E324
E62     ARS   18
        STA   E174
        CLA   0,2
        SBM   3,2
        TMI   E324
        CLA   1,2
        SBM   4,2
        TMI   E324
        CLA   2,2
        SBM   5,2
        TMI   E324
        CLA   0,2
        ADD   3,2
        ADD   E425
        STO   COMMON+9
        ANA   E426
        TNZ   E324
        CLA   COMMON+9
        ARS   18
        STA   E216
        CLA   1,2
        ADD   4,2
        ADD   E425
        STO   COMMON+9
        ANA   E426
        TNZ   E324
        CLA   COMMON+9
        ARS   18
        STA   E220
        STO   E437
        CLA   2,2
        ADD   5,2
        ADD   E425
        STO   COMMON+9
        ANA   E426
        TNZ   E324
        CLA   COMMON+9
        ARS   18
        STA   E222
        CLA   3,2
        ADD   4,2
        SUB   5,2
        SSP   0
        SUB   E430
        TPL   E324
        SXD   COMMON+11,4
        CLA   0,2
        ADD   4,2
```

```
       SUB   2,2
       ARS   18
       STO   COMMON+9
       CLA   1,2
       SUB   2,2
       SUB   3,2
       ARS   18
       LDQ   COMMON+9
       TSX   E315,1
       STO   E431
       CLA   0,2
       SUB   3,2
       ARS   18
       LDQ   E437
       TSX   E331,1
       LDQ   E435
       TSX   E331,1
       STO   E432
       CLA   2,2
       ARS   17
       STA   E177
       ADD   E433
       STA   E175
       LXA   E434,1
E172   CLA   0,1
E173   FAD   0,1
E174   FAD   0,1
E175   FAD   0,1
E176   FSB   0,1
E177   FSB   0,1
       STO   E443
       CLA   0,2
       SUB   3,2
       ARS   18
       STA   E217
       STO   E436
       CLA   1,2
       SUB   4,2
       ARS   18
       STA   E221
       CLA   2,2
       SUB   5,2
       ARS   18
       STA   E223
E216   CLA   0,1
E217   FAD   0,1
E220   FAD   0,1
E221   FAD   0,1
E222   FAD   0,1
E223   FAD   0,1
       FAD   E443
       FDH   E444
       STQ   E443
       CLA   2,2
       SUB   1,2
       ADD   3,2
```

```
        ARS    18
        STO    E440
        CLA    2,2
        SUB    0,2
        SUB    4,2
        ARS    18
        STO    E441
        CLM    0
        STO    E447
E243    CLM    0
        STO    E442
        STO    E445
        LXA    E423,2
E247    CLA    E443,2
        TXH    E253,2,3                IORT   H03AB$
        ADD    E431
        TRA    E254
E253    SUB    E431
E254    STA    E255
E255    CLA    0,1
        FAD    E445
        STO    E445
        TIX    E247,2,1                IORP   +01ABP
        CLA    E443
        FSB    E445
        TSX    E343,4,2
        HTR      *
        STO    COMMON+10
        CLA    E431
        LBT    0
        TRA    E275
        CLA    E447
        FSB    COMMON+10
        STO    E447
        TRA    E300
E275    CLA    E447
        FAD    COMMON+10
        STO    E447
E300    CLA    E432
        SUB    E431
        TZE    E307
        CLA    E431
        ADD    E433
        STO    E431
        TRA    E243
E307    LXD    COMMON+7,2
        LXD    COMMON+8,1
        LXD    COMMON+11,4
        CLA    E447
        TOV    E314
E314    TRA    2,4
E315    TQP    E317
        TMI    E322
E317    TLQ    E323
        LLS    35
        TRA    1,1
```

```
E322   CLM   0
E323   TRA   1,1
E324   LXD   COMMON+7,2
       LXD   COMMON+8,1
       TOV   E327
E327   PXD   0
       TRA     2,4
E331   STO   COMMON+18
       CLA   COMMON+18
       TQP   E335
       TMI   E341
E335   TLQ   E337
       TRA   1,1
E337   LLS   35
       TRA   1,1
E341   CLM   0
       TRA   1,1
E343   STO   COMMON+2
       SSP   0
       LDQ   E417
       TLQ   E406
       LDQ   E422
       SUB   E421
       TMI   E361
       LRS   27
       STA   E355
E354   PXD   6
E355   LLS   0
       DVH   E420
       ARS   8
       RQL   27
E361   ADD   E421
       STQ   COMMON+3
       FAD   E421
       STO   COMMON+4
       SXD   COMMON+5,4
       LXA   E354,4
       CLA   E410
E370   LRS   35
       FMP   COMMON+4
       FAD   E417,4
       TIX   E370,4,1            IORP   +01JCY
       SUB   COMMON+3
       STO   COMMON+3
       CLA   COMMON+2
       TMI   E403
       CLA   E416
       FDH   COMMON+3
       STQ   COMMON+3
E403   CLA   COMMON+3
       LXD   COMMON+5,4
       TRA   2,4
E406   CLA   COMMON+2
       TRA   1,4
E410   TXI   21335,6,28416       TCH     (OV G
       STR   28449,6,29956       IOCT    D4W(J
```

```
        TXI   10409,7,31059        TCH    NC KR
        STR   32319,1,32085        IOCT   VE Y
        TXI   31517,7,32767        TCH       *
        TNX   32744,7,511          IOSP   7   Q
E416    TIX   0,0,768              IORP  +'0000
E417    TIX   13107,6,3938         IORP  + KT'T
E420    TIX   16320,1,25316        IORP  F=M= 0
E421    TIX   0,0,0                IORP  +00000
E422    HTR   0
E423    HTR   6
E424    TIX   0,0,8704             IORP  B80000
E425    HTR   1024
E426    HTR   0,7
E427    PZE   0,0,100              IOCD  01M000
E430    HTR   6
E431    HTR   0
E432    HTR   0
E433    HTR   1
E434    HTR   E452
E435    HTR   0
E436    HTR   0
E437    HTR   0
E440    HTR   0
E441    HTR   0
E442    HTR   0
E443    HTR   0
E444    TIX   0,0,1280             IORP  +D0000
E445    HTR   0
        HTR   E435
E447    HTR   0
E450    HTR   COMMON+18
E451    HTR     CLEB+439
E452    PZE     0
        PZE     0
        TIX   4287,7,354           IORP  +5KZ2
        TIX   17152,5,970          IORP  + 0*'0
        TIX   10718,6,1430         IORP  +FFSP
        TIX   6414,3,1842          IORP  +)SIM
        TIX   18894,0,1957         IORP  + N4P
        TIX   14461,6,2320         IORP  +M+TJ
        TIX   25505,2,2387         IORP  +NCF J
        TIX   8772,5,2457          IORP  +0I-94
        TIX   23911,2,2531         IORP  +PLEVP
        TIX   9680,0,2840          IORP  +*H2G+
        TIX   11907,6,2879         IORP  +* S 3
        TIX   22183,6,2920         IORP  + QV+P
        TIX   15607,0,2963         IORP  + C3TX
        TIX   3495,3,3006          IORP  +  HWP
        TIX   32705,5,3050         IORP  + -  1
        TIX   10638,0,3340         IORP  +U'20
        TIX   10108,1,3363         IORP  +UL0 (
        TIX   24660,5,3386         IORP  +U  10
        TIX   15709,5,3410         IORP  +VB$V
        TIX   10777,0,3435         IORP  +V$2QI
        TIX   5098,6,3459          IORP  +W3/ -
        TIX   27107,6,3484         IORP  +W)WPL
```

```
        TIX    7295,2,3510               IORP   +WWA/
        TIX    7560,0,3536               IORP   +X+1W8
        TIX    24540,0,3562              IORP   +X-5 )
        TIX    27566,1,3842              IORP   +(2
        TIX    15459,4,3855              IORP   +( L/L
        TIX    7380,0,3869               IORP   +( 1TD
        TIX    2082,5,3882               IORP   +(-Q-K
        TIX    31167,2,3896              IORP   +(YGO
        TIX    28006,1,3910              IORP   + 6 VO
        TIX    24344,1,3924              IORP   + D (H
        TIX    19218,2,3938              IORP   + KD*B
        TIX    11718,4,3952              IORP   +  KX6
        TIX    990,7,3966                IORP   +  Y
        TIX    18991,2,3981              IORP   +  DQ
        TIX    32191,6,3995              IORP   + .XW
E521    TIX    7088,4,4010               IORP   + -J
        TIX    8535,2,4025               IORP   + ZB5G
        TIX    3103,1,4040               IORP   + 88
        TIX    22942,0,4055              IORP   + G50
        TIX    1918,1,4070               IORP   + C8
        TIX    5001,2,4085               IORP   + VA 9
        TIX    32207,1,4354              IORP   A42 X
        TIX    7906,7,4361               IORP   A49Z,K
        TIX    27640,4,4369              IORP   A4AO Y
        TIX    25648,2,4377              IORP   A4IF+
        TIX    1698,1,4385               IORP   A4J8+K
        TIX    21113,7,4392              IORP   A4Q 9Z
        TIX    18135,6,4400              IORP   A4 U.G
        TIX    25344,5,4408              IORP   A4Y 'O
        TIX    9767,5,4416               IORP   A50-HP
        TIX    3989,5,4424               IORP   A58Q E
        TIX    7838,5,4432               IORP   A5+R
        TIX    21128,5,4440              IORP   A5H 08
        TIX    10931,6,4448              IORP   A5-S-T
        TIX    9851,7,4456               IORP   A5Q I,
        TIX    17736,0,4465              IORP   A5/4E8
        TIX    1661,2,4473               IORP   A5Z+I
        TIX    27027,3,4481              IORP   A61 OC
        TIX    28143,5,4489              IORP   A69 X
        TIX    4886,0,4498               IORP   A6B1'F
        TIX    22649,2,4506              IORP   A6+EJZ
        TIX    15775,5,4514              IORP   A6K$W
        TIX    16903,0,4523              IORP   A6$487
        TIX    25915,3,4531              IORP   A6T D,
        TIX    9930,7,4539               IORP   A6, .0
        TIX    1599,3,4548               IORP   A74HH
        TIX    807,7,4556                IORP   A7'Y'P
        TIX    7455,3,4565               IORP   A7EIU
        TIX    21438,7,4573              IORP   A7
        TIX    9882,4,4582               IORP   A7OK++
        TIX    5457,1,4591               IORP   A7 9EA
        TIX    8074,6,4599               IORP   A7X/ 0
        TIX    25202,1,4864              IORP   A'0 9S
        TIX    17023,4,4868              IORP   A'4M9
        TIX    12229,7,4872              IORP   A'8  5
        TIX    10774,2,4877              IORP   A' BQF
```

```
        TIX    12614,5,4881             IORP   A'A$56
        TIX    17713,0,4886             IORP   A'F4D/
        TIX    26028,3,4890             IORP   A'+ F*
        TIX    4752,7,4894              IORP   A' ZO+
        TIX    19385,2,4899             IORP   A'LD Z
        TIX    4351,6,4903              IORP   A'P/3
        TIX    25152,1,4908             IORP   A'* 90
        TIX    16216,5,4912             IORP   A' $ H
        TIX    10273,1,4917             IORP   A'VO-J
        TIX    7295,5,4921              IORP   A'ZR/
        TIX    7245,1,4926              IORP   A' 9/
        TIX    10092,5,4930             IORP   A 2- *
        TIX    15804,1,4935             IORP   A 7=W(
        TIX    24350,5,4939             IORP   A = (
        TIX    2930,2,4944              IORP   A ++ S
        TIX    17055,6,4948             IORP   A DUO
        TIX    1156,3,4953              IORP   A IHB4
        TIX    20740,7,4957             IORP   A   44
        TIX    10247,4,4962             IORP   A KK-7
        TIX    2414,1,4967              IORP   A P8N
        TIX    29984,5,4971             IORP   A $ D-
        TIX    27394,2,4976             IORP   A  F*2
E620    CLA    E17
        COM    0
        STA    E434
        CLA    E450
        TRA    E3
COMMON  DUP      1,18
        PZE      0
        DUP      1,5
        PZE      0
 ARRAY  PZE      0
        END
                      *** 'END-OF-FILE' CARD ***
```

```
$ID    465001,LYCURGUS,5,SPRINGER
$IBJOB          LOGIC
$IBFTC LYCURG  LIST,REF
C      LYCURGUS NUCLEAR REACTIONS RELATIVISTIC KINEMATICS PROGRAM
       DIMENSION EL(99),S(5),MW(5),T(99),EBS  (361,2),THETAS(361),LC(361)
      1,AW(5),THETCS   (361,2),EYS(361,2),THETYS(361,2)    ,RJ(361),H(2)
      2,RA(5)
       LOGICAL LAB,LABR
       REAL MX,MEV,LC
       DOUBLE PRECISION  UM,UMB,QS ,AY,PA,E,EC,G,W,R,PBC,PAC,RY,C,CO,SI,
      1B,D,F,EB,EY,COT,AB,THETAC,V,THETAY,A,DCOS,DSIN,DATAN,DSQRT,UMY,UMA
      2,AUMBB,RADIAN,P,PI
       DATA(T(I),I=1,99),(S(I),I=1,5),(
      X                             MW(I),I=1,5),(AW(I),I=1,5)/1HH,2HHE
      1,2HLI,2HBE,1HB,1HC,1HN,1HO,1HF,2HNE,2HNA,2HMG,2HAL,2HSI,1HP,1HS,2H
      2CL,2HAR,1HK,2HCA,2HSC,2HTI,1HV,2HCR,2HMN,2HFE,2HCO,2HNI,2HCU,2HZN,
      32HGA,2HGE,2HAS,2HSE,2HBR,2HKR,2HRB,2HSR,1HY,2HZR,2HNB,2HMO,2HTC,2H
      4RU,2HRH,2HPD,2HAG,2HCD,2HIN,2HSN,2HSB,2HTE,1HI,2HXE,2HCS,2HBA,2HLA
      5,2HCE,2HPR,2HND,2HPM,2HSM,2HEU,2HGD,2HTB,2HDY,2HHO,2HER,2HTM,2HYB,
      62HLU,2HHF,2HTA,1HW,2HRE,2HOS,2HIR,2HPT,2HAU,2HHG,2HTL,2HPB,2HBI,2H
      7PO,2HAT,2HRN,2HFR,2HRA,2HAC,2HTH,2HPA,1HU,2HNP,2HPU,2HAM,2HCM,2HBK
      8,2HCF,2HES,1HP,1HD,3HHE3,3HHE4,1HT,1,1,2,2,1,1.007825,2.014102,3.0
      91603,4.002604,3.016049/
       DATA MEV,RADIAN,PI/931.478,1.7453292519943D-2,3.1415926536/
       DATA HC/197.323/
       RA(1)=0.
       DO 1  J=2,5
       RA(J)=1.2
     1 CONTINUE
       H(1)=1.0
       H(2)=-1.0
     2 CONTINUE
       READ  (2,10)NZX,NA,NB,K,M,DELTA,    UMX,    Q,EA,RI,     (EL(J),J=
      11,K)
       DELTA=DELTA*RADIAN
       UMA=AW(NA)*MEV
       UMB=AW(NB)*MEV
       NUMX=UMX+0.5
       NUMY=AW(NA)+UMX-AW(NB)+.5
       NZY=NZX+MW(NA)-MW(NB)
       RI=RI*UMX**(1.0/3.0)+RA(NA)
       MX=UMX
       UMX=UMX*MEV
C
C
C      BEGIN CALCULATION
C
       UM=UMA+UMX
       PA=DSQRT((EA        )**2+2.*UMA*EA        )
       E=UM+EA
       EC=DSQRT(2.*UMX*E+UMA**2-UMX**2)
       G=E/EC
       PAC=G*PA/E*UMX
       DO     7 J=1,K
       QS=Q-EL(J)
       UMY=UM-UMB-QS
```

```
      A=UM**2+2.0*UMX*EA        +UMB**2-UMY **2
      AY=UM**2+2.0*UMX*EA        +UMY**2-UMB**2
      D=A*E
      RY=PA*AY/E/DSQRT(AY**2-4.*EC**2*UMY**2)
      W=      DSQRT(A**2-4.0*EC**2*UMB**2)
      R=PA*A/E/W
      LAB=DABS(R-1.).LE.1.D-7
      LABR=R.LT.1..OR.LAB
      PBC=W/2.0/EC
      C=G*(1.0-R**2)
      THETA=0.
      DO   5  L=1,M
      IS=1
      THETA=THETA+DELTA
      THETAS(L)=THETA/RADIAN
      CO=DCOS(THETA)
      SI=DSIN(THETA)
      COT=CO/SI
      P=PA*CO
      B=E**2-P**2
      AUMBB=A**2-4.*UMB**2*B
      IF(AUMBB.LT.0.) GO TO 6
      LS=L
      F=P*DSQRT(AUMBB)
    3 CONTINUE
C
C
C     ENERGY OF SCATTERED PARTICLE AND RECOIL
C
      EB=(D+F*H(IS))/2.0/B
      EBS  (L,IS)=(EB-UMB)
      EY =E-EB
      EYS(L,IS)=(EY-UMY)
C
C
C     CENTER OF MASS ANGLES
C
C
C
C     FOR THE SPECIAL CASE IN WHICH RHO EQUALS ONE
C
      IF(LAB)
     1THETAC=DATAN(2.*G*COT/(COT**2-G**2))
      IF(LAB) GO TO 4
C
C
C     FOR THE GENERAL CASE OF RHO NOT EQUAL TO ONE
C
      V=R*DSQRT(G*C+COT**2)
      THETAC=DATAN(C/(COT-V*H(IS)))
    4 CONTINUE
      IF(THETAC.LT.0.) THETAC=THETAC+PI
      THETCS(L,IS)=THETAC/RADIAN
C
C
C     RELATIVISTIC JACOBIAN
```

```
C
      IF(IS.EQ.1)
     1RJ(L)=G*(1.+R*DCOS(THETAC                ))*(SI/DSIN(THETAC ))**3
C
C
C     ANGULAR MOMENTUM TRANSFERRED IN SCATTERING
C
      ULC=DSQRT(PBC**2+PAC**2-2.*PBC*PAC*DCOS(THETAC))*RI
      LC(L)=ULC/HC
C
C
C     RECOIL LAB ANGLE
C
      THETAY=DATAN((R+DCOS(THETAC))/COT/(RY-DCOS(THETAC)))
      IF(THETAY.LT.0.) THETAY=THETAY+PI
      THETYS(L,IS)=THETAY/RADIAN
      IF(IS.EQ.2.OR. LABR)GO TO 5
      IS=2
      GO TO 3
    5 CONTINUE
    6 CONTINUE
      IF(LABR)
     0WRITE (3, 8)T(NZX),NUMX,S(NA),S(NB),T(NZY),NUMY,
     1           QS,EL(J),RI,  MX,G,       EA,R,(THETAS(L),  RJ(L),     T
     2HETCS(L,1),EBS(L,1),EYS(L,1),THETYS(L,1),LC(L),               L=1,
     3LS)
      IF(.NOT.LABR)
     0WRITE (3, 9)T(NZX),NUMX,S(NA),S(NB),T(NZY),NUMY,
     1           QS,EL(J),      MX,G,       EA,R,(THETAS(L),  RJ(L),     T
     2HETCS(L,1),THETCS(L,2),EBS(L,1),EBS(L,2),EYS(L,1),EYS(L,2),THETYS(
     3L,1),THETYS(L,2),L=1,LS)
    7 CONTINUE
    8 FORMAT(1H1///51X,A2,I3,1H(,A3,1H,,A3,1H),A2,I3//
     11X,7HQ VALUEF8.3,15X,12HENERGY LEVELF7.3,15X,6HRADIUSF6.2
     2                      //9X,11HTARGET MASS,F10.6,5X,5HGAMMA,F10.6,
     3         9X,11HBEAM ENERGY,F10.4,7X,3HRHO,F10.7////
     49H PARTICLE,13X,3(8HPARTICLE,2X),1X,2(6HRECOIL,4X)
     5   ,7HMAXIMUM/                                       3X,3HLAB,14X,12
     6HRELATIVISTIC,2X,4HC.M.,6X,3(3HLAB,7X),3HANG
     7                     /2X,5HANGLE,15X,8HJACOBIAN,3X,5HANGLE,5X,2(6HE
     8NERGY,4X),5HANGLE,4X,8HMOMENTUM
     9   ////(F6.1,14X,5F10.4,3X, F5.2))
    9 FORMAT(1H1///51X,A2,I3,1H(,A3,1H,,A3,1H),A2,I3//
     1       37H                             Q VALUE F8.3,27H
     2      ENERGY LEVEL F7.3//9X,11HTARGET MASS,F10.6,5X,5HGAMMA,F10.6,
     3         9X,11HBEAM ENERGY,F10.4,7X,3HRHO,F10.7////
     49H PARTICLE,13X,5(8HPARTICLE,2X),1X,4(6HRECOIL,4X)/3X,3HLAB,14X,12
     5HRELATIVISTIC,2X,2
     6(4HC.M.,6X),6(3HLAB,7X)/2X,5HANGLE,15X,8HJACOBIAN,3X,2(5HANGLE,5X)
     7,4(6HENERGY,4X
     8),2(5HANGLE,5X)////(F6.1,14X,9F10.4))
   10 FORMAT (I3,2I1,I2,I3,1F10.9,F10.7,      2F10.7,F10.8/(8F10.8))
      GO TO 2
      END
          *** DATA 'END-OF-FILE' CARD ***
```

```
$IBFTC FCN     LIST,REF
      SUBROUTINE FCN(N, G, F, X, M1)                                    FCN10030
      DIMENSION BACK(1024),BG(20),CHBG(20)
       DIMENSION G(40),X(40),PD(40),A(5)   ,SIGMA(40),SIGVAR(40)        FCN1
      DIMENSION T(1024)   ,V(1024),W(1024),S(1024),VV(1024),REMARK(11)
      DIMENSION RA(20),RC(20),FITS(1024),EF(40),EX(40)
      IF(M1-1) 60,40,60                                                 FCN10140
40    CONTINUE                                                          FCN10150
      READ(2,906) NBG,(CHBG(I),BG(I),I=1,NBG)
      WRITE(3,927)NBG,(I,CHBG(I),BG(I),I=1,NBG)
      READ  (2,3161)IRUN,NSTR,NFIN                                      FCN10260
       READ  (2,103)N,M,ICAM,MAXJ,IS,IW,DIV                             FCN10270
       WRITE (3,103)N,M,ICAM,MAXJ,IS,IW,DIV                             FCN10290
      M=NFIN-NSTR+1
      WRITE (3,150)N                                                    FCN10300
      WRITE (3,151)M                                                    FCN10310
       WRITE (3,161)ICAM                                                FCN10320
       IF(N-40)665,665,29204                                            FCN10340
29204  WRITE (3,1025)                                                   FCN10390
665    CONTINUE                                                         FCN10350
       READ  (2,1024)( X(I),I=1,N)                                      FCN10420
       WRITE (3,1026)( X(I),I=1,N)                                      FCN10430
      NBG=NBG-1
      DO 165 K=1,MBG
      XU=CHBG(K+1)
      XL=CHBG(K)
      IL=XL
      IU=XU
      DO 160 I=IL,IU
      XI=I
      BACK(I)=BG(K)+(XI-XL)*(BG(K+1)-BG(K))/(XU-XL)
  160 CONTINUE
  165 CONTINUE
      IF(IRUN-NRUN) 3162,3165,3162                                      FCN10440
 3162 READ  (15,3163)NRUN,NCHANL,REMARK                                 FCN10450
      WRITE (3,3182)NRUN,NCHANL,REMARK                                  FCN10460
      READ  (15,3164)(V (I),I=1,NCHANL)
      IF(IRUN-NRUN)3162,3165,3162                                       FCN10480
 3165 CONTINUE
       WRITE (3,1026)(V(I),I=NSTR,NFIN)
       TA=0.0                                                           FCN10650
       DO 26423 I=NSTR,NFIN
       TA=TA+V(I)-BACK(I)
26423   CONTINUE                                                        FCN10680
       DO 26424 I=NSTR,NFIN
       W(I)=1.0                                                         FCN10730
       IF( V (I)  )656,654,656
656    CONTINUE                                                         FCN10750
       W(I)=1.0/V (I)
654    CONTINUE                                                         FCN10770
      T(I)=I
26424  CONTINUE                                                         FCN10800
       C1=-2.773                                                        TABL0150
      TAA=TA  *.93944
      NA=N/3                                                            TABL0190
      TDD=0.
```

```
       DO 12 J=1,NA                                                     TABL0210
      NBJ=2*NA+J                                                        TABL0220
   12 TDD=TDD+X(J)*X(NBJ)
      TC =TAA/TDD
      TG =5.546*TC
60     CONTINUE                                                         FCN10810
       F=0.0                                                            FCN10830
      DO 4 I=1, N                                                       FCN10840
      PD(I) =0.0                                                        FCN10850
      G(I)= 0.0                                                         FCN10860
    4 CONTINUE                                                          FCN10870
      IF(M1-2)350,349,350
350    CONTINUE                                                         FCN10890
       WRITE (3,351)                                                    FCN10900
       DO 5103 J=1,N                                                    FCN10910
5103   SIGMA(J)=0.0                                                     FCN10920
349    CONTINUE                                                         FCN10930
      AC=0.0                                                            FCN11020
      DO5      I= NSTR,NFIN
       WI     =W(I     )
       TB=0.0                                                           TABL0280
       TH=0.0                                                           TABL0290
       DO 11 J=1,NA                                                     TABL0300
       NAJ=NA+J                                                         TABL0310
      NBJ=2*NA+J                                                        TABL0320
      TL=1.0/X(NBJ)
56     EF(J)= (T(I)-X(NAJ))*TL
       EX(J)= EXP( C1*EF(J)**2 )                                        TABL0360
       TI=X(J)*EX(J)
       TB=TB+TI                                                         TABL0740
      PD(NAJ)=TG*TI*EF(J)*TL
      PD(NBJ)=PD(NAJ)*EF(J)
      PD(J)=TC*(    EX(J) )
11     CONTINUE                                                         TABL0800
      IF(M1.EQ.3) CALL STDEV(PD,SIGMA,WI,N)
      FIT=TC*TB +BACK(I)
      TD=FIT-V(I     )
      TE=TD*WI
      F=F+TE*TD                                                         FCN11210
      DO 7 J=1, N                                                       FCN11240
       G(J)=G(J)+2.0*TE*PD(J)                                           FCN11250
    7 CONTINUE                                                          FCN11260
      IF(M1-2) 15,14,15
15     CONTINUE                                                         FCN11290
       FITA=V (I     )-FIT
       FITB=F                                                           FCN11330
       FITC= T(I)
       WRITE (3,346)V (I     ),FIT,FITA,FITB,FITC ,WI
      FITS(I     )=FIT
    9 AC=FIT+AC-BACK(I)
14     CONTINUE                                                         FCN11380
    5 CONTINUE                                                          FCN11390
      IF(M1-2) 683,682,684
  683 SCALEF=F
      WRITE(3,1014) SCALEF
  682 CONTINUE
```

```
      F=F/SCALEF
      DO 703 J=1,N
      G(J)=G(J)/SCALEF
  703 CONTINUE
      GO TO 5105
  684 CONTINUE
 1020 RSC=X(1)                                                          FCN11830
 2020 TC=TC*RSC                                                         FCN11840
      TQ=0.0                                                            FCN11850
 3020 DO 4020 J=1,NA                                                    FCN11860
      NBJ=2*NA+J
 4020 TQ=TQ+X(J)*X(NBJ)
  120 DO 520 J=1,NA                                                     FCN11880
  220 NAJ=NA+J                                                          FCN11890
      NBJ=2*NA+J
  320 RC(J)=X(NAJ)                                                      FCN11900
      RA(J)=X(J)*X(NBJ)/TQ*AC
  520 X(J)=X(J)/RSC                                                     FCN11920
       DO 5107 J=1,N                                                    FCN11930
5107   SIGMA(J)=SQRT( SIGMA(J) ) / SCALEF
      F=F/SCALEF
       CALL SDVAR(M,N,SIGVAR)                                           FCN11950
      F=F*SCALEF
       WRITE (3,1001)                                                   FCN11960
       DO 4462 I=1,N                                                    FCN11970
       WRITE (3,1002)I,X(I),SIGVAR(I),SIGMA(I)                          FCN11980
4462   CONTINUE                                                         FCN11990
    1 WRITE (3,3)X(N),F,TC                                              FCN12000
      WRITE (3,8)(RC(J),RA(J),X (J),J=1,NA)                             FCN12010
      WRITE (3,18)TA,AC                                                 FCN12020
      CALL LYCUR(RA,RC)
      WRITE (3,3168)IRUN,NSTR,NFIN                                      FCN12040
      WRITE (3,3169)                                                    FCN12050
      DO 2830 I=NSTR,NFIN
      LFYZ=FITS(I)/DIV+.5                                               FCN12070
      LVYZ=V(I)/DIV+.5                                                  FCN12080
      CALL GRAPH (LFYZ,44,0)                                            FCN12090
      CALL GRAPH (LVYZ,16,-1)                                           FCN12100
 2830 WRITE (3,2831)T(I)
      WRITE (3,3171)                                                    FCN12120
5105   CONTINUE                                                         FCN12130
      RETURN                                                            FCN12160
100    FORMAT(7I10)                                                     FCN12170
101    FORMAT(7F10.5)                                                   FCN12180
102    FORMAT(5E14.5)                                                   FCN12190
  103 FORMAT (6I10,F5.2,I3)                                             FCN12200
  150 FORMAT(36H  THE NUMBER OF FITTING PARAMETERS =I6)                 FCN12240
  151 FORMAT(29H  THE NUMBER OF DATA POINTS =I6/)                       FCN12250
161    FORMAT(45H  FCN FORCES RETURN TO NEXT RANDOM STEP AFTERI6,       FCN12330
     1 11H ITERATIONS)                                                  FCN12340
346    FORMAT(1H 6F20.6)                                                FCN12350
351    FORMAT(118H0      Y OBSERVED          Y CALCULATED        YOBS - FCN12380
     1 YCAL          (YOBS-YCAL)/YCAL     X OBSERVED          WEIGHTS   )FCN12390
  906 FORMAT(4X,I1,5X,14F5.0)
  927 FORMAT(2X,I1,42H BACKGROUND PTS  POINT   CHANNEL     LEVEL  /(21X,
     *I1,5X,F5.0,5X,F5.0))
```

```
1001    FORMAT(54H0      I            X(I)     SIGVAR(I)        SIGMA(I)     )FCN12440
1002     FORMAT(I6,7E16.8)
1014    FORMAT(9H  SCALEF=F20.5)
1024    FORMAT(16F5.2)                                                      FCN12500
1025    FORMAT(54H0 M OR IW  EXCEEDS 999, OR N EXCEEDS 40 SO EXIT CALLED)FCN12510
1026    FORMAT(10E13.5)                                                     FCN12520
    3 FORMAT(1H1,                                                           FCN12530
     1        16X,20HTHE AVERAGE WIDTH IS,F10.2,3X,6HCHI IS,F15.8,3X,25HTFCN12540
     2HE HEIGHT OF PEAK ONE IS,F10.2)                                       FCN12550
    8 FORMAT (38X,7HCHANNEL,13X,6HCOUNTS,14X,5HRATIO/(34X,F10.3,10X,F10.FCN12560
     11,10X,F10.3))                                                         FCN12570
   18 FORMAT(//                                                             FCN12580
     1        34H THE EXPERIMENTAL TOTAL COUNTS ARE,F10.1,10X,31HTHE CALCFCN12590
     2ULATED TOTAL COUNTS ARE,F10.1)                                        FCN12600
 2831 FORMAT(1H+,F4.0)                                                      FCN12610
 3168 FORMAT(1X ,10HRUN NUMBER,I5,12HFROM CHANNEL,I5, 2HTO,I5)              FCN12620
 3169 FORMAT(6H1*OVF*)                                                      FCN12640
 3171 FORMAT(6H1*OVN*)                                                      FCN12650
 3161 FORMAT(3I5)                                                           FCN12660
 3163 FORMAT(2I6,11A6)                                                      FCN12670
 3164 FORMAT(16F8.0)                                                        FCN12680
 3182 FORMAT(1X,          2I6,11A6)
      END                                                                   FCN12700
```

```
$IBFTC STDEV   LIST,REF
      SUBROUTINE  STDEV(PD,SIGMA,WI,N)
C  STDEV IS NOT CORRECT FOR ANYTHING EXCEPT LINEAR LEAST SQUARE
C SUM(BUT NOT PRODUCT,EXP,LOG) OF GAUSSIANS IS GAUSSIAN
C  SEE SDVAR FOR A COMPLETELY DIFFERENT APPROACH
      DIMENSION  PD(40), SIGMA(40)
      DIMENSION H(40,40),X(40),G(40),S(40),XP(40),GP(40), T(40),GB(40)
      DIMENSION V(3),C(40,40)
      COMMON  F     ,   FP     ,   FB     ,   FO     ,   X      ,   XP
      COMMON  T     ,   S      ,   G      ,   GS     ,   GP     ,   GSP
      COMMON  GB    ,   GSB    ,   GSS    ,   GTP    ,   GTT    ,   H
      COMMON  DELTA,    N      ,   M      ,   L      ,   M1     ,   MS
      COMMON  IT    ,   E      ,   K      ,   P      ,   TO     ,   SL
      COMMON  Z     ,   Q      ,   A      ,   EL     ,   V      ,    C
      DO 1 I=1,N
      TA=0.
      DO 3 J=1,N
      FI=I
      FJ=J
      FIRST=1.
      IF(FIRST)73,74,73
74    CONTINUE
73    CONTINUE
3     TA=TA+H(I,J)*PD(J)
      TA=TA*2.
      SIGMA(I)=SIGMA(I)+TA**2*ABS (WI)
1     CONTINUE
      FIRST=1.
      RETURN
1001  FORMAT(7E16.3)
      END
$IBFTC SDVAR   LIST,REF
      SUBROUTINE SDVAR(M,N,SIGVAR)
C SIGVAR WOULD RESULT IN F INCREASE OF .5*F/(M-N-1)
      DIMENSION SIGVAR(40)
      DIMENSION H(40,40),X(40),G(40),S(40),XP(40),GP(40), T(40),GB(40)
      DIMENSION V(3),C(40,40)
      COMMON  F     ,   FP     ,   FB     ,   FO     ,   X      ,   XP
      COMMON  T     ,   S      ,   G      ,   GS     ,   GP     ,   GSP
      COMMON  GB    ,   GSB    ,   GSS    ,   GTP    ,   GTT    ,   H
      COMMON  DELTA,    N      ,   M      ,   L      ,   M1     ,   MS
      COMMON  IT    ,   E      ,   K      ,   P      ,   TO     ,   SL
      COMMON  Z     ,   Q      ,   A      ,   EL     ,   V      ,    C
      FREE=M-N-1
       IF(FREE)2,2,1
2      FREE=0.
       GOTO 4
1      FREE=1./FREE
4      CONTINUE
       DO 3 J=1,N
      TEMP=H(J,J)
      SIGVAR(J)=SQRT ( FREE*F*TEMP )
3      CONTINUE
       RETURN
      END
```

```
$IBFTC LYCUR    LIST,REF
      SUBROUTINE LYCUR(AREA,CH)
      DIMENSION IAR(20)                                                 LYC40040
      DIMENSION EL(20),S(5),MW(5),T(99),EBS(20),THETAS(20),ULC(20)
     1,AW(5),THETCS(20),THETYS(20),RJ(20)
     2,SD(20)        ,AREA(20),CH(20),DCS(20)
      LOGICAL LAB,LABR
      REAL MX,MEV
      DOUBLE PRECISION  UM,UMB,QS ,AY,PA,E,EC,G,W,R,PBC,PAC,RY,C,CO,SI,
     1B,D,F,EB,EY,COT,AB,THETAC,V,THETAY,A,DCOS,DSIN,DATAN,DSQRT,UMY,UMA
     2,AUMBB,RADIAN,P,PI,THETA
      DATA(T(I),I=1,99),(S(I),I=1,5),(
     X                                     MW(I),I=1,5),(AW(I),I=1,5)/1HH,2HHE
     1,2HLI,2HBE,1HB,1HC,1HN,1HO,1HF,2HNE,2HNA,2HMG,2HAL,2HSI,1HP,1HS,2H
     2CL,2HAR,1HK,2HCA,2HSC,2HTI,1HV,2HCR,2HMN,2HFE,2HCO,2HNI,2HCU,2HZN,
     32HGA,2HGE,2HAS,2HSE,2HBR,2HKR,2HRB,2HSR,1HY,2HZR,2HNB,2HMO,2HTC,2H
     4RU,2HRH,2HPD,2HAG,2HCD,2HIN,2HSN,2HSB,2HTE,1HI,2HXE,2HCS,2HBA,2HLA
     5,2HCE,2HPR,2HND,2HPM,2HSM,2HEU,2HGD,2HTB,2HDY,2HHO,2HER,2HTM,2HYB,
     62HLU,2HHF,2HTA,1HW,2HRE,2HOS,2HIR,2HPT,2HAU,2HHG,2HTL,2HPB,2HBI,2H
     7PO,2HAT,2HRN,2HFR,2HRA,2HAC,2HTH,2HPA,1HU,2HNP,2HPU,2HAM,2HCM,2HBK
     8,2HCF,2HES,1HP,1HD,3HHE3,3HHE4,1HT,1,1,2,2,1,1.007825,2.014102,3.0
     91603,4.002604,3.016049/
      DATA MEV,RADIAN,PI/931.478,1.7453292519943D-2,3.1415926536/
      DATA HC/197.323/
      READ  (2,3 )NZX,NA,NB,K,M,DELTA,    UMX,    Q,EA,         (EL(J),J=
     11,K)                                                                  0130
      READ  (2,4 )THETA,UC,GEOM
      DELTA=DELTA*RADIAN
      UMA=AW(NA)*MEV
      UMB=AW(NB)*MEV
      NUMX=UMX+0.5
      NUMY=AW(NA)+UMX-AW(NB)+.5
      NZY=NZX+MW(NA)-MW(NB)
      MX=UMX
      UMX=UMX*MEV
C
C
C     BEGIN CALCULATION
C
      UM=UMA+UMX
      PA=DSQRT((EA        )**2+2.*UMA*EA        )
      E=UM+EA
      EC=DSQRT(2.*UMX*E+UMA**2-UMX**2)
      G=E/EC
      PAC=G*PA/E*UMX
      DO 1 L=1,K
      QS=Q-EL(L)
      UMY=UM-UMB-QS
      A=UM**2+2.0*UMX*EA        +UMB**2-UMY **2
      AY=UM**2+2.0*UMX*EA        +UMY**2-UMB**2
      D=A*E
      RY=PA*AY/E/DSQRT(AY**2-4.*EC**2*UMY**2)
      W=       DSQRT(A**2-4.0*EC**2*UMB**2)
      R=PA*A/E/W
      LAB=DABS(R-1.).LE.1.D-7
      LABR=R.LT.1..OR.LAB
```

```
      PBC=W/2.0/EC
      C=G*(1.0-R**2)
      THETAS(L)=THETA/RADIAN
      CO=DCOS(THETA)
      SI=DSIN(THETA)
      COT=CO/SI
      P=PA*CO
      B=E**2-P**2
      AUMBB=A**2-4.*UMB**2*B
      F=P*DSQRT(AUMBB)
C
C
C     ENERGY OF SCATTERED PARTICLE AND RECOIL
C
      EB=(D+F       )/2.0/B
      EBS  (L)   =(EB-UMB)
C
C
C     CENTER OF MASS ANGLES
C
C
C
C     FOR THE SPECIAL CASE IN WHICH RHO EQUALS ONE
C
      IF(LAB)
     1THETAC=DATAN(2.*G*COT/(COT**2-G**2))
      IF(LAB) GO TO 2
C
C
C     FOR THE GENERAL CASE OF RHO NOT EQUAL TO ONE
C
      V=R*DSQRT(G*C+COT**2)
      THETAC=DATAN(C/(COT-V        ))
    2 CONTINUE
      IF(THETAC.LT.0.) THETAC=THETAC+PI
      THETCS(L)   =THETAC/RADIAN
C
C
C     RELATIVISTIC JACOBIAN
C
      RJ(L)=G*(1.+R*DCOS(THETAC                    ))*(SI/DSIN(THETAC ))**3
C
C
C     ANGULAR MOMENTUM TRANSFERRED IN SCATTERING
C
      ULC(L)=DSQRT(PBC**2+PAC**2-2.*PAC*PBC*DCOS(THETAC))/HC
    1 CONTINUE
      WRITE (3, 5)T(NZX),NUMX,S(NA),S(NB),T(NZY),NUMY,
     1            QS,          UMX,G,       EA,R
      WRITE (3,6 )THETA,UC,GEOM
      WRITE(3,7)
      DCS(L)=GEOM*AREA(L)*RJ(L)/UC
      IF(M .NE.0) DCS(L)=DCS(L)*SI
      WRITE (3,8 )EL(L),CH(L),DCS(L),THETCS(L)
      IAR(L)=AREA(L)+.5
      WRITE (14,9 )IAR(L),THETA,UC,CH(L),EL(L),EBS(L),       THETCS(L)
```

```
 1,DCS(L),ULC(L),SD(L)
 3 FORMAT (I3,2I1,I2,I3,1F10.9,F10.7,      2F10.7,F10.8/(8F10.8))
 4 FORMAT(7F10.5)
 5 FORMAT(1H1///51X,A2,I3,1H(,A3,1H,,A3,1H),A2,I3//
 11X,7HQ VALUEF8.3
 2                   //9X,11HTARGET MASS,F10.6,5X,5HGAMMA,F10.6, LYC43340
 3          9X,11HBEAM ENERGY,F10.4,7X,3HRHO,F10.7////)          LYC43350
 6 FORMAT(11X,9HLAB ANGLEF10.3,22X,6HCHARGEF10.3,13X,18HGEOMETRICAL F
 1ACTORF10.3//)                                                   LYC43480
 7 FORMAT (12X,6HENERGY,24X,7HCHANNEL,22X,12HDIFFERENTIAL,22X,4HC.M./
 112X,5HLEVEL,25X,6HNUMBER,22X,13HCROSS SECTION,21X,5HANGLE/)     LYC43500
 8 FORMAT(8X,F10.3,20X,F10.3,20X,F10.3,20X,F10.3)                 LYC43510
 9 FORMAT(1X,I6,1X,F5.1,1X,F7.1,1X,F7.2,1X,F6.3,1X,F6.3,1X,F5.1,F11.4
 *,1X,F4.3,F8.6)
52 RETURN                                                         LYC43520
   END
```

```
$IBMAP GRAF
       ENTRY   GRAPH
GRAPH  SAVE    1,2,4
       CLA*    3,4
       TZE     *+8
       TMI     ADD1
       SUB     =100
       TZE     ADD1
       TMI     ADD1
       CLA =100
       TRA *+3
ADD1   ADD     =100
       TMI     *-1
       ADD     =18
       LRS     35
       DVH     =6                R IN AC.  Q INMQ.
       XCA                       Z IN AC. R IN MQ
       ALS     18
       STD     TEST1      WORDS TO BLANK
       MPY     =6
       XCA
       STA     SHIFT
       AXT     1,1
       AXT     0,2
       CAL     =H
TEST1  TXH     *+4,1,**
       SLW     Z,2
       TXI     *+1,2,-1
       TXI     *-3,1,1
*                                PLACE M IN PROPER POSITION FOR WRITING
       CAL*    4,4
       ALS     30
       ORA     =H0
       XCL
       CAL     =H
SHIFT  LGR     **
       STQ     Z,2
       SXA     NW,1
*                                PLOT AL
       CAL     Z
       ALS     6
       ARS     6
       STO     Z
       CLA*    5,4
       TZE     *+6
       TMI     *+3
       CAL     =H000000
       TRA     *+4
       CAL     =H+00000
       TRA     *+2
       CAL     =H 00000
       ORS     Z
       CALL    .FWRD.(.UN03.,FORMAT)
       CALL    .FSLO.(Z,NW)
       TSX     .FFIL.,4
       RETURN  GRAPH
Z      BSS     20
FORMAT BCI     1,(20A6)
NW     BSS     4
Y      BCI     1, XXXXX
       END
                    *** 'END-OF-FILE' CARD ***
```

REFERENCES

1. A. E. Litherland, J. A. Keuhner, H. E. Grove, M. A. Clark, and E. Almqvist, Phys. Rev. Letters 7, 98 (1961).
2. A. M. Lane and E. D. Pendlebury, Nucl. Phys. 15, 39 (1960).
3. D. Blum, P. Barreau, and J. Bellicard, Phys. Letters 4, 109 (1963).
4. J. S. Blair, Yugoslav Summer Meeting of Physicists (1962).
5. N. Austern and J. S. Blair, to be published.
6. R. H. Bassel, G. R. Satchler, and R. M. Drisko, Proceedings of the 3rd Conference on Reactions Between Complex Nuclei, Asilomar, 1963 (University of California Press, Berkeley, 1964).
7. J. Saudinos, R. Beurtey, P. Catillon, R. Chaminade, M. Crut, H. Faraggi, A. Papineau, and J. Thirion, Compt. rend. 252, 260 (1961).
8. E. K. Hyde, I. Perlman, and G. T. Seaborg, The Nuclear Properties of the Heavy Elements, Vol. I (Prentice-Hall, Inc., Englewood Cliffs, New Jersey, 1964), p. 150.
9. C. Williamson and J. P. Boujot, Tables of Range and Rate of Energy Loss of Charged Particles of Energy 0.5 to 150 MeV, unnumbered Saclay report (1962).
10. R. E. Ellis and L. Schecter, Phys. Rev. 101, 636 (1956).
11. G. E. Fisher, Phys. Rev. 96, 704 (1954).
12. R. G. Summer-Gill, Phys. Rev. 109, 1591 (1958).
13. J. H. Elliott, Nucl. Instr. Methods 12, 60 (1961).
14. F. S. Goulding and D. A. Landis, "Lawrence Radiation Laboratory Design," in Proceedings of Conference on Instrument Techniques in Nuclear Pulse Analysis, Monterey, 1963.
15. W. C. Davidson, Argonne National Laboratory Report ANL-5990-Rev., 1959.
16. P. M. Endt and C. van der Leun, Nucl. Phys. 34, 1 (1962).
17. V. J. Ashby and H. C. Cation, Tables of Nuclear Reaction Q-values, Lawrence Radiation Laboratory Report UCRL-5419, 1959.
18. C. M. Braams, Phys. Rev. 101, 1764 (1956).
19. H. P. Leenhouts and P. M. Endt, Phys. Letters 5, 69 (1963).

20. K. Alder, A. Bohr, T. Huus, B. R. Mottelson, and A. Winther, Rev. Mod. Phys. 28, 432 (1956).
21. A. Bohr and B.R. Mottelson, Mat.-fys. Medd. Dan. Vid. Selsk. 27, No. 16 (1953).
22. A. Messiah, Quantum Mechanics, Vol. 2 (North-Holland Publishing Co., Amsterdam, 1962).
23. R. Hofstadter, Rev. Mod. Phys. 28, 214 (1956).
24. B. L. Cohen, Phys. Rev. 105, 1549 (1957).
25. B. L. Cohen and A. G. Rubin, Phys. Rev. 111, 1568 (1958).
26. R. W. Bauer, A. M. Bernstein, G. Heymann, E. P. Lippincott, and N. S. Wall, Ca^{40} (α,α'): A Test of Particle-Hole Calculations (to be submitted to Phys. Letters).
27. K. Yogi, H. Ejiri, M. Furukawa, Y. Ishizaki, M. Koike, K. Matsuda, Y. Nakajima, I. Nonaka, Y. Saji, E. Tanaka, and G. T. Satchler, Phys. Letters 10, 186 (1964).
28. J. J. Kraushaar, W. S. Gray, and R. A. Kenefick, private communication.
29. A. E. Litherland, J. A. Kuehner, H. E. Grove, M. A. Clark, and E. Almqvist, Phys. Rev. Letters 7, 98 (1961).
30. J. S. Blair, Phys. Rev. 115, 928 (1959).
31. S. I. Drozdov, Soviet Phys. JETP 1, 591 (1955).
32. E. V. Inopin, Soviet Phys. JETP 4, 764 (1957).
33. J. S. Blair, D. Sharp, and L. Wilets, Phys. Rev. 125, 1625 (1962).
34. B. Buck, Phys.Rev. 127, 940 (1962).
35. J. R. Meriwether, A. Bussiere, B. G. Harvey, and D. J. Horen, Phys. Letters 11, 299 (1964).
36. A. M. Boldin, V. I. Gol'danskii, I. L. Rozenthal, Kinematics of Nuclear Reactions (Pergamon Press, London, 1961).
37. A. Leon, Lawrence Radiation Laboratory Space Laboratory Internal Working Paper No. 20, 1964.
38. R. Fletcher and M. J. D. Powell, The Computer Journal 6, 163 (1963).
39. J. S. Blair, University of Washington, private communication, 1964.
40. H. P. Leenhouts, University of Utrecht, private communication, 1963.